



저작자표시-비영리-변경금지 2.0 대한민국

이용자는 아래의 조건을 따르는 경우에 한하여 자유롭게

- 이 저작물을 복제, 배포, 전송, 전시, 공연 및 방송할 수 있습니다.

다음과 같은 조건을 따라야 합니다:



저작자표시. 귀하는 원저작자를 표시하여야 합니다.



비영리. 귀하는 이 저작물을 영리 목적으로 이용할 수 없습니다.



변경금지. 귀하는 이 저작물을 개작, 변형 또는 가공할 수 없습니다.

- 귀하는, 이 저작물의 재이용이나 배포의 경우, 이 저작물에 적용된 이용허락조건을 명확하게 나타내어야 합니다.
- 저작권자로부터 별도의 허가를 받으면 이러한 조건들은 적용되지 않습니다.

저작권법에 따른 이용자의 권리는 위의 내용에 의하여 영향을 받지 않습니다.

이것은 [이용허락규약\(Legal Code\)](#)을 이해하기 쉽게 요약한 것입니다.

[Disclaimer](#)

August 2020

Ph.D. Dissertation

**Automated Methods For  
Analysis Of Stem Cell-derived  
Cardiomyocytes At The Single-  
Cell Level With A Label-free  
Digital Holographic Microscope**

**Graduate School of Chosun University**

**Department of Computer Engineering**

**Ezat Ahmadzadeh**

라벨이없는 디지털 홀로그램  
현미경으로 단일 세포 수준에서  
줄기 세포 유래 심근 세포의  
분석을위한 자동화 된 방법

2020 년 8 월 28 일

조선대학교 대학원

컴 퓨 터 공학 과

이잠 아흐마드자데흐



**Automated Methods for Analysis  
of Stem Cell-derived  
Cardiomyocytes At the Single-  
Cell level With a Label-Free  
Digital Holographic Microscope**

**Advisor: Professor Shin Seokjoo**

**This Thesis is submitted to the Graduate School of  
Chosun University in partial fulfillment of the  
requirements for the award of a Ph.D. degree**

**2020 년 5 월**

**Graduate School of Chosun University**

**Department of Computer Engineering**

**Ezat Ahmadzadeh**

## 이장의 박사학위논문을 인준함

위원장 조선대학교 교수 이충규(인)

위원 조선대학교 교수 신석주(인)

위원 조선대학교 교수 권구락(인)

위원 조선대학교 교수 강문수(인)

위원 대구경북과학기술원 교수 문인규(인)

2020년 07월

조선대학교 대학원

This dissertation is lovingly dedicated to my compassionate mother Masome Rahimi. Her patience, encouragement, and constant love have regulated my life.

## ACKNOWLEDGEMENTS

First and foremost, praises and thanks to God, the Almighty, for His blessings throughout my Ph.D. course to complete successfully.

I am most grateful to the members of my committee (**Prof. Inkyu Moon, Prof. Shin Seokjoo, Prof. Goo-Rak Kwon, Prof. Moon Soo Kang, Prof. Chung Ghiu lee**) for their time, encouragement, and expertise throughout this project.

Special thanks go to the chairman of my committee, **Prof. Moon Soo Kang** for his keen attention to detail and his demand for goodness. There are people in everyone's lives who make success both possible

I would like to express my profound thanks and appreciation to my advisor, **Prof. Inkyu Moon** who helped me do a lot of research, and I came to know so many new things by providing invaluable guidance throughout this Ph.D. course. I am extremely grateful to **Prof. Shin Seokjoo** who allowed me to continue the Ph.D. course. It was a great privilege and honor to be his student.

I would like to thank my wonderful sisters, brother, sister in law and brother-in-law for their support who helped me staying abroad and tolerate being far from them for a long time and my Ph.D. course wouldn't be completed without their support and encouragement over the years.

I also want to dedicate this dissertation to my little niece "**Rozhan Ahmadzadeh**" which I love the most.

Last but not least I dedicate this dissertation to my late father "**Ali Ahmadzadeh**" gone forever and left a void which can't be filled. I miss you beyond words.

Finally, my thanks and appreciation go to all the people who have supported me to complete the research work directly or indirectly.

Thank you



## Table of Contents

<b>DEDICATION.....</b>	<b>VI</b>
<b>ACKNOWLEDGEMENTS.....</b>	<b>VII</b>
<b>TABLE OF CONTENTS .....</b>	<b>IX</b>
<b>LIST OF TABLES.....</b>	<b>XII</b>
<b>LIST OF FIGURES .....</b>	<b>XIII</b>
<b>ABBREVIATIONS .....</b>	<b>XX</b>
<b>ABSTRACT .....</b>	<b>XXI</b>
<b>초록 .....</b>	<b>XXIII</b>
<b>1 INTRODUCTION.....</b>	<b>1</b>
A. MOTIVATIONS.....	6
B. OBJECTIVES OF RESEARCH.....	7
C. ORGANIZATION OF THE RESEARCH .....	8
<b>2 THE STUDY OF STEM CELL-DERIVED CARDIOMYOCYTES BY DIGITAL HOLOGRAPHIC MICROSCOPY TECHNIQUE: .....</b>	<b>10</b>
A. AUTOMATED SINGLE CARDIOMYOCYTE CHARACTERIZATION BY NUCLEUS EXTRACTION FROM DYNAMIC HOLOGRAPHIC IMAGES USING FULLY CONVOLUTIONAL NEURAL NETWORK ....	13

a.	Abstract:.....	13
b.	Motivations and introduction:.....	14
c.	Cardiomyocytes preparations .....	15
d.	Results and discussions:.....	16
e.	Conclusion .....	32
B.	LABEL-FREE MOTION CHARACTERIZATION OF HUMAN CARDIOMYOCYTES AT THE SINGLE-CELL LEVEL USING HOLOGRAPHIC IMAGING FOR CARDIOTOXICITY SCREENING ....	33
a.	Motivations and introduction:.....	33
b.	Cardiac cell motion tracking with Farneback optical flow .....	35
c.	Workflow and beating signal extraction.....	37
d.	Results and discussion .....	41
e.	Conclusions.....	51
C.	AUTOMATED MOTION CHARACTERIZATION OF DRUG-TREATED CARDIOMYOCYTES AT THE SINGLE CELL-LEVEL WITH DIGITAL HOLOGRAPHIC IMAGING..	52
a.	Abstract.....	52
b.	Motivation and introduction .....	53
c.	Material and methods.....	55
d.	Results and discussion. ....	59
e.	Conclusions.....	70
D.	INTEGRATED PLATFORM FOR SIMULTANEOUSLY MONITORING HUMAN CARDIOMYOCYTES CONTRACTILE MOTION AND KINETICS FORCE GENERATION AT THE SINGLE-CELL LEVEL FROM HOLOGRAPHIC IMAGING INFORMATICS .....	71
a.	Abstract.....	71
b.	Motivation and introduction .....	72
c.	Materials and methods .....	74
d.	Results and discussion .....	80

e. Conclusions: ..... 89

**3 CONCLUSION AND FUTURE RESEARCH OPPORTUNITIES.....90**

**4 REFERENCES.....91**

## List of Tables

Table 2.1: Description of cardiomyocyte dynamic parameter quantification .....	24
Table 2.2: The Dice coefficient analysis of the proposed method against the U-Net model ....	28
Table 2.3: Description of dynamic parameters measured for each extracted single cardiac cell .....	40
Table 2.4: Definition of terms and analysis parameters .....	59
Table 2.5: Quantitative parameters and corresponding description measured from the whole slide QPI cardiomyocyte of the control sample .....	60
Table 2.6 Description of kinematic parameters measured for each extracted single cardiac cell .....	77
Table 2.7 Description of temporal parameters measured for each extracted single cardiac cell ... .....	79

## List of Figures

Figure 2. 1 Schematic representation of a Digital Holographic Microscope .....	9
Figure 2. 2 (a) A recorded hologram (a three-dimensional (3D) section of the hologram is shown in the inset). (b) the main three bandwidths of the hologram are separated using fourior transform. (c) a spatial filter is used to filter out the real image bandwidth and remove the other bandwidths. (d) shows the numerical reconstruction of the hologram which gives the amplitude image and (e) phase image after the phase unwarping .....	12
Figure 2.3: (a) QPIs of multiple CMs, (b) beating activity comparison of the ROI against Non-ROI. The inset shows the marked with the red line .....	14
Figure 2.4: The proposed FCN network architecture for cardiac cells nucleus section extraction consists of the following elements: Parallel multi-pathway features concatenation (blue box) consists of different kernel sizes: $1 \times 1$ , $3 \times 3$ , and $5 \times 5$ .made up of a convolucional layer + batch normalization layer (BN) + rectified linear unit (Relu). max-pooling layer size is $2 \times 2$ with a stride of two. The dense connection technique is used for efficient gradient propagation along with residual connections that are denoted with dotted red arrows .....	17
Figure 2.5: (a) the QPI of CMs (yellow bar denotes $20\mu\text{m}$ ). (b) a portion of the original phase image is magnified to indicate patches. (c) Corresponding ground truth patches with denoted ROI shown in yellow color and non-ROI dark blue color portions .....	20
Figure 2.6: Results of the CM's nucleus extraction using the proposed FCN-based method in comparison with the U-Net network model. (a) Original phase image of multiple cardiac cells obtained by DHM. (b) Predicted mask using our trained FCN-based model. (c) The results of the U-Net network model. (d) Ground truth mask extracted manually.....	21
Figure 2.7: the whole-slide QPI of multiple CMs beating profile reconstruction before and after	

nucleus extraction. (a) and (b) QPI multiple CMs before ROI extraction and corresponding beating activity profile respectively. (c) and (d) the QPI after the ROI extraction using the proposed method marked with green line and corresponding beating activity profile..... 22

Figure 2.8: The quantitative phase image of multiple CMs in which single CMs are marked to be extracted for further quantification. (b) the corresponding beating profile of single CMs #1 to #6, (c) details on quantification parameters of single CM beating profile..... 26

Figure 2.9: Single CMs beating profile (#1- #6 ). The sampling frequency was 10Hz ..... 26

Figure 2.10: the beating activity temporal parameter quantification results ..... 27

Figure 2.11: The learning curves and confusion matrix of pixel classification using the proposed FCN-based model versus the U-Net model. (a) and (b) the learning curve of the proposed FCN Model in comparison with the U-Net model and corresponding loss curves respectively. (c) Confusion matrix for pixel classification of the proposed model. (d) Confusion matrix for pixel classification of the U-Net model..... 29

Figure 2.12:(a) the ROI marked with green line on the original QPI before Hoechst nuclear staining, (b) The original QPI with nuclei section stained using the Hoechst nuclear staining method overlaid on the segmented image. The segmented sections are mostly included nuclei..... 30

Figure 2.13: (a) representation of the optical flow method for pixel displacement estimation. The black pixels correspond to the pixel position at the time (t), and white pixels correspond to the pixel position at the time (t+dt). (b) Multi-resolution leveling of the image with three levels. The image resolution at each level is downsized. The tracking begins at the lowest level finishes at the highest level.....36

Figure 2.14. The overview of the workflow for motion tracking of single cardiac cells and beating profile visualization using motion speed calculation .....38

Figure 2.15. Single CM contractile motion characterization using optical flow analysis. A close-up image

of a single CM with superimposed motion vectors on the cell for (a) contraction, (b) relaxation and (c) resting state, respectively, (first row) and corresponding heat map generated from absolute motion (second row). The contractile center refers to a region from which contractions are maximized. (d) details on quantification parameters explained in Table 1. (e) beating activity profile of a single cell .....39

Figure 2.16: Real-time motion tracking of single CMs with the optical flow and contractility analysis using heat maps: (a), (b) and (c) motion vectors superimposed on the single CM image representing the motion direction for contraction, relaxation and resting beating cycle, respectively, shown in the first row. The corresponding contractility heat map is shown in the second row. The contractile centers are encircled and shown in warmer colors on the heat map. (d) The beating activity profile derived from dry mass redistribution motion speed calculation by absolute motion in the entire image over time using Eq. (14) .....42

Figure 2.17: Results of different parameters of beating profile of the single extracted cells.....43

Figure 2.18: Visual and numerical synchronization analysis. (a) 3D representation of single CM’s beating profile synchronization. (b) Cross-correlation analysis between different pairs of individual CMs .44

Figure 2.19: Whole slide QPI of multiple cardiomyocytes motion characterization. The sample is recorded at 10Hz frequency. (a) Whole slide QPI of multiple CMs with superimposed motion vectors for contraction beating status, (b) corresponding heat map, (c) beating activity profile. (Maximum contraction speed: 1.4 [ $\mu\text{m/s}$ ]; Maximum relaxation speed: 0.8 [ $\mu\text{m/s}$ ]; Contraction period:0.58 [s]; Relaxation period: 0.63 [s]; Beating period: 2.1 [s]; Resting period: 0.75 [s]).....45

Figure 2.20: The whole slide QPI Motion speed measurement of fixed cardiomyocytes versus live cardiomyocytes .....46

Fig. 2. 21. Single-CM contractile motion analysis in control (Ctrl) and drug-treated conditions in response to 166nM of isoprenaline. (a) Whole-slide QPI contractile motion analysis in control and drug-treated conditions, (b) single-beat contractile motion comparison in control and drug-treated conditions. (c) Motion waveforms of single CMs #1 to #4 extracted in control conditions. (d)

Quantification result comparison in the control conditions (blue points) versus drug-treated conditions (red points) at the single-cell level. (e) Single CMs #1 to #4 extracted after isoprenaline treatment. (f) Average of each quantification parameter for all extracted single cells in control (blue bars) versus drug-treated conditions (red bars). All statistical comparisons were carried using an unpaired student t-test. .... 47

Figure. 2. 22. cardiomyocytes contractile motion analysis in control (ctrl) and drug-treated conditions in response to 500  $\mu$ M of E-4031. (a) Whole-slide QPI contractile motion analysis in control versus drug-treated conditions in response to 500  $\mu$ M of E-4031. (b) Single beat contractile motion comparison in control versus drug-treated conditions. (c) Motion waveforms of single CMs #1 to #4 extracted in the control conditions and (d) quantification result comparison at the single-cell level of the control conditions (blue points) versus drug-treated conditions (red points). e) Single CMs #1 to #4 extracted after 500- $\mu$ M E-4031 treatment. (f) Average of each quantification parameter for all extracted single cells in the control conditions (blue bars) versus drug-treated conditions (red bars). All comparisons were carried out using an unpaired student t-test ..... 49

Figure 2.23: The overview of the workflow for motion tracking of single cardiac cells and beating profile visualization using motion speed calculation. (a) cardiomyocytes phase image after numerical reconstruction with multiple cardiac cells. (b) single cardiac cell manually extracted with a size of 100 $\times$ 100 pixels. Consequently, 3D median filter with the size of 2 $\times$ 2 $\times$ 2 was applied for noise reduction, (c) optical flow procedure for cardiac cell's contractile motion speed measurement,(d)(e),(f) motion vectors supper imposed on cell's phase image for contraction, relaxation, and resting beating activity respectively and corresponding heatmap generated from absolute motion shown in the second row (The contractile center shown in warmer color on heat map refers to a region from which contractions are maximized),(g) beating activity profile of a single CM generated from cell's motion speed measurement..... 56

Figure 2.24: Representation of a single cardiac cell's motion waveform generated using contractile motion speed calculation and the definition of the multi-parameters. The inset shows details of



multi-parameters calculated from beating activity described in table 2.4 .....58

Figure 2.25: Representation of action potential motion speed evaluation of whole slide QPI in the presence of different drugs versus the control condition. The bar charts on the right side show the variation of a critical parameter expressed in terms of mean and SD for control and treated conditions. (a)The contractile motion of whole slide QPI of multiple CMS in control and drug-treated conditions in response to 200nM sertindole, (b) in response to 500µM E-4031, (c) in response to 500nM isoprenaline and their corresponding quantification results.....61

Figure 2.26: Multiple parameter measurements per each individual extracted cells in response to the sertindole with different concentrations. The corresponding effect of the drug by increasing the concentration on each cell's behavior was separately investigated .....64

Figure 2.27: Effect of sertindole on critical parameters of the average population of single cells. The graph shows a summary of the changes in the mean and standard deviation. The unpaired t-test was performed to detect significant differences between average groups .....64

Figure 2.28: Multiple parameter measurements per each extracted cells treated with different concentrations of isoprenaline drug. The effect of the drug by increasing the concentration on each cell behavior is investigated .....65

Figure 2.29: Characterization of the Effect of isoprenaline with different concentrations on critical parameters of the average population of single cells. The graph shows the changes in the mean and standard deviation of each quantification parameters calculated from the average of the single cells population. The unpaired T-test was performed .....66

Figure 2.30: Assessment of multiple parameters per each cardiac cells. The effect of the E-4031 different concentrations of the drug on each cardiomyocyte is shown .....67

Figure 2.31: Characterization of the effect of E-4031 with different concentrations on critical parameters of the average population of single cells. The graph shows a summary of the changes in mean and standard deviation calculated from the average of the single cells population.....68

Figure 2.32: The average resting period of single cells population in the presence of different drug

concentrations of E-4031, isoprenaline, and sertindole .....68

Figure 2.33. Steps of single CM dry mass extraction using a fully convolutional neural network. (a) original QPI of multiple CMs, (b) single CMs captured using the FCN model marked with the green line, inset shows a single CM dry mass denoted with a green line (top), 3D representation of single CM dry mass (bottom). ..... 75

Figure 2.34 The workflow of single CMs kinematic beating activity signal extraction. Single CM dry mass extracted using FCN method with superimposed motion vectors for contraction (a), relaxation (b), resting (c) (top) and their corresponding heat map (bottom), (d) Single CM’s contractile force profile, (e) single CM motion speed profile (f), motion acceleration profile, (g) motion velocity profile. . . ..... 76

Figure 2.35. Schematic of single cells kinematic signals quantification using contraction-relaxation peak identification method..... 78

Figure 2.36. Details of beating activity related temporal parameters quantification calculated from motion speed waveform explained in the table 2.7 ..... 79

Figure 2.37 Single CMs (#1 to #3) autonomous mechanics beating activity signals ..... 81

Figure 2.38. Single CM beating activity-related temporal parameter quantification results ..... 82

Figure. 2.39. Single CM kinetic beating activity quantification results..... 83

Figure. 2.40. Cardiomyocytes response to 166  $\mu\text{M}$ , 500  $\mu\text{M}$  of E-4031 drug kinetic force generation, and beating activity temporal parameters analysis in control (ctrl) versus drug-treated conditions. (a) whole-slide QPI contractile force profile in control versus drug-treated conditions in response 166  $\mu\text{M}$  , 500  $\mu\text{M}$  of E-4031(a ,b), (c) quantification results in comparison of the control conditions (blue bars) versus drug-treated conditions (red bars) ..... 84

Figure. 2.41. Cardiomyocytes response to 166 nM, 500 nM of isoprenaline drug kinematic force generation and beating activity temporal parameters analysis in control (ctrl) versus

drug-treated conditions. Whole-slide QPI contractile Force profile in control versus drug-treated conditions in response to 166 nM (a), 500 nM (b) of isoprenaline, (c) quantification result comparison of the control conditions (blue bars) versus drug-treated conditions (red bars) ..... 85

## Abbreviations

DHM: Digital Holographic Microscopy

CM: Cardiomyocytes

FFT: Fast Fourier Transform

FCN: Fully convolutional neural network

AP: Action Potential

MO: Microscope Objective

hiPSC-CMs: Human-induced pluripotent stem cell-derived cardiomyocytes

QP-DHM: Quantitative Phase Digital Holographic Microscopy

QPI: Quantitative Phase Images

2D: 2-dimensional

3D: 3-dimensional

4D: 4-dimensional

## Abstract

### **Automated Methods for Analysis of Stem Cell-derived Cardiomyocytes At the Single-Cell level With a Label-Free Digital Holographic Microscope**

By: Ezat Ahmadzadeh

Advisor: Shin Seokjoo

Department of Computer Engineering

Graduate School of Chosun University

Digital holographic microscopy (DHM) providing quantitative phase images (QPIs), is a promising tool in the field of label-free biological sample analysis. The QPIs obtained from DHM made it possible to study micrometer-sized living cells. The cell's dry mass can be monitored by DHM which provides a label-free QPI of living cells. Cardiomyocytes (CMs) are the main contractile elements of the heart leading to pump the blood to the entire body through the vessels by spontaneous contraction-relaxation cycle in a synchronized manner by electrical stimuli generated by pacemaker cells. Human-induced pluripotent stem cell-derived cardiomyocytes (hiPSC-CMs) are elastic elements used for human disease modeling, cardiotoxicity screening *in vitro*. The hiPSC-CMs are also been utilized for myocardium therapy due to the limitations of the heart cells for regeneration. There are crucial issues regarding stem cell therapy with the transfer and survival of the implanted stem cells in the myocardium. While CM spontaneous contraction-relaxation beating activity, the cell tissue frequently shortens and lengthens. The CM's proper functionality depends on fiber flexibility. While cardiac cell's beating activity, dry mass redistribution can be monitored with DHM.

In this dissertation, we report on different automated methods that allow us to study

single cardiomyocytes in a noninvasive manner. DHM is perfectly suited for single cardiac cell characterization by providing a quantitative time-lapse phase image. We have proposed several approaches for studying and analyzing single cardiomyocytes. Cardiomyocyte's nucleus section can efficiently reflect the beating pattern of single cells. Therefore, our single CM characterization approaches mainly performed using the cell's nucleus section. To this end, we extracted a single cardiomyocyte which mainly includes the nucleus section, and afterward, I proposed different computational algorithms for single CM motion characterization and the effects of pharmacological substances on single CM motion speed and different temporal parameters extraction. Furthermore, I proposed a method based on FCN and optical flow for Single CM contractile kinetics and force generation of a cardiac muscle cell using the ability of DHM in measuring single cells dry mass.

[KEYWORDS]: Human Cardiomyocytes analysis, Digital Holographic Microscopy, Single Cardiomyocytes Characterization, High content screening

## 초록

정량적 위상 이미지 (QPI)를 제공하는 디지털 홀로그래프 현미경 (DHM)은 라벨이없는 생물학적 샘플 분석 분야에서 유망한 도구입니다. DHM에서 얻은 QPI를 통해 마이크로 미터 크기의 살아있는 세포를 연구 할 수있었습니다. 세포의 건조 질량은 DHM에 의해 모니터링 될 수 있으며, 이는 살아있는 세포의 라벨이없는 QPI를 제공합니다. 심근 세포 (CM)는 심장 박동기 세포에 의해 생성 된 전기 자극에 의해 동기화 된 방식으로 자발적 수축-이완 사이클에 의해 혈관을 통해 혈관을 통해 전신으로 혈액을 펌핑하게하는 심장의 주요 수축성 요소이다. 인간-유도 다 능성 줄기 세포-유래 심근 세포 (hiPSC-CM)는 인간 질병 모델링, 시험 관내 심독성 스크리닝에 사용되는 탄성 요소이다. hiPSC-CM은 또한 재생을위한 심장 세포의 한계로 인해 심근 치료에 이용된다. 심근에서 이식 된 줄기 세포의 전달 및 생존에 관한 줄기 세포 치료에 관한 중요한 문제가있다. CM 자연 수축 이완 박동 활동 동안, 세포 조직은 종종 단축되고 연장된다. CM의 적절한 기능은 섬유 유연성에 달려 있습니다. 심장 세포의 박동 활동 동안 DHM을 사용하여 건조 대량 재분배를 모니터링 할 수 있습니다.

이 논문에서, 우리는 비 침습적 인 방식으로 단일 심근 세포를 연구 할 수 있도록하는 다른 자동화 된 방법에 대해보고합니다. DHM은 정량적 시간 경과 위상 이미지를 제공함으로써 단일 심장 세포 특성화에 완벽하게 적합합니다. 우리는 단일 심근 세포를 연구하고 분석하기위한 여러 가지 접근법을 제안했습니다. 심근 세포의 핵 섹션은 단일 세포의 박동 패턴을 효과적으로 반영 할 수 있습니다. 따라서 우리의 단일 CM 특성화 방법은 주로 세포의 핵 섹션을 사용하여 수행됩니다. 이를 위해, 우리는 주로 핵 섹션을 포함하는 단일 심근 세포를 추출한 후, 단일 CM 모션 특성화 및 단일 CM 모션 속도 및 다른 시간적 파라미터 추출에 대한 약리학 적 물질의 효과에 대한 상이한 계산

알고리즘을 제안 하였다. 또한, 단일 세포 건조 질량 측정을 측정하기 위한 DHM의 능력을 사용하여 단일 CM 수축 운동학 및 심장 근육 세포의 힘 생성을 위한 FCN 및 광학 흐름에 기초한 방법을 제안했습니다



# 1 Introduction

The main contractile elements of the human heart consist of cardiomyocytes (CMs) muscle cells that pump the blood to the body by spontaneous contraction–relaxation cycle in a coordinated manner [1]. Human-induced pluripotent stem cell-derived cardiomyocytes (hiPSC-CMs) are used for modeling human disease, cardiotoxicity, and therapy *in vitro* and stem cell therapy [2]. In the case of stem cell therapy, there are some issues including the transfer and survival of the implanted stem cells in the myocardium [3]. DHM has the capability of monitoring cell dry mass redistribution while spontaneous beating activity.

New drug development deals with many crucial issues most importantly it's adverse effects on the cardiovascular system. Therefore the drug's adverse effects on the cardiovascular system need to be investigated before releasing it to the market. Different methods have been proposed for CM characterization *in vitro* to reduce drug development costs with cardiotoxicity application including patch clamping [4, 5], calcium imaging [6, 7], and image processing-based contraction-relaxation studies [8, 9]. The mechanics-based methods are also extensively applied for CM characterization [10] which requires more expertise and costly equipment. Besides, the above-mentioned methods reported multiple CMs characterization methods while single CM characterization, not an easy undertaking. Therefore, it is crucial to need to conduct high throughput and reliable *in vitro* methods for single CM characterization. The hiPSC-CMs can be efficiently characterized solely by the nucleus section redistribution monitoring which provides less noisy and more informative rhythmic beating patterns for subsequent characterization. Therefore I proposed to divide the entire QPI image further into ROI (nucleus) and non-ROI which includes surrounding cytoplasm and membrane. CMs have different shapes, sizes, and orientations [11]. A deep learning-based method can extract discriminative features from the ROI considering sufficient training samples [12, 13]. Deep fully convolutional neural network (FCN)-based architectures have been successfully applied for the medical image segmentation field.

However, conventional deep learning-based methods cannot extract discriminative features when the target object and the other objects in the image are similar in terms of intensity, location, shape, and size. This phenomenon leads to the poor performance of the U-Net architecture one of the most popular deep learning models for medical image segmentation. Single CM characterization can be very helpful for cardiotoxicity screening and drug adverse effects on single cardiac cells.

The adverse effect of the drug on cardiac cells can cause a disturbance in cardiac cell's motion behavior. In the second study, we discuss the method for single cardiomyocyte's motion characterization. It has become increasingly important to develop high throughput, low-cost, and fully automated solutions to characterize hiPSC-CMs motion at a single-cell level without the need for manually tuning software parameters or physical or biochemical alternation in long-term monitoring. Finally, to simplify low-cost real-time monitoring of the hiPSC-CMs at the single-cell level, the algorithm must be fast without the need for parallel implementation. The state-of-the-art methods have mainly discussed cardiomyocytes motion tracking based on the block-matching methods.

Another problem CM motion characterization methods are that they are mainly based on image segmentation or block-matching technique that performs tracking by the search for the specific attributes of a moving group of pixels called macroblock including corners, edges. While a single cardiac cell's beating activity, cell shape undergoes large deformation which makes tracking a challenging task to find the best-matched block in the next video sequence frame. The Farneback dense optical flow method performs tracking by measuring the displacement of each pixel on the image [14,15] Furthermore, using the non-invasive property of DHM and optical flow-based analysis, cells remain intact for long-term monitoring. Using motion waveforms generated from the cell's contractile motion speed measurement, the cell's dynamic parameters including the contraction period, relaxation period, and resting period can be automatically quantified. Generally, video-based cardiomyocytes motion characterization methods have

several advantages over traditional methods for studying cell's functionality including the need for little training for personnel, no external hardware except the microscope while revealing information about actual biomechanical timing.

In the second study, we present a new and fully automated platform that performs real-time contractile motion characterization of CMs at the single-cell level using Farneback dense optical flow method and time-lapse QPI imaging. The proposed method overcomes the limitations of the current state-of-the-art methods. In our proposed schema first, we perform real-time motion tracking at the single-cell level using a Farneback dense optical flow method to measure contractile motion speed with individual pixel motion sensitivity. In this way, the cell's motion waveform is generated from dry mass redistribution during the autonomous cardiac activity. Then, we implemented a computational algorithm, to further characterize the dynamic nature of the cardiac contractile motions. The proposed method can detect high-resolution contractile centers. Since our assessment method is at the single-cell level, the CMs synchronization can be qualitatively assessed. To further demonstrate the power of the proposed method, we also applied several whole slides QPI of multiple cardiomyocytes for motion characterization and the generated motion waveform is quantified. The validation of the proposed CM characterization method is performed by the speed measurement of the fixed cardiomyocytes versus live cardiomyocytes. Besides, the impact of camera image accusation speed on the cardiac cell's motion speed estimation is assessed and the resulting beating profile for each camera frame rate is investigated. Furthermore, the noise sensitivity of the proposed method was examined by artificially adding different levels of noise to the image stacks and the impact on the resulting beating profile was quantified. We demonstrate the application of the proposed method for cardiotoxicity screening by analyzing the pharmacological effects of isoprenaline (166 nM) and E-4031 (500  $\mu$ M) on the response of a single CM's contractile speed in comparison to control conditions. The platform was validated by speed measurements of fixed cardiomyocytes versus live cardiomyocytes, single-CM synchronization testing, and a noise sensitivity analysis.

The third study subject discusses the developing method to alleviate the major concerns in the drug development process which is cardiotoxicity and the potential effect of candidate compounds on the cardiovascular function and precise risk measurement. The quantitative phase digital holographic microscopy (QP-DHM) provides high acquisition speed quantitative phase images of cell structure and dynamics in a label-free manner. DHM can provide accurate quantitative visualization of human cardiomyocytes derived from induced pluripotent stem cells (hiPSC-CMs) dynamics which are transparent or semi-transparent microscopic objects [15–23]. Hence, DHM is particularly effective to study CM's dynamics. As a result, significantly valuable information regarding the cell's dynamics of dry mass redistribution can be obtained in a label-free manner [24]. Drug attrition is one of the main contributors to the high expense of drug development. The Human induced pluripotent stem cell (hiPSC-CMs) technology, showed to be an alternative model for in vitro cardiotoxicity screening for new compounds human disease modeling, cardiotoxicity, and therapy in vitro [25, 26]. Due to the presence of different ion channels in cardiomyocytes, the sole reliance on cell line models, puts human lives at risk. Drugs that cause cardiac arrhythmia manifest by alternation in CMs physiological behaviors (dry mass redistribution) such as changes in the contraction-relaxation motion speed, beat frequency, contraction period, relaxation period and motion patterns of cardiomyocytes. Therefore, high throughput preclinical cardio-safety assessment methods for CM characterization in cardiotoxic screening are crucially in demand. Many authors have reported methods for CM characterizing for the whole slide of multiple cardiomyocytes analysis [4-10]. The proposed methods require expensive equipment or specific expertise which demonstrates the shortcomings of simplifying methods for CM motion characterization while they lack of single-cell level analysis. Optical flow-based real-time motion characterization methods are low-cost and high throughput methods capable of monitoring CM contractile activity without physical touching which maintains the sample's paradigm [27-31]. The above mentioned CM motion analysis methods are mainly based block-matching, image registration, and edge detection methods which are not accurate enough

for single CM motion characterization. The Farneback dense optical flow method performs tracking by measuring the displacement of each pixel on the image suitable for CM's contractile kinetic analysis at the single-cell level. Meanwhile, This approach allows evaluating the CM motion characterization at the single-cell level and further quantification of several parameters. We believe single CM kinetic quantification can provide valuable information about interpretation kinetics of single drug-treated CMs.

In our third study, we characterized single CM kinetics in control and drug-treated conditions using various concentrations by combining quantitative phase digital holographic microscopy (QP-DHM) with Farneback dense optical flow. The cardiomyocytes QPI was obtained using DHM and seven single CMs in the control and drug-treated conditions were manually extracted. Afterward, the Farneback dense optical flow method was applied to monitor the dynamic, rhythmic beating patterns and biomechanical contractile motion waveform was generated. The motion field was shown by motion vectors in a real-time manner. The system was able to sensitively and quantitatively detect the cardiac functional behavior treated with E-4031, isoprenaline, and sertindole in real-time. Following this, a computational algorithm was implemented to characterize the contractile motion of single cardiomyocytes from the motion waveform signal and multiple parameters related to the periodicity of CM's beating activity profile were measured. All quantification parameters such as (contraction motion speed, relaxation motion speed, contraction period, relaxation period, resting period) and their standard deviation were measured at the single-cell level and the population average was computed. Our results demonstrated the E-4031 compound declines the contraction-relaxation motion speed compared to control condition while isoprenaline increases the contraction-relaxation motion speed. The sertindole causes an increase in contraction motion speed while the relaxation motion speed is reduced compared to the control condition. Overall, the sensitivity of the proposed method to effectively detect the periodicity of the beating profile makes the proposed method well suited for the early preclinical safety assessment of cardiotoxic compounds.

In my fourth study I present a novel contactless and low cost *in vitro* platform allowing us simultaneous monitoring of the cardiac mechanical beating activity and force generation at the single-cell level from digital holographic imaging informatics. Our proposed method is a combination of the fully convolutional neural network and optical flow method which can return functional parameters for *in vitro* single CM motion and force generation analysis simultaneously. In the first step, we extracted single cardiac cells and removed the unnecessary background using a fully convolutional neural network. Secondly, we tracked the spatial-temporal coordinates  $x, y$  of the cell dry mass while beating activity using the Farneback optical flow method. This allowed us to monitor contractile force along with multiple parameters related to dynamic beating activity of the cell (contractile force, speed, velocity, acceleration, contraction period, relaxation period, resting period, beating period). The applicability of CM contractile kinetics and force generation of the proposed method was tested to reveal the pharmacological effects of two cardiovascular drugs, isoprenaline (166nM, 500nM) and E-4031 (166  $\mu$ M, 500 $\mu$ M), on whole slide QPI of multiple cardiomyocytes compared to the control condition. Validation of our approach was tested by measuring the contractile force generation of live cardiomyocytes versus fixed cardiomyocytes.

## A. Motivations

The cardiomyocytes are transparent or semi-transparent. Therefore the DHM technique is suitable to study these cells by providing quantitative 3D visualization of the cardiomyocytes cells which cant be provided by conventional 2D microscopy. By using quantitative phase images one can monitor dry mass redistribution of the cardiac cells without labeling and destruction of the cell structure. Therefore it can be used for real-time monitoring of the cell activity in sensitive cells while preserving the shape and structure. The labeling techniques such as labeling can

change the nature of the cells and consequently change the results. Besides, the quantitative phase images provided by the DHM technique can provide the 3D measurement of cell structure the different cells such volume, project surface area, and biological cells. The DHM capability of non-invasive visualization of cell structure has been utilized for studying different types of cells like (protozoa, bacteria, plant cells, blood cells, nerve cells, or stem cells).

Overall, the motivations can be listed as below:

- 1- DHM can provide a quantitative phase image to study transparent or semitransparent cells.
- 2- It is non-invasive thus the cell's original shape will be preserved.
- 3- It is label-free thus cells are not treated by a material.
- 4- It uses weak leaser source so the original shape of the cell is not changed.
- 5- It can provide a 3-dimensional cell structure.
- 6- It can provide time-lapses imaging (4D- imaging) suitable for studying cardiomyocytes beating activity over time.

## **B. Objectives of Research**

The objectives of this researchs are to find automated methods for analyzing stem cells-derived cardiomyocytes characteristics at the single-cell level. Also, monitoring the functional behavior of CMs over time, for example, dynamic and motion characterization of the single cardiac cells as a function of time is possible by DHM.

The objectives can be listed as:

- To study the automated method for single cardiomyocytes characterization.
- To study automated methods for motion characterization of single cardiomyocytes.
- To study automated methods for motion characterization of single drug-treated cardiomyocytes according to the abilities of DHM.
- To study the automated methods to analyze the contractile kinetics and force generation of single drug-treated cardiomyocytes according to the DHM's

abilities.

## **C. Organization of the Research**

The organization of this thesis is as follows. Chapter 2 gives an overview of the digital holographic microscopy method for cardiomyocytes study and 4 reports on the automated methods for studying the dynamic characterization of the single stem cell-derived using the ability of the DHM technique. Chapter 3 provides concluding remarks and future research opportunities. Chapter 4 reports on the references used in this research.



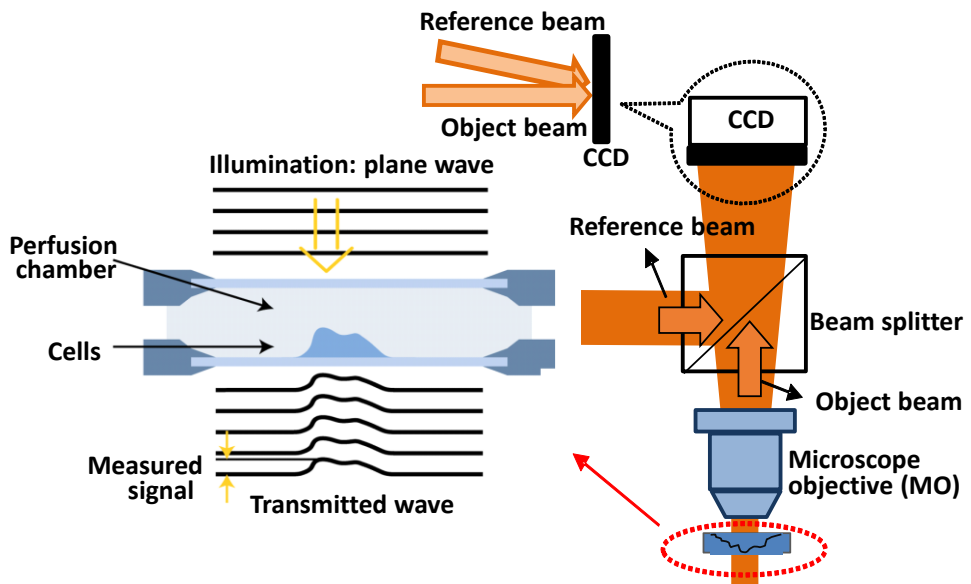


Figure 1.1: Schematic representation of a Digital Holographic Microscope.

## 2 The study of Stem Cell-derived Cardiomyocytes by digital holographic microscopy technique

The off-axis DHM is used to obtain the phase image of CMs in this research. In the off-axis configuration, the laser source is divided into an object and reference beams (see Fig.2 1). The microscope objective (MO) magnifies the object wave and CCD camera records the hologram generated by the interference of the magnified object wave (O) and the reference wave (R) incident at a small angle “ $\theta$ ” to provide the off-axis property. Figure 2.2 (a) shows the recorded hologram of CMs, which can be expressed as the sum of four terms:

$$I_H(x, y) = |R|^2 + |O|^2 + R^*O + RO^*, \quad (1)$$

where  $|R|^2$  is the intensity of the reference wave and  $|O|^2$  is that of the object wave.  $R^*$  and  $O^*$  denote the complex conjugates of the two waves. Since hologram is recorded in off-axis configuration, the Fourier transform of the hologram can separately represent bandwidth of real image, virtual image, and zero-order noise as shown in (see Fig. 2.2 (b)). To separate the real image from the twin image and zero-order noise, a spatial filter in the frequency domain is designed. This filter can only preserve the bandwidth of the real image and eliminates the unwanted bandwidth (see Fig. 2.2 (c)). Finally, a hologram is reconstructed (see Fig. 2.2 (d)) by illuminating it with a replica of the plane reference wave (RD):

$$R_D(k, l) = A_R \exp \left[ i \left( \frac{2\pi}{\lambda} \right) (k_x k \Delta x + k_y l \Delta y) \right], \quad (2)$$

where  $A_R$  is the amplitude of the reference wave,  $\lambda$  is the wavelength of the illumination light,  $\Delta x$  and  $\Delta y$  are the sampling intervals in the hologram plane,  $k$ , and  $l$  are integers and  $k_x$  and  $k_y$  are wave vectors. The reconstruction in the observation plane is obtained by a numerical

calculation of scalar diffraction in the Fresnel approximation, which is expressed as:

$$\Psi(m,n) = \frac{\exp(i2\pi d/\lambda)}{(i\lambda d)} \Phi(m,n) \exp\left[\frac{i\pi}{\lambda d}(m^2\Delta\xi^2 + n^2\Delta\eta^2)\right] \times \text{FFT}\left\{R_D(k,l)I_H^F(k,l) \times \exp\left[\frac{i\pi}{\lambda d}(k^2\Delta x^2 + l^2\Delta y^2)\right]\right\}_{m,n}, \quad (3)$$

where  $d$  is the distance between both planes,  $k, l, m,$  and  $n$  are integers ( $-N/2 \leq k, l, m, n \leq N/2$ ;  $N \times N$  is the number of pixels in the CCD camera),  $\Delta\xi = \lambda d / N\Delta x$  and  $\Delta\eta = \lambda d / N\Delta y$  are the sampling intervals in the observation plane,  $\text{FFT}$  is the fast Fourier transform.  $I_H^F$  is the filtered hologram, and  $\Phi(m,n)$  is the digital phase mask to compensate for the phase aberrations caused by the MO calculated by:

$$\Phi(m,n) = \exp\left[\frac{-i\pi}{\lambda D}(m^2\Delta\xi^2 + n^2\Delta\eta^2)\right], \quad (4)$$

A fine adjustment of “ $D$ ” can be performed in the absence of fringes by removing the reconstructed phase distribution in some area of the image where a constant phase is presumed [32,33]. “ $D$ ” must be set to counterbalance the wave-front curvature according to the distance between MO and specimen, and MO and the image plane evaluated by:

$$\frac{1}{D} = \frac{1}{d_i} \left(1 + \frac{d_o}{d_i}\right), \quad (5)$$

Where  $d_i$  is the distance between MO and image plane and  $d_o$  is the distance between the specimen and MO. The phase image (see Figure 2 (e)) is obtained by the argument of:

$$\phi(m,n) = \tan^{-1} \left\{ \frac{\text{Im}[\Psi(m,n)]}{\text{Re}[\Psi(m,n)]} \right\}, \quad (6)$$

The resulted phase values are between  $-\pi$  and  $+\pi$ ; thus, the result is given by modulo  $2\pi$  and sometimes discontinuities with values near  $2\pi$  appear. Phase unwrapping operation converts

the undesired phase values into desired ones by adding or subtracting  $2\pi$  from the pixel value. The optical path difference (OPD) and phase values are exchangeable, and are obtained by the following equation:

$$OPD(x, y) = \frac{\lambda \times \phi(x, y)}{2\pi}, \quad (7)$$

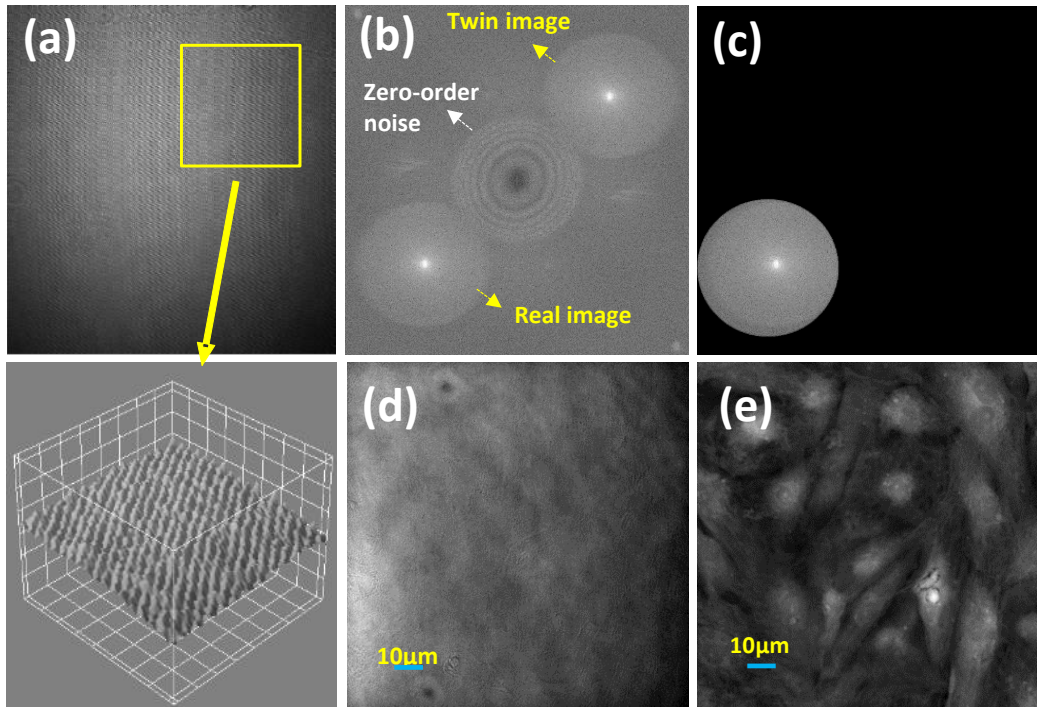


Figure 2. (a) A recorded hologram (a three-dimensional (3D) section of the hologram is shown in the inset). (b) the main three bandwidths of the hologram are separated using fourior transform. (c) a spatial filter is used to filter out the real image bandwidth and remove the other bandwidths. (d) shows the numerical reconstruction of the hologram which gives the amplitude image and (e) phase image after the phase unwarping.

## **A. Automated single cardiomyocyte characterization by nucleus extraction from dynamic holographic images using fully convolutional neural network**

### **a. Abstract:**

The time-lapse quantitative images (QPIs) obtained from digital holographic microscopy (DHM) can be validly used for characterizing human-induced pluripotent stem cell-derived cardiomyocytes (hiPSC-CMs) beating activity. The CM's nucleus section can precisely reflect the associated rhythmic beating pattern of the CM suitable for subsequent beating pattern characterization. In our first study, we describe an automated method to characterize single CMs by nucleus extraction from QPIs and subsequent beating pattern reconstruction and quantification. However, accurate CM's nucleus extraction from the QPIs is a challenging task due to the variations in shape, size, orientation, and lack of special geometry. In this study, we proposed a new fully convolutional neural network (FCN)-based network architecture for accurate CM's nucleus extraction using pixel classification techniques. Afterward, the beating activity of every single cell was reconstructed using the extracted nucleus section for subsequent characterization. The results show that the beating profile extracted from the CM's nucleus section is less noisy and more informative compared whole image slide. In this way, the CMs can be characterized at the single-cell level. Consequently, we extracted multiple single CMs from the whole slide QPIs and the beating profile of every single CM was characterized.

## b. Motivations and introduction:

Accurate ROI determination is a crucial task. To this end, we carried out the dynamic beating activity comparison between the ROI and non-ROI. Figure 2.3 shows the overall schema of the beating profile comparison of the ROI against the non-ROI section. Figure 2.3(a) shows the QPI image of multiple CMs obtained from DHM. The beating activity comparison result is shown in Fig. 2.3:(b). The QPIs in this study are related to the optical path difference (OPD). The beating profile was reconstructed using the spatial variance between two consecutive QPI images proposed in [17]. The OPD variance reflects the CMs beating activity of the cell dry mass redistribution occurring while the spontaneous contraction-relaxation. Since the OPD value of the ROI is much higher than the non-ROI, the OPD variance in the ROI can precisely reflect beating activity. No beating activity is observed in the non-ROI section.

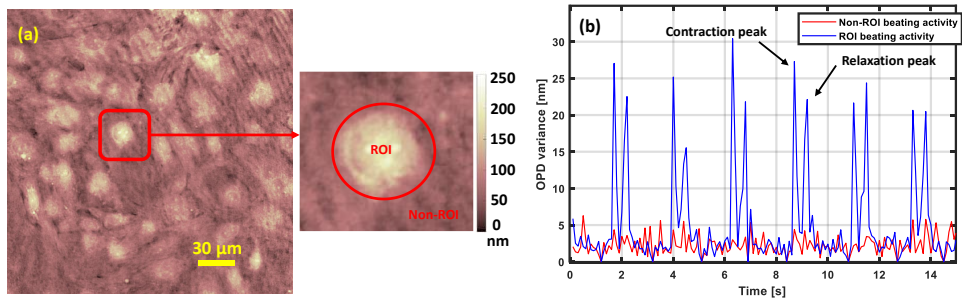


Figure 2.3: (a) QPIs of multiple CMs obtained from digital holographic microscopy, (b) beating activity comparison of the ROI against Non-ROI. The inset shows the marked with the red line.

### c. Cardiomyocytes preparations

Human-induced pluripotent stem (iPS) cell-derived CM obtained from Cellular Dynamics Int. (Madison, WI) were cultured and grown according to the manufacturer's instructions for 14 days before recording the hologram. Measurements were acquired in a Chambridge WP incubator system with a 96-well plate (LCI, South Korea) set at 37°/5% CO<sub>2</sub> with high humidity. Images were recorded by a commercially available DHM T-1001 from LynceeTec SA (Lausanne, Switzerland) equipped with a motorized stage (Märzhäuser Wetzlar GmbH & Co. KG, Wetzlar, Germany, ref. S429). Images were obtained using a Leica 20×/0.4NA objective (Leica Microsystems GmbH, Wetzlar, Germany, ref. 11566049). The CCD resolution is 1920 ×1200 pixel (the hologram size is 1024×1024 efficient for FFT computation). The phase stability of imaging system is around  $\Delta\varphi=0.05^\circ$ , which in studying the biological samples with limited reflective index is equivalent to a thickness of several nanometers. The 666nm laser source delivered intensity of ~200W/cm<sup>2</sup> to the specimen plane, which is nearly six orders of magnitude less light, and the required exposure time was only 0.4ms. 540 holograms were recorded at a sampling frequency of 10Hz.

#### **d. Results and discussions:**

Deep learning methods have many applications in medical image analysis especially for medical image segmentation [35, 36]. Convolutional neural networks are a type of deep learning methods based on the sequential application of the convolutional layer. In CNN consists of a sequential application of the convolution layers. Each convolutional layer provides one feature hierarchies at a specific level. A convolution filter is formed by shared weights to the same output. In CNN's the layer weights and biases are randomly initialized. CNN captures features of input data via multiple consecutive convolution kernels followed by max-pooling layers for data dimension reduction. CNN mainly comprises three main elements as follows. 1) A set of learnable filters namely convolutional layers to extract local and global features from the image. 2) an activation function and 3) a max-pooling layer that combines the local feature specification to reduce the data dimensions. The max-pooling operation used for the down-sampling purpose which obtains the maximum value of each filter in the convolution layer. The summation of each convolution layer is applied to a nonlinear function named as a rectified linear unit (ReLU) as an activation function. The ReLU function is a nonlinear function applied to increase the nonlinearity of the CNN feature maps. A fully convolutional neural network (FCN) is a type of CNN in which the last layer of the CNN namely fully connected layer is replaced with another convolution layer [37].



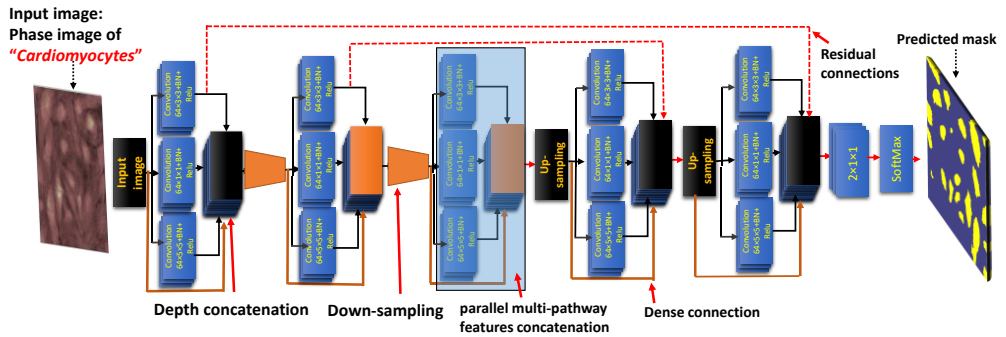


Figure 2.4: The proposed FCN network architecture for cardiac cells nucleus section extraction consists of the following elements: Parallel multi-pathway features concatenation (blue box) consists of different kernel sizes:  $1 \times 1$ ,  $3 \times 3$ , and  $5 \times 5$ . made up of a convolutional layer + batch normalization layer (BN) + rectified linear unit (Relu). max-pooling layer size is  $2 \times 2$  with a stride of two. The dense connection technique is used for efficient gradient propagation along with residual connections that are denoted with dotted red arrows.

### ***Proposed network model***

The proposed FCN based method consists of the following elements fo CMs nucleus section extraction. The proposed FCN architecture consists of parallel multi-pathways features concatenation with dense connection blocks and residual connections [38]. The overall structure and building blocks of the proposed network architecture are shown in Figure 2.4. The overall network structure leads to a better training performance when compared to the U-Net model meanwhile it improves the pixel classification accuracy. The proposed FCN-based network model’s building blocks are briefly explained below:

### ***Parallel multi-pathways features concatenation***

In multi-pathways features concatenation technique, different feature maps extracted by various kernel sizes are concatenated. The commonly used convolutional kernel size is  $3 \times 3$ . But its challenging to determine the best kernel size for the task in hand. Therefore, we have used different kernel sizes in parallel with the sizes of  $1 \times 1$ ,  $3 \times 3$ , and  $5 \times 5$  followed by batch normalization (BN) and rectified linear unit (ReLU) Followed by feature concatenation at the end. Max-pooling layer with the size of  $(2 \times 2)$  with a stride of 2 have been utilized to reduce the data dimension.

### ***Dense connection***

In our proposed method we used dense connection blocks explained in [39]. Within each dense block, layers are directly connected with their preceding layers, which is implemented via the concatenation of feature maps in subsequent layers. The major advantages of dense connection blocks can be mentioned as efficient gradient propagation to prevent vanishing gradient occurs in deep networks and reuse of the feature extracted in previous layers instead of relying only on the features from the last layer. This technique results in better network performance.

### ***Residual connection***

Residual connection technique is to utilize skip connections, or short-cuts to jump over some layers that facilitate the training of deep networks [40, 41]. The shorter connection between layers close to the output and input yields better performance, reduces the number of parameters, and easier to train. The max-pooling operations in convolutional neural networks may cause to lose some crucial spatial information on the image. These skip connections retrieve the lost spatial information inside the consecutive spatial information. We proposed to use the skip connections in our proposed model. In our proposed schema the output of the standard  $3 \times 3$  convolutional layer prior to the pooling operation is connected to the corresponding output in the up-sampling section.

### ***Patch extraction***

For better training of deep learning-based methods having a large dataset is crucial. In the case of cardiac cells it is crucial to make such a big dataset. To create sufficient samples, we proposed to extract patches from the original image. The proposed patch extraction method, significantly increase the number of samples to a sufficient level for training of FCN-based deep learning models. The sliding window method has been utilized for patch extraction of the QPI containing multiple CMs and capturing patches along with corresponding ground truth (manually extracted). The extracted patches are with a size of  $32 \times 32$  pixels in a non-overlapping manner. Figure 2.5 shows the patch extraction method using the sliding window technique.

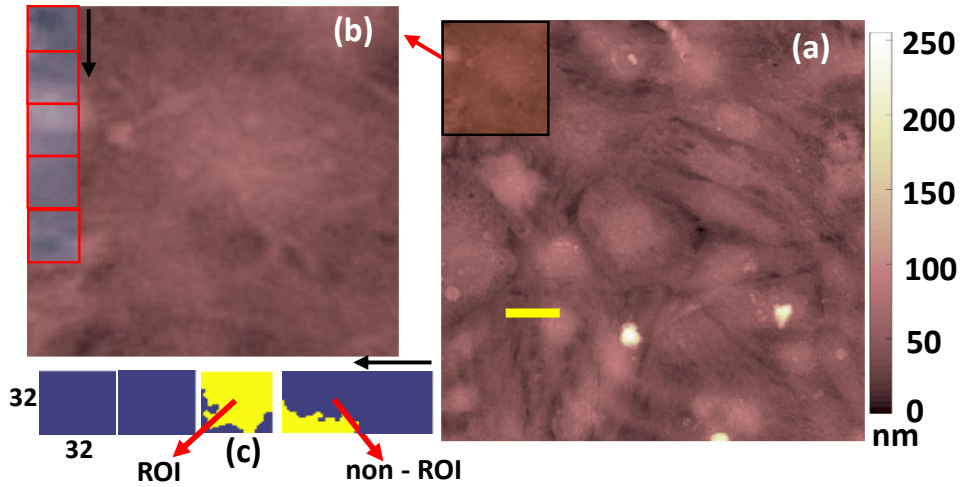


Figure 2.5: (a) the quantitative phase image of CMs (yellow bar denotes 20µm). (b) a portion of the original phase image is magnified to indicate patches. (c) Corresponding ground truth patches with denoted ROI shown in yellow color and non-ROI dark blue color portions.

After we manually annotated the ground truth image, we trained the proposed network by using the training dataset images (generated by patch extraction method) and their corresponding ground truth labels. The total extracted patch was 2500 along with corresponding ground truth. The training dataset 80% of the whole dataset ( $n = 2000$ ) and 20% ( $n = 500$ ) is used as a test dataset.

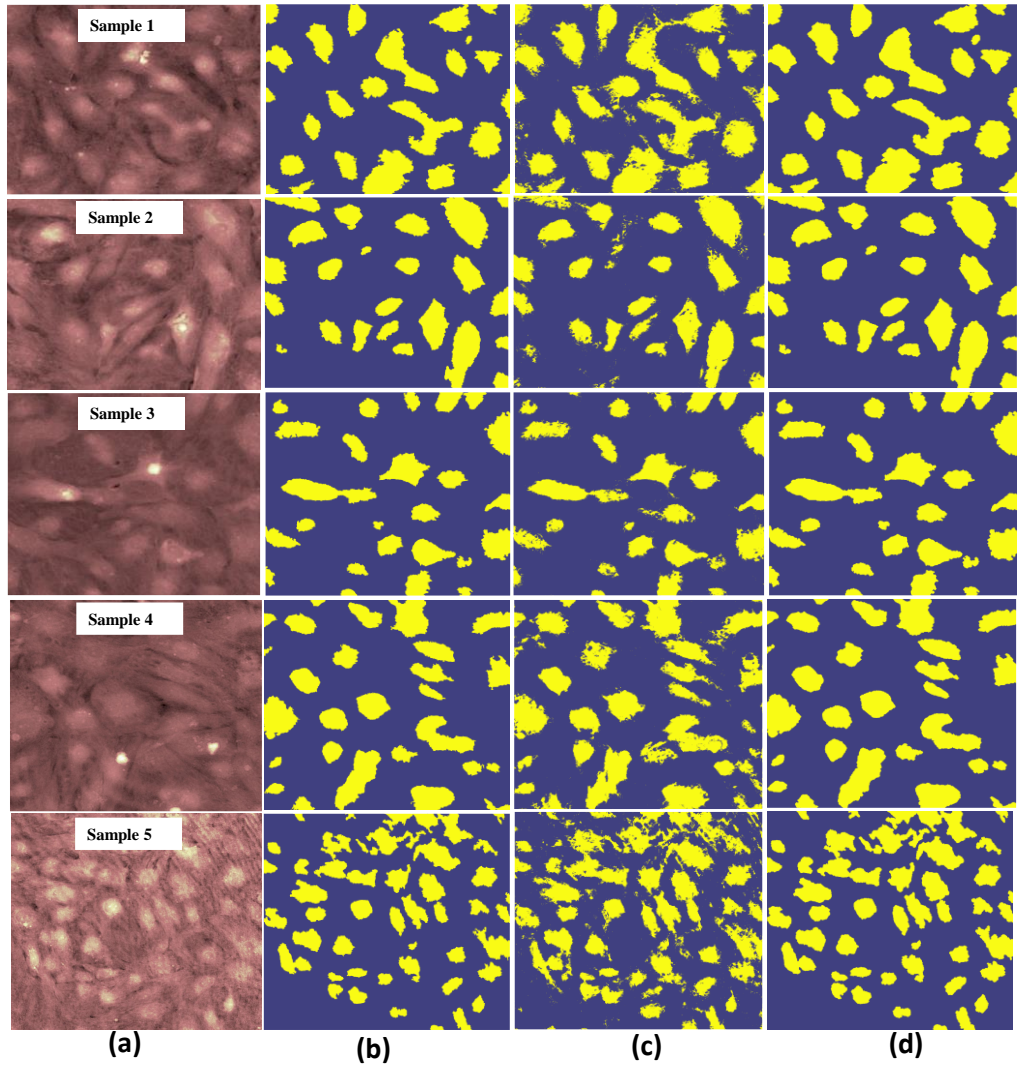


Figure 2.6: Results of the CM's nucleus extraction using the proposed FCN-based method in comparison with the U-Net network model. (a) Original phase image of multiple cardiac cells obtained by DHM. (b) Predicted mask using our trained FCN-based model. (c) The results of the U-Net network model. (d) Ground truth mask extracted manually.

The experimental result using the test image after training of the proposed network model for cardiac cells nucleus extraction containing multiple cardiac cells (see Figure. 2.6(a)). The visual evaluation of network performance predicted masks using the proposed network model and predicted mask by the U-Net network model are shown in Fig. 2.6 (b), (c), respectively. The ground truth mask is shown in Fig. 2.6 (d). The experimental results show that the predicted mask by the U-Net is highly over and under segmentation.

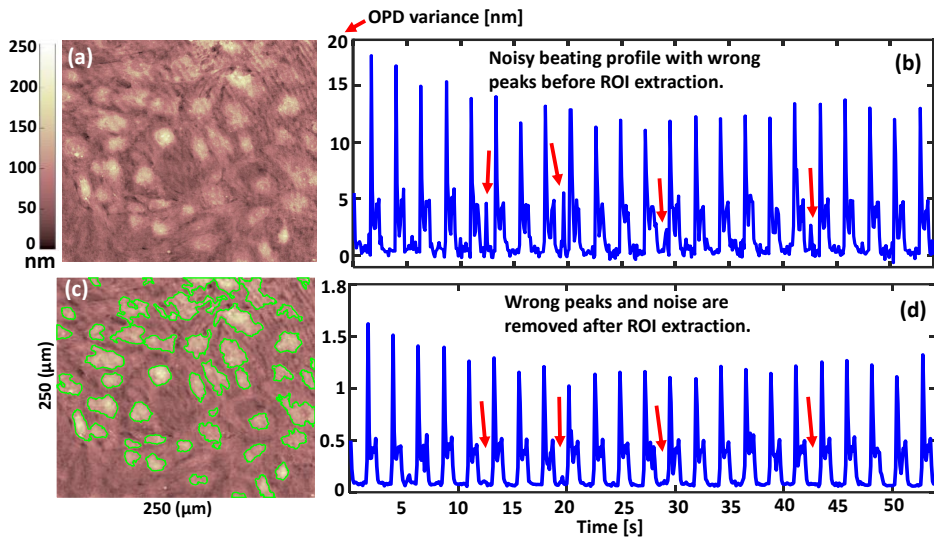


Figure 2.7: the whole-slide QPI of multiple CMs beating profile reconstruction before and after nucleus extraction. (a) and (b) QPI multiple CMs before the nucleus extraction and corresponding beating activity profile respectively. (c) and (d) the QPI after the nucleus extraction using the proposed method marked with green line and corresponding beating activity profile.

### ***Single cardiomyocytes beating profile quantification***

Our proposed approach includes two main steps. In the first step of our proposed method, a single cardiac cell nucleus section was extracted and the resulting mask image is multiplied by each QPI image in the sequence. secondly, in our proposed approach we reconstructed a single CM beating profile by calculation of the spatial variance between two consecutive image frames explained in [42]. Using our proposed approach, we can reconstruct beating profile using this parameter which is sensitive to the redistribution of dry mass within cardiomyocytes to monitor the characteristics of the cardio beating over time using the following equation:

$$opd_{var} = \text{var}[opd_i - opd_{i-1}], \quad (8)$$

where  $opd_i$  and  $opd_{i-1}$  are the  $i$ th and  $i-1$ th images. Specifically,  $opdvar$  ( $OPD$  variance) reflects the time course of the cell dry mass redistribution while CM beating activity. The  $opdvar$  signal reflects the beating activity signal of the single CM and yields information about AP durations. After a single CM beating activity extraction, we can measure multiple different parameters regarding every single CM's beating profile. Descriptions of quantification parameters are explained in Table 2.1.

Table 2.1: Description of cardiomyocyte dynamic parameter quantification.

	Parameters	Description
Contraction	Beat rate	The total number of contraction peaks in one minute (number of red points in Fig. 2.8(b)).
	Beating interval AVG [see #1 in Fig. 2.8(c)]	The time between two adjacent contraction peaks.
	Contraction period AVG [see #2 in Fig. 2.8(c)]	The average time between the Start-of-Contraction and End-of-Contraction points.
	Contraction period STD	The standard deviation of the contraction beating period.
Relaxation	Relaxation period AVG [see #3 in Fig. 2.8(c)]	The average time between Start-of-Relaxation to the End-of-Relaxation points.
	Relaxation period STD	The standard deviation of the
Resting	Resting period AVG	The average time between the End-of-
	Resting period STD	The standard deviation of the resting

To evaluate the accuracy of the proposed method for single CM beating activity characterization, we extracted six individual cells from the whole slide QPI of cardiomyocyte (see Figure 2.8(a)) and the corresponding beating profile was reconstructed using from Eq. (8) (see Fig.2.8(b)). Afterward, multiple parameters regarding every single CM's beating activity profile was measured.



For single CMs beating activity quantification using the nucleus section extraction, we need to detect two main peaks of the contraction and relaxation. To this end, we used the Otsu thresholding method. In most of the cases, the contraction peak has a higher amplitude value than the relaxation peak. Therefore first peaks which in most cases have a larger amplitude value stands for contraction and the relaxation peak is the second peak. Afterward, three auxiliary points 1) Start-of-Contraction, 2) End-of-Contraction, and 3) End-of-Relaxation shown in Fig 2.8(c) are defined using contraction and relaxation peaks. Locating the auxiliary points are found as follows: the End-of-Contraction point (Start-of-Relaxation) (see Fig 2.8(c) blue color points) is obtained by finding the smallest amplitude value between contraction and corresponding relaxation peaks. The Start-of-Contraction point and the End-of-Relaxation are detected using a search strategy around the contraction and relaxation peaks. Then the time difference between End-of-Contraction (Start-of-Relaxation) and End-of-Relaxation is considered a relaxation period. The time difference between Start-of-Contraction and corresponding End-of-Contraction point specifies the contraction period. The time difference between two consecutive contraction peaks determines the beating intervals. The resting period is the time difference between End-of-Relaxation and the next Start-of-Contraction point. The extracted features of the beating profile and the corresponding descriptions are presented in Table 2. 1

The beating activity profile reconstructed from cells #1, cell #2, cell #3, cells #4, cell #5, and cell #6 with detected contraction and relaxation peaks and auxiliary point for precise single CM characterization are shown in figure 2:9.

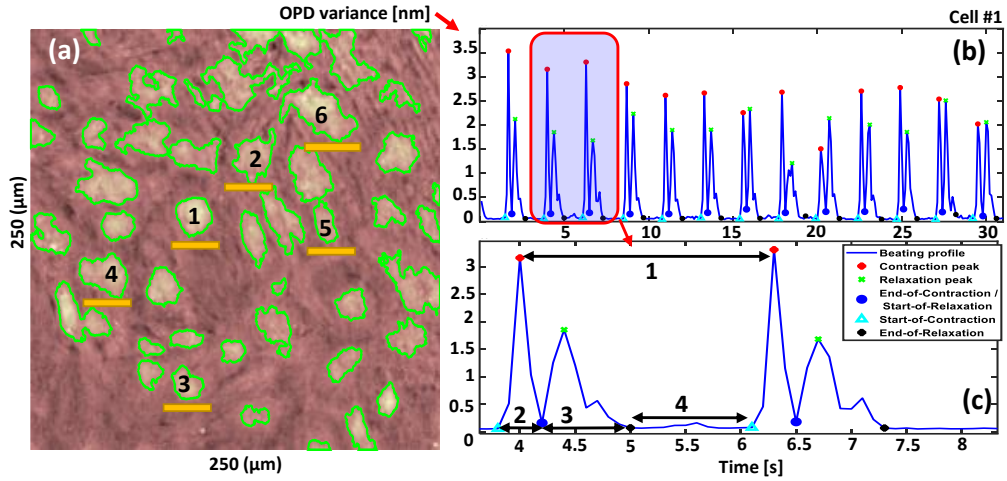


Figure 2.8: The quantitative phase image of multiple CMs in which single CMs are marked to be extracted for further quantification. (b) the corresponding beating profile of single CMs #1 to #6, (c) details on quantification parameters of single CM beating profile.

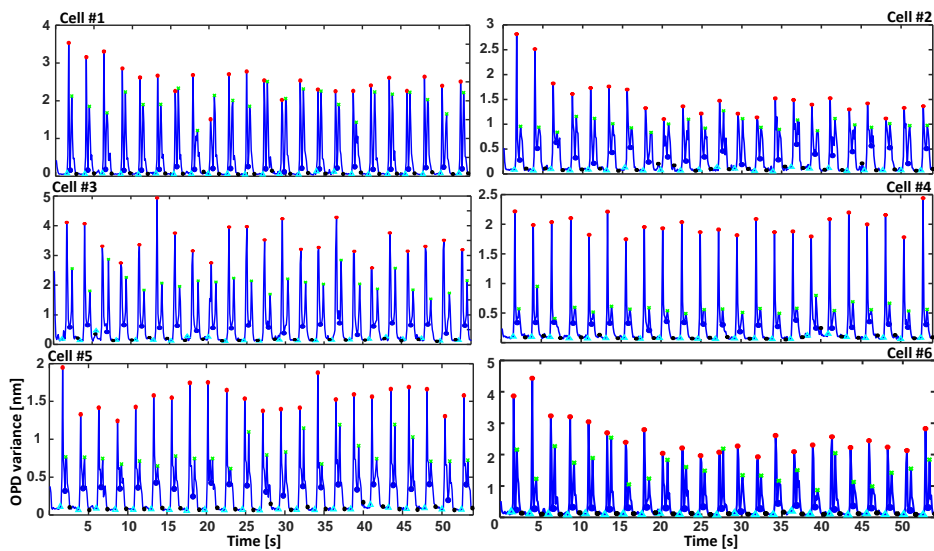
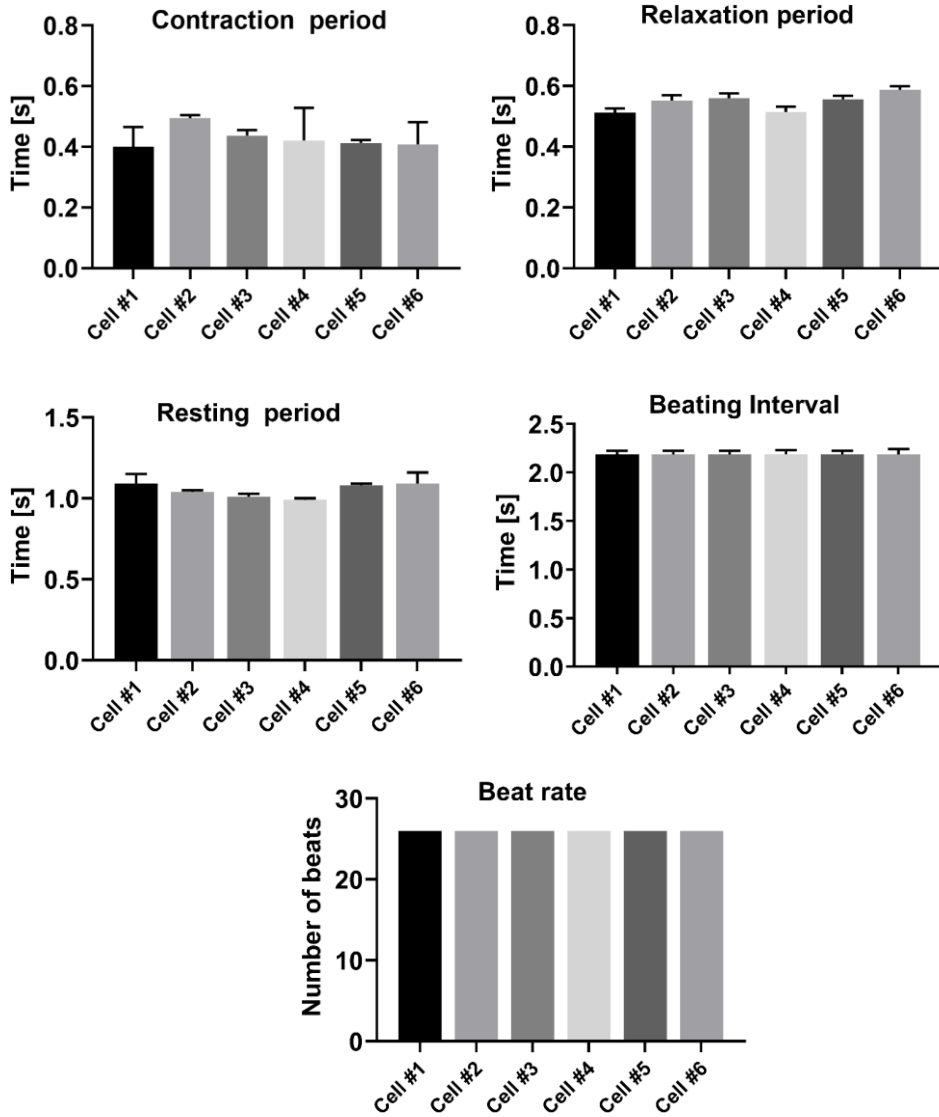


Figure 2.9: Single CMs beating profile (#1- #6). The sampling frequency was 10Hz.



2.10: the beating activity temporal parameter quantification results.

We evaluated the proposed's method training performance by the learning curve evaluation and the corresponding loss compared with the U-Net model (see Figure 2.11(a), (b)). As shown in Figure 2.11(c), the classification accuracy rate using the proposed FCN-based method 99.76% and 99.28%, respectively while the same evaluation for the U-Net model shows 93.69% and 91.25% accuracy (see Figure 11(d)). Besides, we evaluated the segmentation performance of the proposed method against the U-Net model from the statistics point of view. The proposed method's performance was evaluated for each of the whole slide images separately. The Dice similarity coefficient analysis was performed and the experimental results in comparison with the U-Net model are shown in Table 2.2. The Dice coefficient is calculated using the following equation:

$$DSC = \frac{2TP}{FP + 2TP + FN}, \quad (9)$$

where  $TP$ ,  $FP$ , and  $FN$  denote the numbers of true positive, false positive, and false negative respectively.

Table 2.2: The Dice coefficient analysis of the proposed method against the U-Net model.

Samples number	Dice (%)	
	Proposed FCN	U-Net model
Sample #1	96	88
Sample #2	95	89
Sample #3	94	88
Sample #4	96	87
Sample #5	97	88

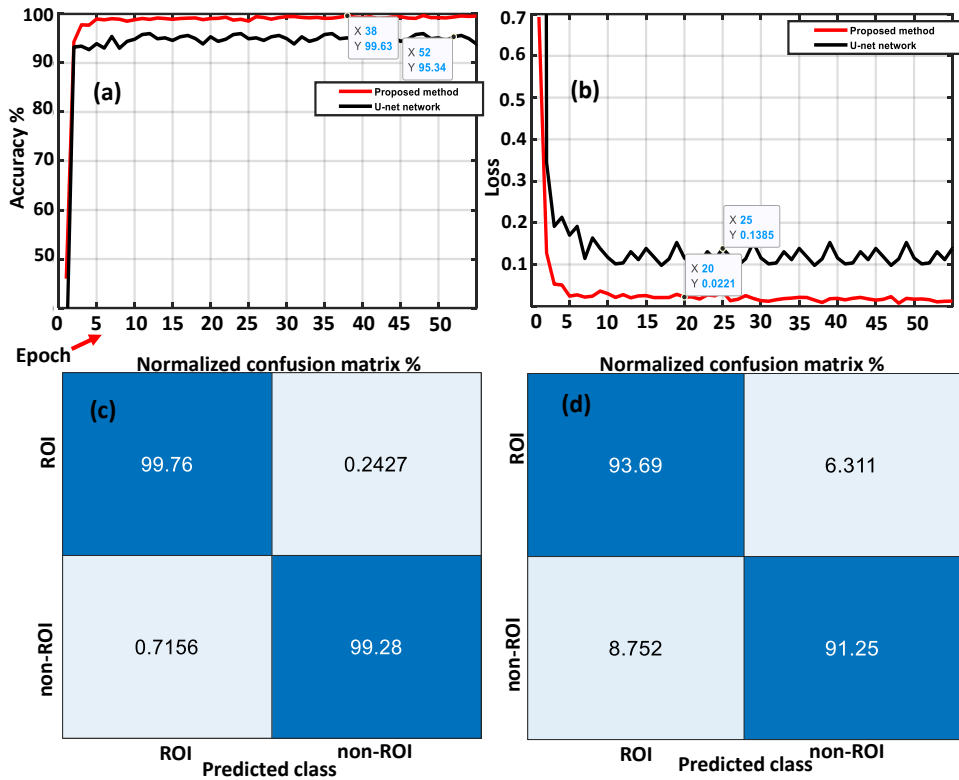


Figure 2.11: The learning curves and confusion matrix of pixel classification using the proposed FCN-based model versus the U-Net model. (a) and (b) the learning curve of the proposed FCN Model in comparison with the U-Net model and corresponding loss curves respectively. (c) Confusion matrix for pixel classification of the proposed model. (d) Confusion matrix for pixel classification of the U-Net model.

### ***Proposed method validation***

To validate whether the segmentation area includes nuclei, one sample is stained with Hoechst dye. We applied our segmentation method before and after nuclei staining and ROI and non-ROI sections are marked for the visual comparison. As one can see from Figure. 2.12, the ROI section mainly includes the nuclei section (nuclei is marked in blue color).

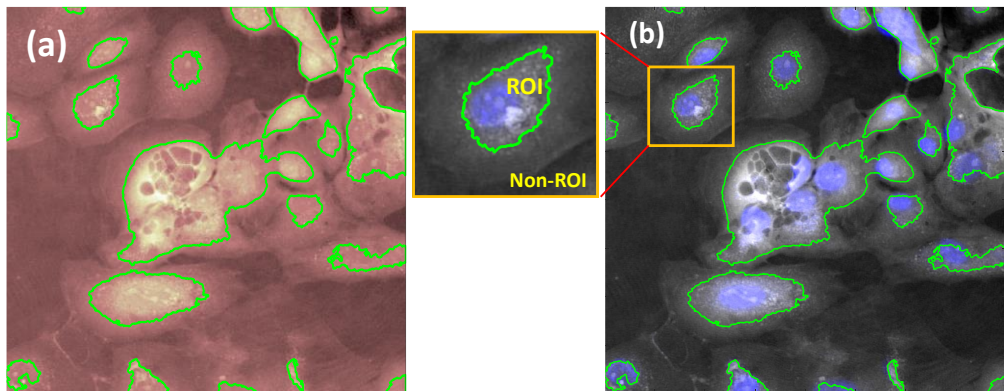


Figure 2.12: the ROI marked with green line on the original QPI before Hoechst nuclear staining, (b) The original QPI with nuclei section stained using the Hoechst nuclear staining method overlaid on the segmented image. The segmented sections are mostly included nuclei

### ***Discussion***

The CM characterization at the single-cell level is crucially important for *in vitro* drug compound testing and cardiotoxicity screening. The single CM's beating activity can efficiently

be characterized solely by the nucleus section redistribution monitoring. In this project, I proposed a single CM characterization method using nucleus extraction. In this schema, I considered the CM's nucleus section as the (ROI) surrounding cytoplasm and membrane were considered as non-ROI. The beating activity profile of every single CM was reconstructed using the OPD variance calculation between the successive QPI frames.

The experimental results show that the CM beating profile reconstructed from the extracted nucleus is less noisy and more informative for further characterization. On the other hand, the OPD variance in the non-ROI section leads to create a noisy beating profile with multiple wrong peaks causing difficulties for further CM characterization. Due to the specific attributes of the nucleus section, we proposed a novel FCN-based method for nucleus extraction combined with further analysis which allows cardiac cell characterization at single-cell levels. The proposed platform can be integrated into other technologies for precise single CM characterization. The proposed FCN-based architecture showed a better segmentation performance when compared to the one of the popular deep learning-based biomedical image segmentation U-Net model. To further examine the potential of the proposed method, we extracted multiple isolated CMs from segmentation results and multiple parameters regarding the beating profile of every single cell are measured.

### e. Conclusion

In this study, a single CM's beating activity profile was characterized using nucleus extraction. In this schema, I have proposed an automated FCN-based platform for CM's nucleus extraction. After single CM's nucleus extraction, the beating activity profile of the single CM was reconstructed using OPD variance calculation between successive image frames. Afterward, a computational algorithm was used to characterize beating activity profile and multiple parameters regarding the beating activity profile of every single CM was extracted including ( beating period, contraction period, relaxation period, resting period ). The experimental results demonstrated that the cardiac cell nucleus section (referred to as ROI) from QPI can effectively reflect the beating pattern suitable for CM characterization at the single-cell level. We proposed a novel FCN-based method to discriminate CM's nucleus section from other sections of cardiac cells using pixel classification techniques. The predicted mask is used for further characterization of dynamic contraction-relaxation of single CM. We evaluated the proposed model's segmentation mask prediction using pixel classification accuracy along with network training accuracy and dice similarity coefficient metrics. In the next step, I extracted several single CM's, and the beating activity profile was efficiently characterized. Multiple parameters associated with the dynamic beating profile of each cell was measured. The Single CM beating profile quantification is precisely performed using contraction-relaxation peak detection and multiple auxiliary points.



## **B. Label-free Motion Characterization of Human Cardiomyocytes at the Single-cell Level using Holographic Imaging for Cardiotoxicity Screening**

### **a. Motivations and introduction:**

Real-time single CMs motion characterization from QPI sequences can reveal the periodicity of contraction and the characteristic changes. Many methods have been reported on CM motion characterization. Cell-based biosensors are widely used tools for CM characterization. The limitations of these methods include the need for specific high-cost hardware, sensors, and trained personnel, as well as cardiomyocytes to be cultured on specialized materials. However, it has become increasingly important to develop high throughput, low-cost and fully automated solutions to motion characterization iPSC-CMs at a single-cell level without manually tuning of software parameters and/or physical or biochemical alternation for long-term monitoring.

optical flow-based real-time motion characterization methods are low-cost and high throughput methods capable of monitoring cardiomyocyte contractile activity without physical touching which preserves the sample's originality. The motion vectors generated by the optical flow method can reveal valuable information related to the CM's contractility and health which is difficult to acquire using traditional image processing or mechanical investigations techniques [43]. Finally, to simplify low-cost real-time monitoring of the hiPSC-CMs at the single-cell level, the algorithm must be fast without the need for parallel implementation.

Many attempts have been made to create such a simplified platform for CM motion characterization [44–50]. For example, [50] made a video-management platform using segmentation to specify the beating region with a user-defined threshold on the average change in signal intensity. The above-mentioned methods require manual tuning of many parameters. Another problem with these methods is that they are mainly based on image segmentation or

block-matching technique that performs tracking by a search for the specific attributes of a moving group of pixels called macroblock including corners and edges. While a single CM's beating activity, cell shape undergoes large deformation which makes tracking a challenging task to find the best-matched block in the next video sequence frame. The Farneback dense optical flow method performs object tracking by measuring the displacement of each pixel on the image [51, 52]. Furthermore, using the non-invasive property of DHM and optical flow-based analysis, cells remain intact for long-term monitoring. Using motion waveforms generated from the cell's motion speed measurement, the cell's dynamic parameters including the contraction period, relaxation period, and resting period can be automatically quantified. Generally, video-based CM motion characterization methods have several advantages over traditional methods for studying cell's functionality including the need for little training for personnel, no external hardware except the microscope while revealing information about actual biomechanical timing.

In this work, a new and fully automated platform is presented that performs real-time single CM's motion characterization using Farneback dense optical flow method and time-lapse QPI imaging. The proposed method overcomes the limitations of the current state-of-the-art methods. In our proposed schema first, we perform real-time CM motion tracking at the single-cell level using a Farneback dense optical flow method to measure contractile motion speed with individual pixel displacement sensitivity. In this way, the cell's motion waveform was generated from dry mass redistribution monitoring during the autonomous CM's beating activity. Afterward, we implemented a computational algorithm to further characterize the dynamic nature of the CM's contractile motions. The proposed method can detect high-resolution contractile centers. Since the measurements are at the single-cell level, the CMs synchronization can be qualitatively assessed. To further demonstrate the power of the proposed method, we also applied several whole slides QPI of multiple cardiomyocytes for motion characterization and the generated motion waveform is quantified. The validation of the proposed CM characterization method was performed by the speed measurement of the fixed cardiomyocytes versus live

cardiomyocytes. Furthermore, the noise sensitivity of the proposed method was examined by artificially adding different levels of noise to the image stacks and the impact on the resulting beating profile was quantified. We demonstrate the application of the proposed method for cardiotoxicity screening by analyzing the pharmacological effects of isoprenaline (166 nM) and E-4031 (500  $\mu$ M) on the response of a single CM's contractile speed in comparison to control conditions.

### b. Cardiac cell motion tracking with Farneback optical flow

The optical flow is an approach for motion estimation of the moving object between consecutive movie frames in the computer vision field. Figure 2.13a shows a schematic representation of the optical flow method for pixel displacement estimation in two successive image frames where  $I(x,y,t)$  denotes the pixel position in the first image frame (reference frame) and  $I(x+dx, y+dy, t+dt)$  refers to the pixel displacement in the subsequent frame (current frame). In the first step of the Farnebak optical flow method, the algorithm generates a hierarchy of image resolution levels from the original image using Gaussian pyramids, where each level has a lower resolution compared to the previous level (see Figure. 2.13(b)). The tracking process starts with the lowest resolution and continues to the highest resolution. Consequently, the displacement of two local patches in consecutive image frames is calculated by approximating the neighborhood of each pixel with a quadratic polynomial as in the following equation [53].

$$I(x) \approx X^T Ax + b^T x + c, \quad (10)$$

where  $A$  stands for symmetric matrix,  $b$  is a vector and  $c$  is a scalar. The vector  $x$  denotes a  $1 \times 2$  vector consisting of  $x$  and  $y$  variable, and  $A$  is a symmetric matrix  $2 \times 2$  of unknowns that containing information about the even parts of the signal and  $c$  is unknown scaler. The first neighborhood is approximated by the following equation:

$$I_1(x) = X^T A_1 x + b_1^T x + c, \quad (11)$$

The new neighborhood, affected by displacement  $d$ , is calculated as follows:

$$\begin{aligned}
 I_2(x) &= I_1(x-d) = (x-d)^T A_1(x-d) + b_1^T(x-d) + c_1 \\
 &= x^T A_1 x + (b_1 - 2A_1 d)^T x + d^T A_1 d - b_1^T d + c_1 \\
 &= x^T A_2 x + b_2^T x + c_2,
 \end{aligned}
 \tag{12}$$

Using the different coefficients from the two polynomials  $I_2(x)$  and  $I_1(x-d)$  gives:  $A_2 = A_1$ ,  $b_2 = b_1 - 2A_1 d$ , and  $c_2 = d^T A_1 d - b_1^T d + c_1$ . The distance,  $d$ , that is used to approximate the optical flow is obtained by the following equation:

$$d = -\frac{1}{2} A_1^{-1} (b_2 - b_1),
 \tag{13}$$

The tracking is refined in each resolution level by initializing from the lowest resolution level and continuous to the highest resolution. The detected tracking points at each resolution level are the base point for the next level. In this way, a large displacement can be detected.

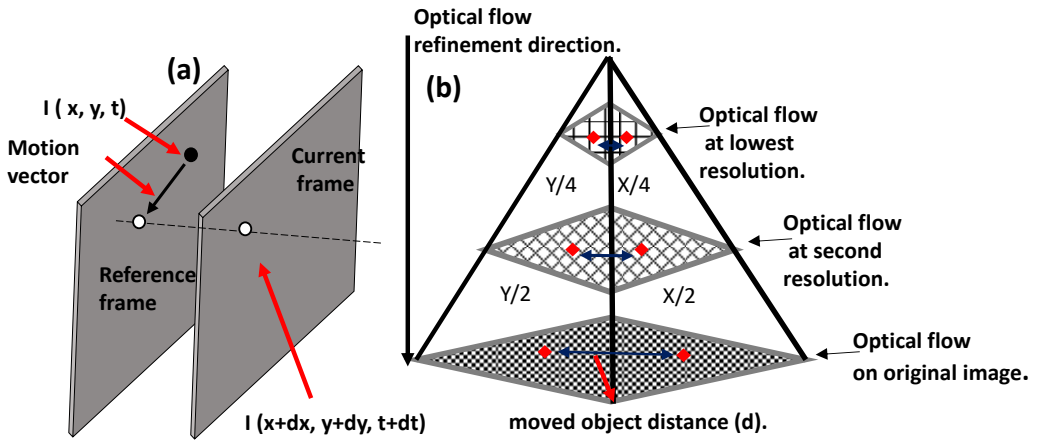


Figure 2.13: (a) representation of the optical flow method for pixel displacement estimation. The black pixels correspond to the pixel position at the time ( $t$ ), and white pixels correspond to the pixel position at the time ( $t+dt$ ). (b) Multi-resolution leveling of the image with three levels. The image resolution at each level is downsized. The tracking begins at the lowest level finishes at the highest level.

### c. Workflow and beating signal extraction

The workflow of our approach starts with a video recording of beating cardiomyocytes. Afterward, ten single cells are manually extracted from different parts of the cardiomyocytes QPI (see Figure 2.14). The extracted single CMs are the size of 100×100 pixels (28μm). While the cardiac cell's beating activity, by repeating the optical flow procedure shown in (Figure 2.14) for each pixel of QPI image, an array of the motion vectors will be generated which shows the CM's motion direction and the CM's movement speed is calculated.

The extracted region was subjected to motion tracking analysis mostly includes the nuclei of the cell, assuming that the cell nuclei represent the motion center of single cells. The beating activity profile is generated from the CM motion speed calculation during beating activity using the following equation:

$$Speed_{\mu m/s} = \frac{Displacement}{Time} = \frac{\sqrt{(dx)^2 + (dy)^2}}{Time}, \quad (14)$$

where  $dx$  and  $dy$  are displacements in  $x$  and  $y$  directions estimated by Farneback algorithm representing CM motion in the  $x$  and  $y$  direction, and time is considered as the time between two consecutive frames. Once the motion speed profile is generated, one can find the contraction and relaxation peaks obtained by the automated peak identification method along with multiple auxiliary points for CM's physiological behavior quantification.

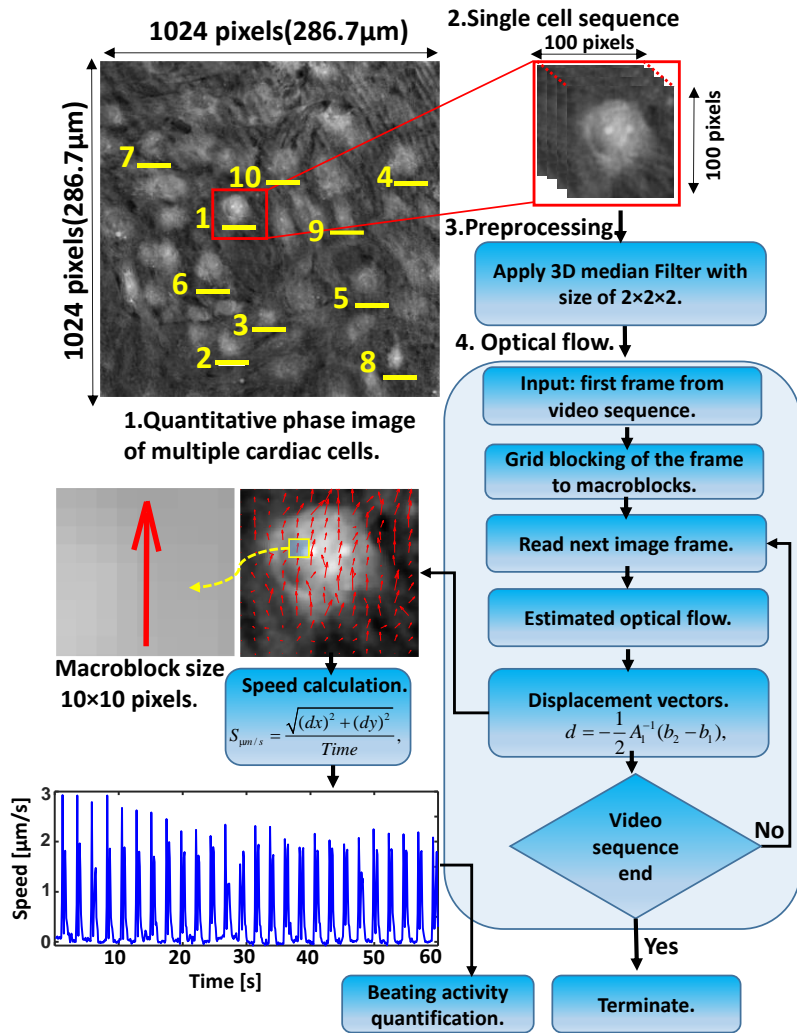


Figure 2.14. The overview of the workflow for motion tracking of single cardiac cells and beating profile visualization using motion speed calculation.

A single cardiac cell with superimposed motion vectors on the image referring to the motion directions for different bating statuses is shown in Figure. 2.15.

The first row of the Figure. 2.15(a),(b),(c) corresponds to the contraction, relaxation, and resting status respectively. It can readily be seen that during contraction and relaxation, motion vectors are indicating opposite directions. In contrast, vectors indicate no motion (displacement) in the

resting status. Optical flow can summarize temporal information about CM's beating activity using heat maps of the magnitude of motion vectors. The maps provide a rapid overview of the movement in different parts of the image. The corresponding heat map generated from absolute motion for each status is also shown (see the second row of Figure 2.15 (a), (b) and (c)). Heat map represents the specific regions of the cells which is a center of contraction. The region in which maximum contraction occurs is called the contractile center.

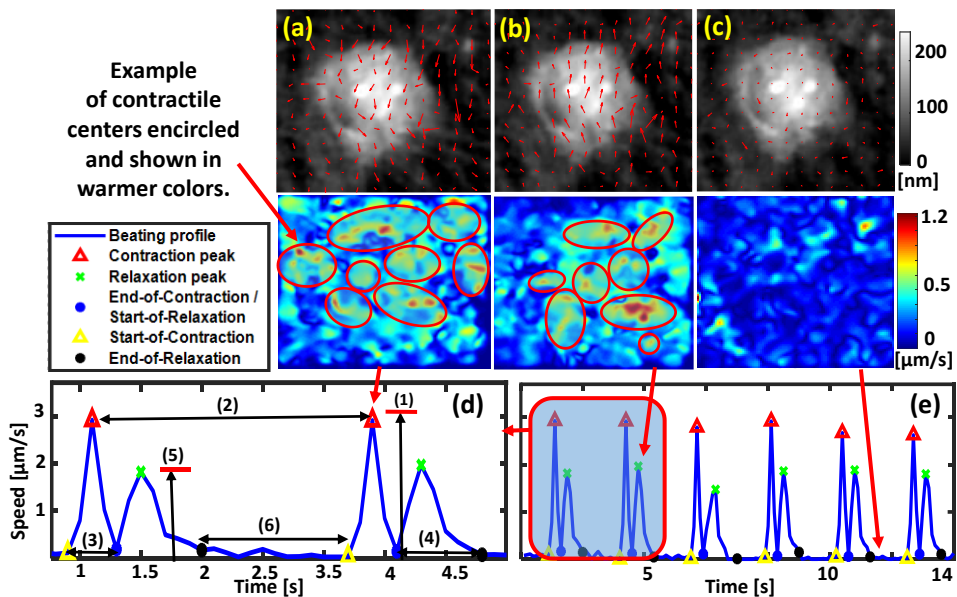


Figure 2.35: Single CM contractile motion characterization using optical flow analysis. A close-up image of a single CM with superimposed motion vectors on the cell's image for (a) contraction, (b) relaxation, and (c) resting states respectively (top) and corresponding heat map generated from absolute motion (bottom). The contractile center refers to a region from which contractions are maximized, (d) details on quantification parameters explained in Table 2.3, (e) a single CM's beating activity profile.

As shown in the second row of Figure 2.15 (a), (b) and (c) (bottom) while cell's contraction status, more contractile centers are observed on the heat map image compared to relaxation status. It leads to generate higher motion speed for contraction status and lower motion speed for relaxation status. In contrast, the heat map shows almost no contractile centers in resting status

which leads to nearly zero value for motion speed. Note that image noise may cause a very small contractile center on the heat map in resting status. The single CM's motion speed monitoring can reveal details of the beating activity temporal parameters(See Figure 2.15(e)). To calculate the characteristics of the single CM's activity from the motion speed signal, single beating profiles are extracted. It requires two main peaks of contraction and relaxation and three auxiliary points 1) Start-of-Contraction, 2) End-of-Contraction and 3) End-of-Relaxation. The representation of these points is shown in Figure. 2.15(d)[78].

Table 2.3: Description of dynamic parameters measured for each extracted single cardiac cell.

Dynamic parameter		Description
Contraction	Maximum contraction speed [see #1 in Fig. 2.15(d)]	The average amplitude of contraction peaks.
	Beating period [see #2 in 2.15 (d)]	The time between two adjacent contraction peaks.
	Contraction period [see #3 in 2.15 (d)]	The average time between the Start-of-Contraction and End-of-Contraction points.
Relaxation	Relaxation period [see #4 in Fig. 2.15 (d)]	The average time between Start-of-Relaxation to the End-of-Relaxation points.
	Maximum relaxation speed [see #5 in Fig. 2.15 (d)]	The average amplitude of relaxation peaks.
Resting	Resting period [see #6 in Fig 2.15 (d)]	The average time between the End-of-Relaxation to the next Start-of-Contraction points.



#### **d. Results and Discussion**

Heat map analysis of absolute motion is used to monitor the contractile centers for four different isolated CM (Figure 2.16 (a), (b), (c) second row) as examples (only four cells are shown;). The motion vectors indicate opposite directions to each other during contraction and relaxation (Figure 2.16 (a), (b), (c) first row). As shown in Figure. 2.16 (d), motion occurred at regular intervals. During the CM resting status, the motion vectors and heat map are too weak which specifies the cell is almost immobile. The proposed motion characterization method allows us to study the high-resolution contractile centers. Note that there is a cell-to-cell variation in the magnitude of speed value, whereas the CM's beating rate and other characteristics related to the physiological aspects of the sample (contraction-relaxation period, etc.) are nearly the same. Then the maximum relaxation speed. Figure 2.16 also indicates that the contraction period is shorter than the relaxation period due to the presence of different ion channels and transporters expressed in cardiomyocytes membrane and the mechanisms by which their activities are sequentially orchestrated while cell contract and relax. The average beating rate and average beating period are similar for all cells.

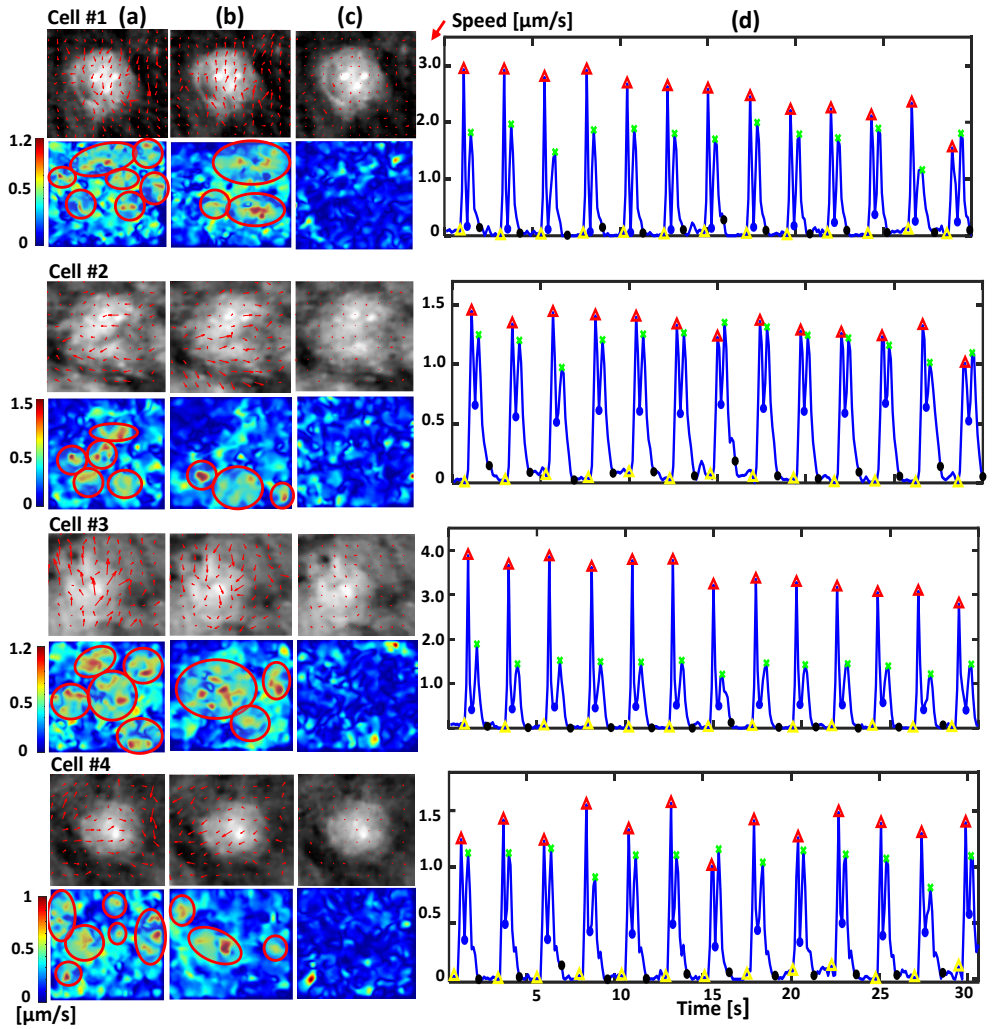


Figure 2.16: Real-time motion tracking of single CMs with the optical flow and contractility analysis using heat maps: (a), (b) and (c) motion vectors superimposed on the single CM image representing the motion direction for contraction, relaxation and resting beating cycle, respectively, shown in the first row. The corresponding contractility heat map is shown in the second row. The contractile centers are encircled and shown in warmer colors on the heat map. (d) The beating activity profile derived from dry mass redistribution motion speed calculation by absolute motion in the entire image over time using Eq. (14).

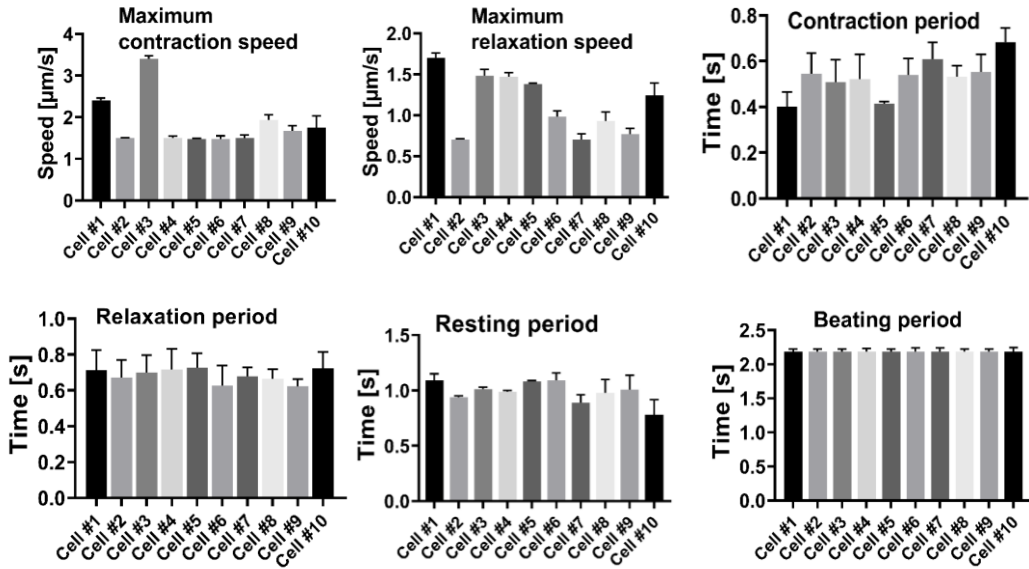


Figure 2.17: Results of different parameters of beating profile of the single extracted cells.

### Synchronization analysis

Since our analysis is at the single-cell level, it can provide reliable synchronization analysis. Figure 2.18 shows the synchronization investigation for all extracted single CMs. As shown in (Figure 2.18(a)) the temporal activity (contraction and relaxation) in different periods beat with the same frequency. Cross-correlation analysis can be applied for synchronization investigation between single CM's beating activity signals. Figure 2.18(b) shows the cross-correlation evaluation in which the maximal cross-correlation value is on the time lag zero. It shows that CM signals are perfectly synced in time.

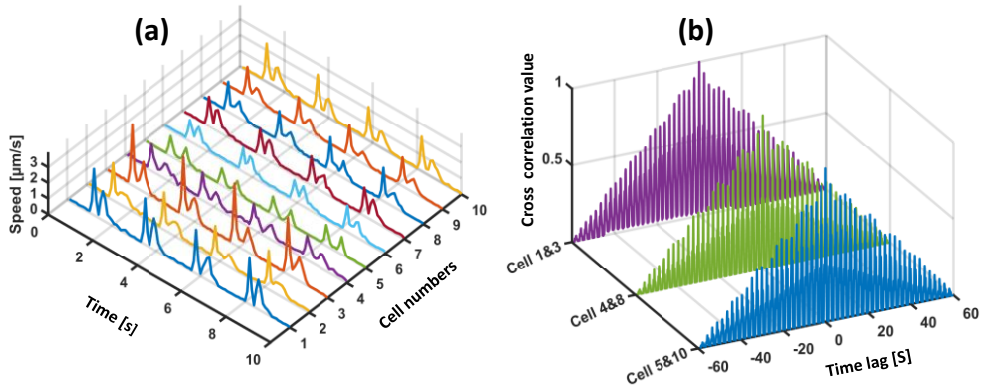


Figure 2.18: Visual and numerical synchronization analysis. (a) 3D representation of single CM's beating profile synchronization. (b) Cross-correlation analysis between different pairs of individual CMs.

### *Whole slide image motion analysis*

To demonstrate the robustness of the proposed CM motion characterization method, we applied the proposed method for motion characterization of the whole slide QPI samples of multiple CMs. Figure 2.19(a) shows the whole slide QPI with superimposed motion vectors for contraction beating status and the corresponding heat map is shown in Figure 2.19(b). The beating activity profile with detected contraction-relaxation peaks and auxiliary points is shown in Figure 2.19(c).

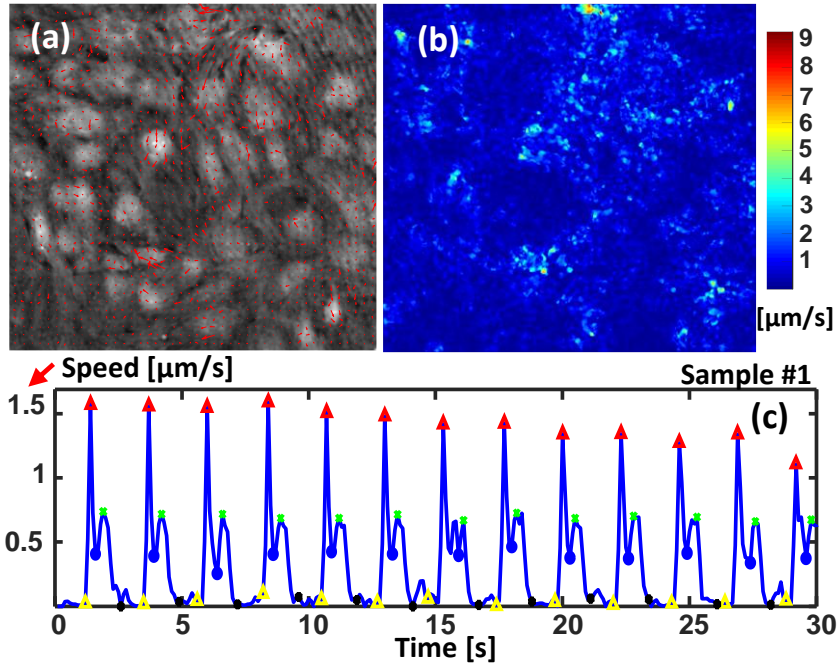


Figure 2.19: Whole slide QPI of multiple cardiomyocytes motion characterization. The sample is recorded at 10Hz frequency. (a) Whole slide QPI of multiple CMs with superimposed motion vectors for contraction beating status, (b) corresponding heat map, (c) beating activity profile. (Maximum contraction speed: 1.4 [ $\mu\text{m/s}$ ]; Maximum relaxation speed: 0.8 [ $\mu\text{m/s}$ ]; Contraction period: 0.58 [s]; Relaxation period: 0.63 [s]; Beating period: 2.1 [s]; Resting period: 0.75 [s]).

### ***Verification of motion tracking method***

#### ***Fixing cardiomyocyte cells***

We performed verification of the proposed CM motion characterization method by applying the proposed method to measure the speed of fixed cardiomyocytes versus live cardiomyocytes shown in Figure 2.20(a). Cardiomyocytes were fixed using a 4% formalin solution (Sigma-Aldrich) incubated for 15 min at room temperature (RT). Subsequently, cells were washed three times with phosphate-buffered saline (PBS) for 10 min at RT. 1500 images at 50Hz sampling

frequency were acquired before and after cell fixation and motion speed for both samples were evaluated.

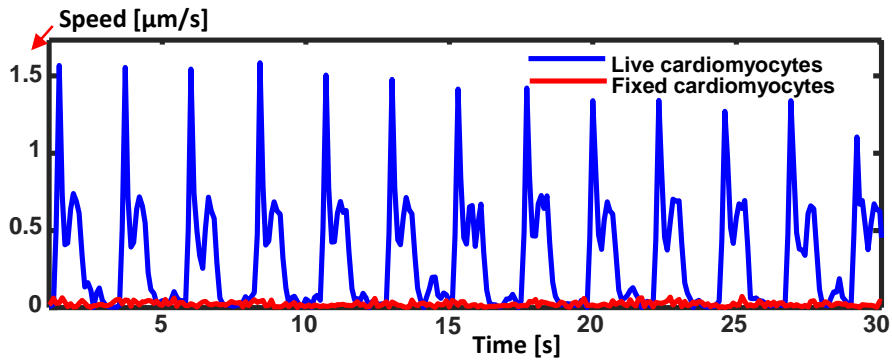


Figure 2.20: The whole slide QPI Motion speed measurement of fixed cardiomyocytes versus live cardiomyocytes.

***Monitoring the pharmacological effects of compounds on cardiomyocytes' AP waveform***

Next, we applied the platform to test the response to pharmacological compounds on single CMs' motion activity. We analyzed the effects of an hERG channel blocker (E-4031) and an adrenergic receptor agonist (isoprenaline) on cardiomyocytes' contractile speed using the proposed platform. We treated multiple cardiomyocytes with 166 nM of isoprenaline and 500 μM of E-4031 and compared the beating activity parameters to those obtained in the control conditions.

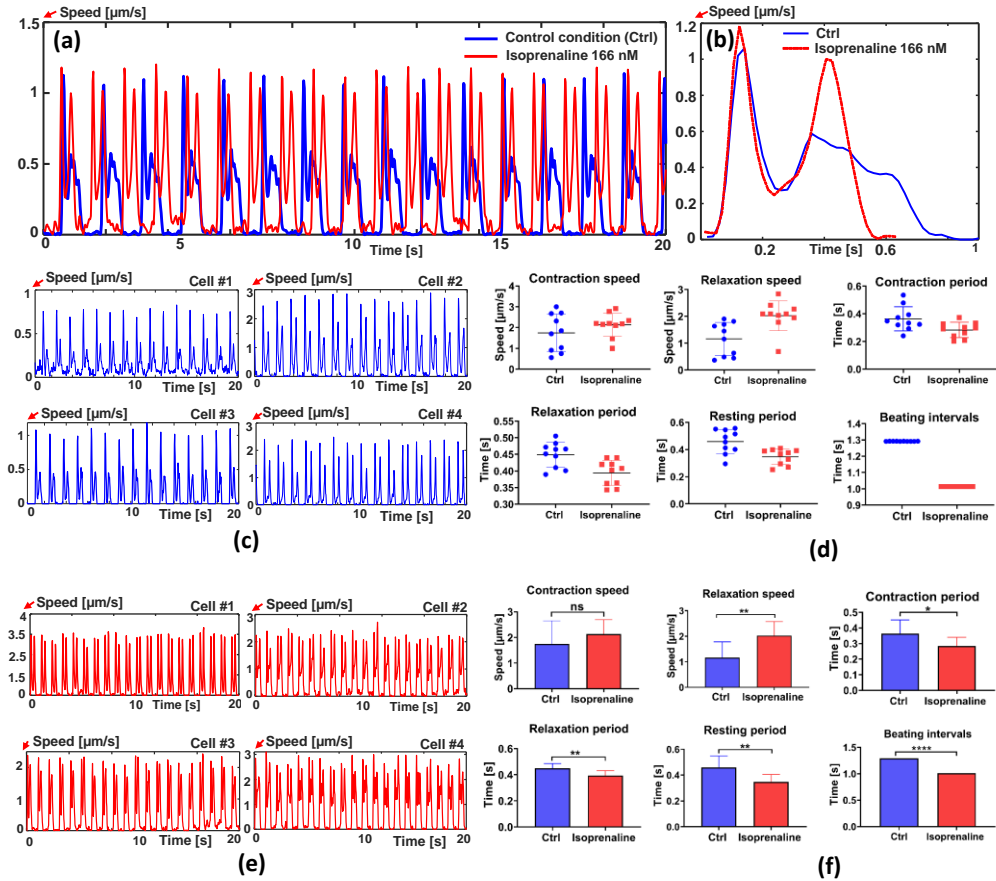


Fig. 2. 21. Cardiomyocytes motion speed analysis in control (Ctrl) and drug-treated conditions in response to 166 nM of isoprenaline. (a) Whole-slide QPI contractile motion analysis in control and drug-treated conditions, (b) single-beat contractile motion comparison in control and drug-treated conditions. (c) Motion waveforms of single CMs #1 to #4 extracted in control conditions. (d) Quantification result comparison in the control conditions (blue points) versus drug-treated conditions (red points) at the single-cell level. (e) Single CMs #1 to #4 extracted after isoprenaline treatment. (f) Average of each quantification parameter for all extracted single cells in control (blue bars) versus drug-treated conditions (red bars). All statistical comparisons were carried using an unpaired student t-test.

Fig. 2.21a shows the contractile speed of the whole-slide QPI of multiple CMs in control and drug-treated conditions in response to 166 nM of isoprenaline. Fig. 2.21b demonstrates an example of single beat profiles of a whole-slide QPI with a comparison between the control and drug-treated conditions. The contraction-relaxation speed increased in drug-treated conditions compared to the control conditions. Figs. 2.21(c) and (e) show examples of single-CM beating profiles of cells #1 to #4 extracted in control (blue beating profile) and isoprenaline-treated conditions (shown in red). Single-cell parameter quantification results are compared in Fig. 2.21d. A summary of the compound addition effects is presented in Fig. 2.21f.

The unpaired student's t-test analysis shows that cardiomyocytes responded to isoprenaline with a significant increase in relaxation speed during the contraction speed, but it was not significantly increased compared to the control condition. The resting period was significantly shortened and caused a significant increase in the beating frequency. The bars represent the mean and standard deviation (SD) for each quantification parameter.



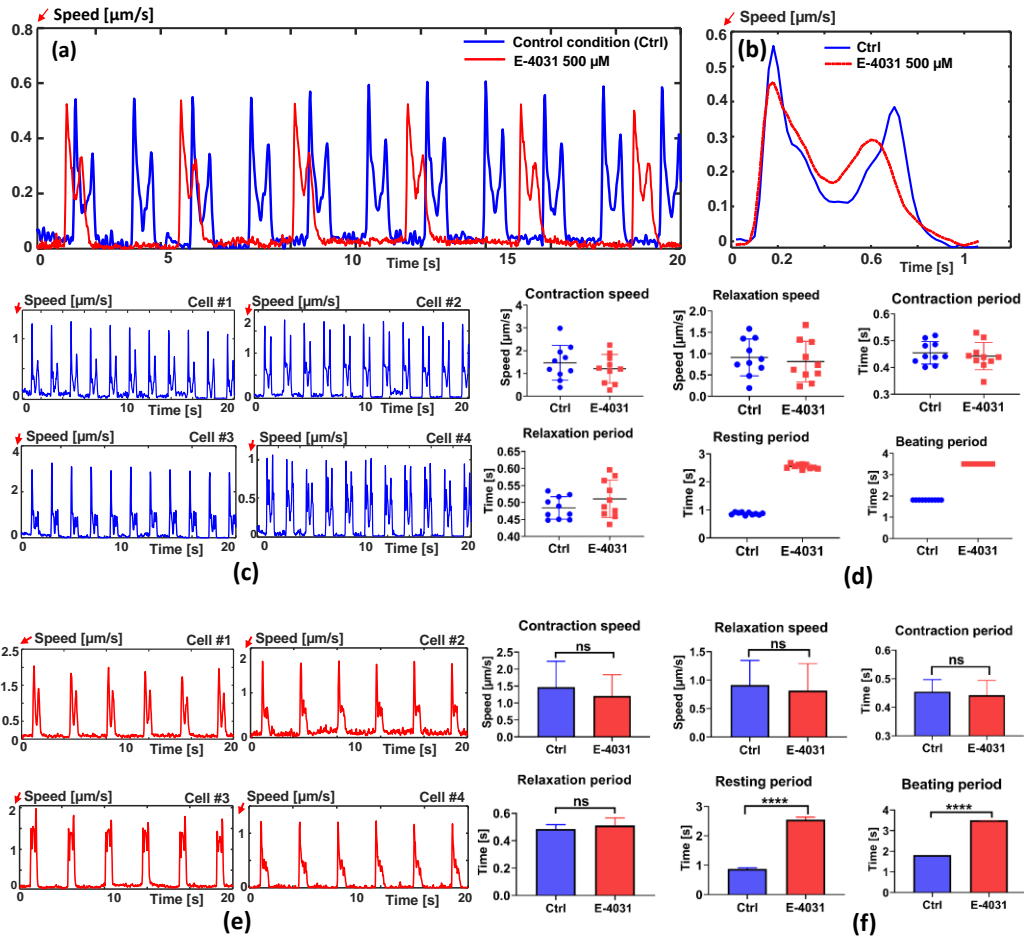


Fig. 2. 22. cardiomyocytes contractile motion analysis in control (ctrl) and drug-treated conditions in response to 500  $\mu\text{M}$  of E-4031. (a) Whole-slide QPI contractile motion analysis in control versus drug-treated conditions in response to 500  $\mu\text{M}$  of E-4031. (b) Single beat contractile motion comparison in control versus drug-treated conditions. (c) Motion waveforms of single CMs #1 to #4 extracted in the control conditions and (d) quantification result comparison at the single-cell level of the control conditions (blue points) versus drug-treated conditions (red points). e) Single CMs #1 to #4 extracted after 500- $\mu\text{M}$  E-4031 treatment. (f) Average of each quantification parameter for all extracted single cells in the control conditions (blue bars) versus drug-treated conditions (red bars). All comparisons were carried out using an unpaired student t-test.

The effects of E-4031 on AP were tested at both the whole-slide QPI and single-cell levels. The single-CM beating patterns for cells #1 to #4 are given in Figs.2.22 (c) and (e). A comparison of

the beating profile quantification parameters was performed at the single-cell level, as shown in Fig. 2.22(d). We observed a contractile response of a CM to the E-4031 drug, which demonstrated that the average AP of all single CMs' contractile speeds decreased compared to the control conditions.

The average resting period for all extracted single CMs in drug-treated conditions demonstrated almost the same value, which shows significant prolongation compared to the control conditions. Thus, there was a significant decrease in the beating period. Some single CMs' motion profiles exhibited irregular beating patterns after drug treatment. The average results of each quantification parameter for all extracted single cells are shown in Fig. 2.22f. The bars represent the mean and SD for each quantification parameter of all extracted single cells.

## ***Discussion***

We have proposed a motion characterization platform for single hiPSC-CMs using the optical flow method combined with digital holographic imaging for cardiotoxicity application. We obtained detailed information about CM functionality from generating the CM beating activity profile based on the cell's speed calculation. Quantification of the beating profile was performed for every extracted single cell using our automated peak identification method. Validation of the proposed CM characterization method was performed by measuring the contractile speed of fixed cardiomyocytes versus live cardiomyocytes and a noise sensitivity analysis.

Based on experimental results, we demonstrated that the proposed method and quantification have the potential to be used in high-throughput analysis of hiPSC-CMs in compound cardiotoxicity screening. Our results revealed quantification features of the beating profile, including the contraction period, relaxation period, and resting period. Also, we investigated the beating synchronization of the single CMs using the proposed method. Finally,

we validated the applicability of the proposed platform for cardiotoxicity screening at the single-cell level by monitoring the effects of E-4031 (500  $\mu$ M) and isoprenaline (166 nM) compounds on multiple single cardiomyocytes' beating activity-related parameters in comparison to control conditions. The cardiomyocytes responded to the E-4031 by decreasing their contractile speed and prolonging their resting period, thus decreasing their beating frequency. The isoprenaline caused an increase in AP speed with a decrease in resting period, thus increasing the beating frequency. Finally, we averaged each quantification result for all extracted single CMs (10 single CMs) in control conditions and drug-treated conditions. In summary, our results prove that the proposed method can be used for synchronization analysis and cardiotoxicity screening. More specifically, the Farneback method can perfectly generate motion vectors for single cardiac muscle cells. Other advanced tracking algorithms may or may not be able to generate the same vectors, but designing a new tracking algorithm is not the purpose of this study. Overall, the experimental results demonstrated that the proposed approach can efficiently and accurately reveal detailed quantification results about the pharmacological effects of a drug on single cardiac cells for cardiotoxicity screening and predictive toxicology.

### **e. Conclusions**

In this paper, we have proposed an optical flow-based method for CM contractile motion characterization at the single cell-level obtained from quantitative phase images by DHM. The system comprises two parts: First, the real-time motion of single cardiac cells is tracked using the Dense Farneback optical flow method, which provides a vector field that is used for automated, user-independent and robust monitoring of cell motion. Second, the computational algorithm quantifies the beating activity profile of every extracted single cell which is derived from the cell's contractile motion speed. This enables multiple parameters related to beating activity to be measured. Our study demonstrates that the heat map of the absolute motion field can be successfully used to identify the contractile region during cell beating activity, which

offers automated, motion tracking and functional monitoring of individual cells. We also performed visual and numerical synchronization at the single-cell level. We believe that our proposed method can be useful for automated high-content screening of drug-induced cardiotoxicity and maturation analysis of CM.

## **C. Automated Motion Characterization Of Drug-Treated Cardiomyocytes At The Single Cell-Level With Digital Holographic Imaging**

### **a. Abstract**

In this study, we combined quantitative phase digital holographic microscopy (QP-DHM) imaging informatics with a Franeback dense optical flow method for manipulation-free *in vitro* motion characterization of single human cardiomyocytes (hiPS-CMs) in control and drug-treated conditions. We screened the toxicities of three drugs, (E-4031, isoprenaline, and sertindole) with various concentrations. While spontaneous contraction-relaxation of single CMs, cellular deformation was detected using QP-DHM imaging with motion vector analysis generated by the Franeback dense optical flow method, and the cell's motion waveform was generated which quantitatively reflected CM's functional behaviors. Following this, we developed a computational algorithm for further characterizing of the single CM's functional behaviors and several parameters related to the beating profiles were calculated. Several single CMs were extracted from the whole slide quantitative phase image (QPI) of multiple CMs and quantification parameters were calculated per every single CM. Besides, a population average, as well as standard deviations, were computed. In the presence of E-4031, the contraction-

relaxation motion speed is declined compared to corresponding control condition while the contraction-relaxation motion speed is increased in response to isoprenaline. In response to sertindole, the contraction motion speed is raised while the relaxation motion speed is reduced compared to the control condition with significant prolongation in the relaxation period. High concentrations of all drugs showed significant alternation in beating frequency. The outcomes of the experimental results offer insights into the interpretation of single CM's kinetics

### **b. Motivations and introductions:**

One of the major concerns in the drug development process is cardiac toxicity and the potential effect of candidate compounds on the cardiovascular function and precise risk measurement is challenging. The quantitative phase digital holographic microscopy (QP-DHM) provides high acquisition speed quantitative phase images of cell structure and dynamics in a label-free manner. DHM can provide accurate quantitative visualization of human cardiomyocytes derived from induced pluripotent stem cells (hiPSC-CMs) dynamics which are transparent or semi-transparent microscopic objects. Hence, DHM is particularly effective to study CM's dynamics. As a result, significantly valuable information regarding the cell's dynamics of dry mass redistribution can be obtained in a label-free manner. The human myocardium contains an estimated 2 to 3 billion of spontaneously beating cardiomyocytes cells to pump the blood to the entire body with synchronized beating activity<sup>10</sup>. Drug attrition is one of the main contributors to the high expense of drug development. The hiPSC-CMs technology showed to be an alternative model for cardiotoxicity screening, human disease modeling, cardiotoxicity, and therapy *in vitro*. Due to the presence of different ion channels in cardiomyocytes, the sole reliance on cell line models, puts human lives at risk. Drugs that cause cardiac arrhythmia manifest by alternation in CMs physiological behaviors (dry mass redistribution) such as changes in the contraction-relaxation motion speed, beat frequency, contraction period, relaxation period and motion patterns of cardiomyocytes. Therefore, high

throughput preclinical cardio-safety assessment methods for CM characterization in cardiotoxic screening are crucially in demand

In our current study, we characterized single CM kinetics in control and drug-treated conditions using various concentrations by combining quantitative phase digital holographic microscopy (QP-DHM) with Farneback dense optical flow. The cardiomyocytes QPI was obtained using DHM and seven single CMs in the control and drug-treated conditions were manually extracted. Afterward, the Farneback dense optical flow method was applied to monitor the dynamic, rhythmic beating patterns and biomechanical contractile motion waveform was generated. The motion field was shown by motion vectors in a real-time manner. The system was able to sensitively and quantitatively detect the cardiac functional behavior treated with E-4031, isoprenaline, and sertindole in real-time. Following this, a computational algorithm was implemented to characterize the contractile motion of single cardiomyocytes from the motion waveform signal and multiple parameters related to the periodicity of CM's beating activity profile were measured. All quantification parameters such as (contraction motion speed, relaxation motion speed, contraction period, relaxation period, resting period) and their standard deviation were measured at the single-cell level and the population average was computed. Our results demonstrated the E-4031 compound declines the contraction-relaxation motion speed compared to control condition while isoprenaline increases the contraction-relaxation motion speed. The sertindole causes an increase in contraction motion speed while the relaxation motion speed is reduced compared to the control condition. Overall, the sensitivity of the proposed method to effectively detect the periodicity of the beating profile makes the proposed method well suited for the early preclinical safety assessment of cardiotoxic compounds.

## c. Materials and Methods

### *Sample preparation*

Human-induced pluripotent stem (iPS) cell-derived CMs obtained from Cellular Dynamics Int. (Madison, WI) were cultured and grown according to the manufacturer's instructions for 14 days before recording a hologram. Measurements were acquired in a Chambridge WP incubator system with a 96-well plate (LCI, South Korea) at 37°C with 5% CO<sub>2</sub> and high humidity. Images were recorded by a commercially available DHM T-1001 from LynceeTec SA (Lausanne, Switzerland) equipped with a motorized stage (Märzhäuser Wetzlar GmbH & Co. KG, Wetzlar, Germany, ref. S429). Images were acquired using a Leica 20×/0.4NA objective (Leica Microsystems GmbH, Wetzlar, Germany, ref. 11566049). The camera resolution was 1920 × 1200 pixels (the hologram size was 1024×1024, which is efficient for FFT computation).

For drug-treated CMs, a sequence was recorded before treatment for the control conditions. Then the drug was added, and after 15 minutes of incubation, the images were recorded again.

### *Pre-processing*

**Median filter:** Median filter is a widely used noise removal method from image or signal by moving through the entire image and replacing the pixel value by the median value of the neighborhood while preserving the edges. In this experiment, we applied a 3D median filter with a window size of 2×2×2 for noise reduction.

### *Postprocessing*

**Average filter:** To remove unwanted peaks on the motion waveform which may negatively affect the quantification, we applied a moving average filter with a span of 4 (unweighted mean of 4

points of motion waveform). This filtering can efficiently reduce part of the noise that appears in the CM's contractile motion waveform which causes multiple peaks in different beating states.

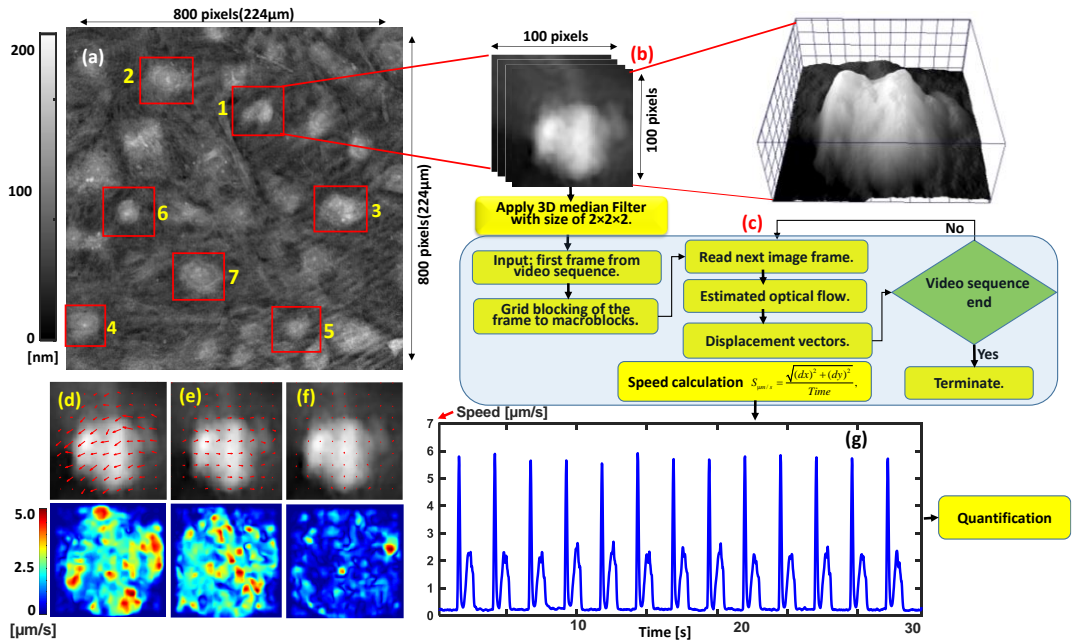


Figure 2.23: The overview of the workflow for motion tracking of single cardiac cells and beating profile visualization using motion speed calculation. (a) cardiomyocytes phase image after numerical reconstruction with multiple cardiac cells. (b) single cardiac cell manually extracted with a size of 100×100 pixels. Consequently, 3D median filter with the size of 2×2×2 was applied for noise reduction, (c) optical flow procedure for cardiac cell's contractile motion speed measurement, (d)(e)(f) motion vectors super imposed on cell's phase image for contraction, relaxation, and resting beating activity respectively and corresponding heatmap generated from absolute motion shown in the second row (The contractile center shown in warmer color on heat map refers to a region from which contractions are maximized), (g) beating activity profile of a single CM generated from cell's motion speed measurement.

We extracted seven single CMs from different parts of the whole slide QPI of multiple CMs (see Fig. 2.23(a)). The QPIs with the multiple CMs are a resolution of 800×800 pixels (224μm). Single cells are manually extracted with a size of 100×100 pixels (28μm). We assume that CM's nuclei part is the center of motion while contraction-relaxation beating activity. The motion waveform is generated from CM's motion speed calculation while spontaneous contraction-



relaxation beating activity using the following equation:

$$Speed_{\mu m/s} = \frac{Displacement}{Time} = \frac{\sqrt{(dx)^2 + (dy)^2}}{Time}, \quad (15)$$

where  $dx$  and  $dy$  are displacements in  $x$  and  $y$  directions estimated by Farneback algorithm representing CM motion in the  $x$  and  $y$  direction, and time is considered as the time between two consecutive image frames. By calculation of the average displacement magnitude of all pixels in  $x$  and  $y$  direction against time, we were able to obtain contractile motion speed. Afterward, we extracted several parameters related to the contractile motion profile. Fig 2.23 shows the workflow of the proposed method single CMs are formed in different shapes and sizes. Seven single CMs are extracted from each QPI of multiple cardiomyocytes. While cell's spontaneous contraction-relaxation, the motion vectors overlayed on the image of single hiPS-CM indicate the opposite direction (see Fig 2.23(d,e)). The motion vectors exhibited shorter length demonstrating slower motion speed during the relaxation period compared to the contraction period. The contractile centers on the corresponding heatmap of contraction status demonstrate a broader region is being contracted compared to relaxation status while the heat map shows no movement in the resting state. After a beating cycle (one contraction-relaxation) the cell inters into the resting state in which the motion vectors show no direction(see Fig 2.23(f)).

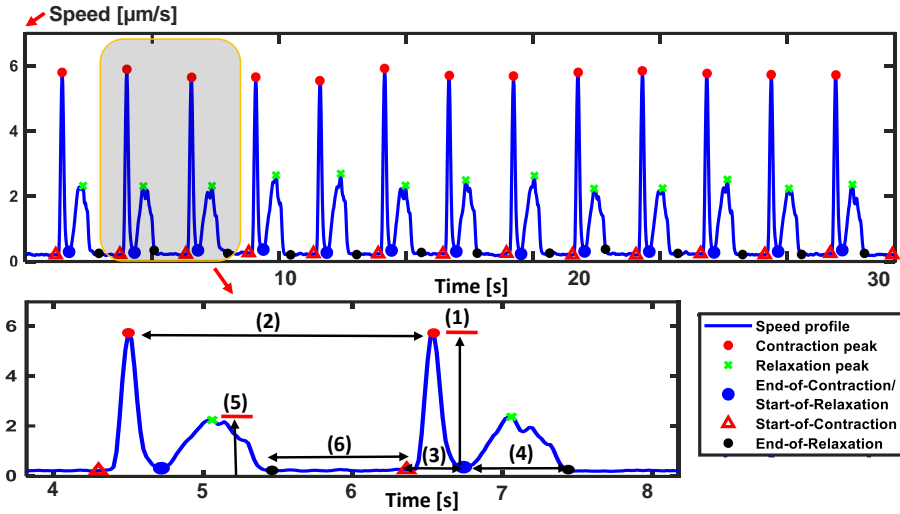


Figure 2.24: Representation of a single cardiac cell's motion waveform generated using contractile motion speed calculation and the definition of the multi-parameters. The inset shows details of multi-parameters calculated from beating activity described in table.2.4

### *Cardiomyocytes dynamic parameter measurement*

It is crucial to use multiple parameters to evaluate the effects of compounds for precise capturing the irregularity and dynamics of the beating profile. Fig.5 shows a motion waveform of single CM generated from motion speed calculation which consists of a sequence of positive peaks for contraction-relaxation and the contractile motion waveform is quantified through contraction-relaxation peaks identification [87]. Different methods have been proposed to find the QRS complex [54-56]. In our proposed method, We calculated the characteristics of the single cardiac cell's beating activity using two main peaks of contraction-relaxation and three auxiliary points 1) Start-of-Contraction, 2) End-of-Contraction and 3) End-of-Relaxation shown in the Figure. 2.24. The extracted temporal parameters and the corresponding descriptions are explained in Table 2.4

Table 2.3: Definition of terms and analysis parameters.

	Dynamic parameter	Description
Contraction	Maximum contraction speed [see #1 in Fig. 2.24 (Inset)].	The average amplitude of contraction peaks.
	Beating period [see #2 in Fig 2.24 (Inset)]	The time between two adjacent contraction peaks.
	Contraction period [see #3 in Fig 2.24 (Inset)]	The average time between the Start-of-Contraction and End-of-Contraction
Relaxation	Relaxation period [see #4 in Fig 2.24 (Inset)]	The average time between Start-of-Relaxation to the End-of-Relaxation points.
	Maximum relaxation speed [see #5 in Fig. 2.24 (Inset)]	The average amplitude of relaxation peaks.
Resting	Resting period [see #6 in Fig. 2.24 (Inset)]	The average time between the End-of-Relaxation to the next Start-of-Contraction points.

### Statistical analysis

The average result of the population for every measured parameter is compared to the control condition in the unpaired student t-test. Data are presented as means  $\pm$  SD. The value was expressed and compared using the raw values. (\*P < 0.05); (\*\*P < 0.01); (\*\*P < 0.001); (\*\*\*\*P < 0.0001).

## d. Results and discussions

### *Whole slide QPI analysis*

In evaluating different perspectives of cardiotoxicity assay of different compounds used in this experiment, we measured multiple parameters that can distinguish among possible drug mechanisms of action. We first tested the compound effect on beat rate frequency changes of the waveforms compared in control conditions and treated conditions due to the direct effects of the drug on particular ion channels. The beat rate frequency changes were observed in the contractile motion patterns of the whole slide QPI of multiple hiPSC-CMs compared to the control condition depending on the compound's mechanism of action.

The drug effect on the motion waveform manifests by changing the beat rate as a direct

consequence. The cardiomyocytes responded to isoprenaline with action potential shortening upon increases in stimulation frequency by increasing the drug concentration and increase in the beating frequency. The High concentration (500[nM]) of isoprenaline markedly increased the beating rate. The High concentration of E-4031 and, sertindole similarly demonstrated a reduction in beating frequency were 500 [ $\mu$ M] of E-4031 and 200 [nM] of sertindole significantly declined the beat frequency similarly. The cardiac cells in control condition share common characteristics. We quantified three whole slide QPI of multiple cardiomyocytes samples in the control condition as the representative for all control conditions and corresponding quantification parameters are demonstrated in table 2.5

Table 2.4: Quantitative parameters and corresponding description measured from the whole slide QPI cardiomyocyte of the control sample.

Parameter	Description	Values (Mean $\pm$ STD)
Maximum contraction speed	The average amplitude of contraction peaks.	1.5 $\pm$ 0.0209 [ $\mu$ m/s]
Beating period	The time between two adjacent contraction peaks.	1.8 $\pm$ 0.0086 [s]
Contraction period	The average time between the Start-of-Contraction and End-of-Contraction points.	0.352 $\pm$ 0.0158 [s]
Relaxation period	The average time between Start-of-Relaxation to the End-of-Relaxation points.	0.532 $\pm$ 0.0221 [s]
Maximum relaxation speed	The average amplitude of relaxation peaks.	1.1 $\pm$ 0.0176 [ $\mu$ m/s]
Resting period	The average time between the End-of-Relaxation to the next Start-of-Contraction points.	0.62 $\pm$ 0.0203 [s]

### ***Drug effects on contractile motion speed***

To characterize pharmacological effects on CMs contractile motion speed, we carried out the comparison of contraction motion speed before and after drug addition. However, the additional parameters are also evaluated to precisely evaluate the effect of drugs. We evaluated the

Sertindole, E-4031, and isoprenaline effects on CM motion speed along with other critical parameters and measure the contraction motion speed prior and after drug addition. Sertindole is the second generation of antipsychotic medication phenylindole-derived compound that functions as an antagonist at a portion of receptor systems [57].

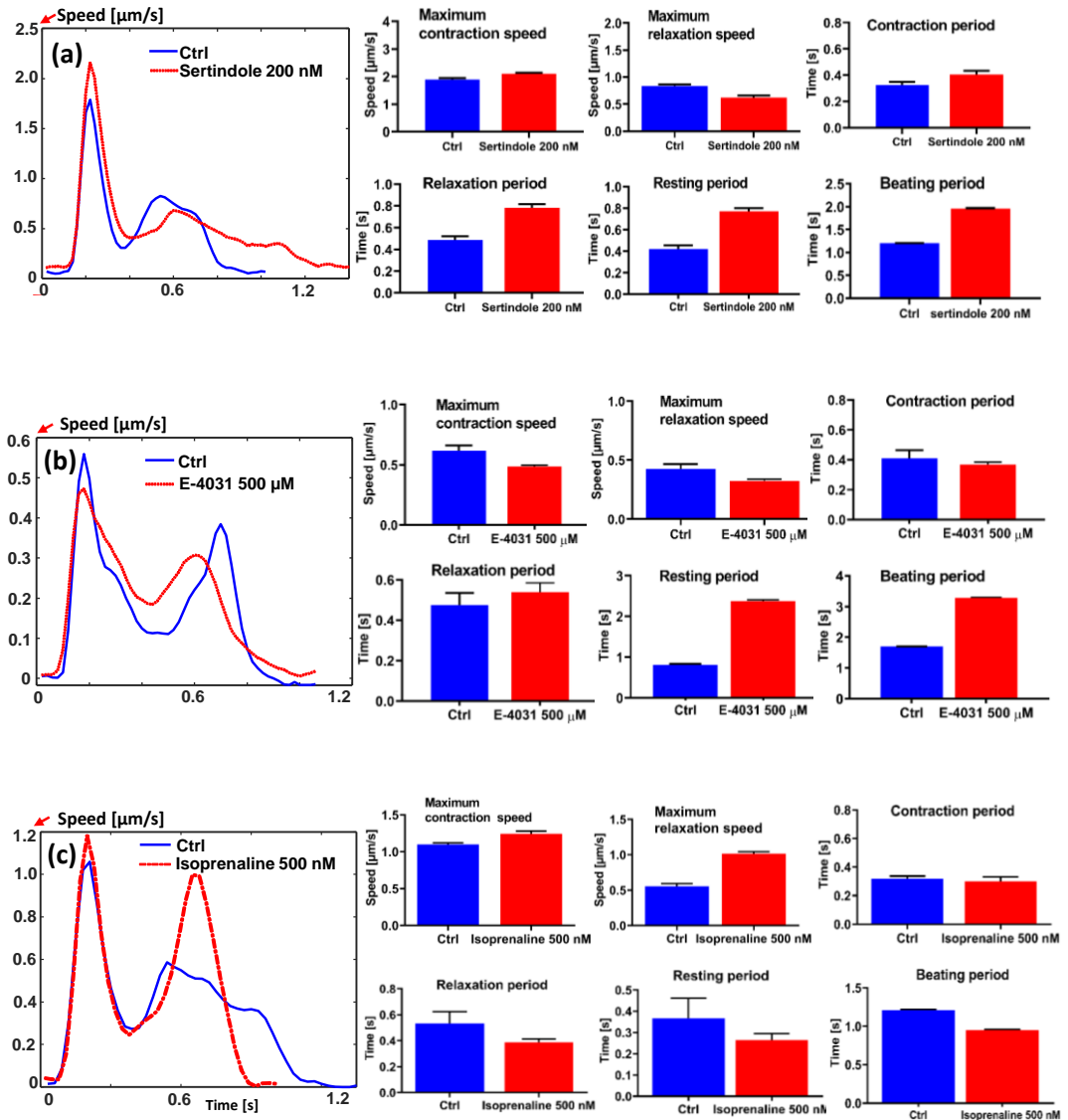


Figure 2.25: Representation of action potential motion speed evaluation of whole slide QPI in the presence of

different drugs versus the control condition. The bar charts on the right side show the variation of a critical parameter expressed in terms of mean and SD for control and treated conditions. (a) The contractile motion of whole slide QPI of multiple CMS in control and drug-treated conditions in response to 200nM sertindole, (b) in response to 500 $\mu$ M E-4031, (c) in response to 500nM isoprenaline and their corresponding quantification results.

The left panels of Fig 2.25 show the drug-treated cardiomyocyte motion speed evaluation versus control condition and the right panels show cardiomyocyte multi parameters measurements results. Figure 6(a) shows the contractile motion speed of the whole slide QPI in response to 200nM sertindole and corresponding quantification results. The Sertindole effect manifested by an increase in CM contraction motion speed while a decline in relaxation motion speed and repolarization being prolonged as a direct consequence. Afterward, we investigated the effect of E-4031 on CM's motion waveform. E-4031 is a potent and selective blocker of the inactivating inward rectifying potassium current (HERG channel). It has been previously reported that the treatment of cardiac cells with E-4031 significantly slowed the heart rate increased myocardial Ca<sup>2+</sup> uptake and attenuated the loss of intracellular K<sup>+</sup> in cardiac cells. Figure 2.23(b) shows the contractile motion of the whole slide QPI of the multiple CMs in control and drug-treated conditions in response to 500 $\mu$ M of E-4031, the contraction-relaxation motion speed is declined. The comparison of the critical parameters in control and drug-treated conditions in the presence of 500 $\mu$ M of E-4031 shows the contraction period is slightly decreased while it caused a prolongation in the relaxation period. The corresponding beating period and resting period are significantly raised thus the beating rate is declined. Finally, we carried out a similar experiment to evaluate the effects of the Isoprenaline. The isoprenaline compound is a beta-1 and beta-2 adrenergic receptor agonist that exert their effects through a G-alpha stimulatory second messenger system. Beta-1 adrenergic receptors primarily concentrate on the heart. The terminal effects of activation of beta-1/or 2 adrenergic receptors are an increase in intracellular calcium. By increasing the slope of phase 4, cardiac cells reach the threshold at a faster rate, resulting in the characteristic increased heart rate and higher contractility [58]. Figure

2.25 (c) shows the contractile motion waveform of the whole slide QPI of the hiPS-CM in control and drug-treated conditions in response to 500nM isoprenaline and corresponding quantification results. As can be seen from Fig. 2.23(c), contraction-relaxation motion speed is raised compared to the control condition in response to 500nM isoprenaline. The contraction-relaxation period, resting period, and beating period are declined.

### ***Quantification at the single-cell level***

To quantify the motion waveform related parameter at the single-cell level, First, we extracted seven single CMs and motion waveforms were generated using contractile motion speed measurement. Secondly, the computational algorithm was applied to extract several quantification parameters related to the motion waveform. Quantification parameters are measured for every single cell and a population average was computed in control and drug-treated conditions to represent the motion characteristics in response to each drug concentration. Consequently, we can observe changes in critical parameters before and after drug treatment. Since our current analysis captures the drug effects on the discrete population of individual cells, it is plausible that differences in contractile motion speed observed after averaging the population. The graph pad prism 8 software is used to conduct statistical analysis to detect significant differences between groups for other critical parameters.

### ***Effects of sertindole treatment***

The Sertindole effect manifested in CM with repolarization being prolonged as a direct consequence. Figure 2.26 shows the quantification of different parameters per each cell. By increasing the drug concentration, the contraction upstroke motion speed is raised while the relaxation motion speed is declined compared to the control condition. Also, alternation in critical parameters was observed including prolongation in the relaxation period, beating period,

resting period.

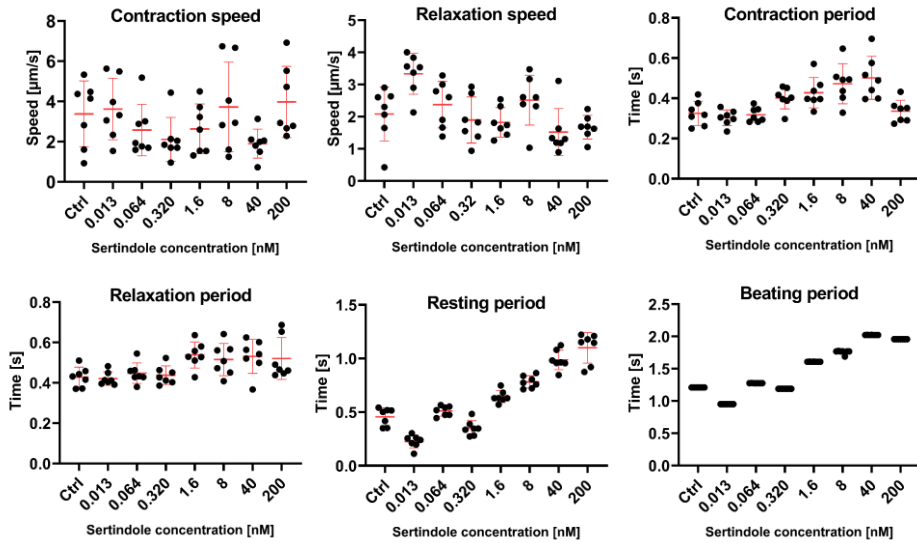


Figure 2.26 Multiple parameter measurements per each individual extracted cells in response to the sertindole with different concentrations. The corresponding effect of the drug by increasing the concentration on each cell's behavior was separately investigated.

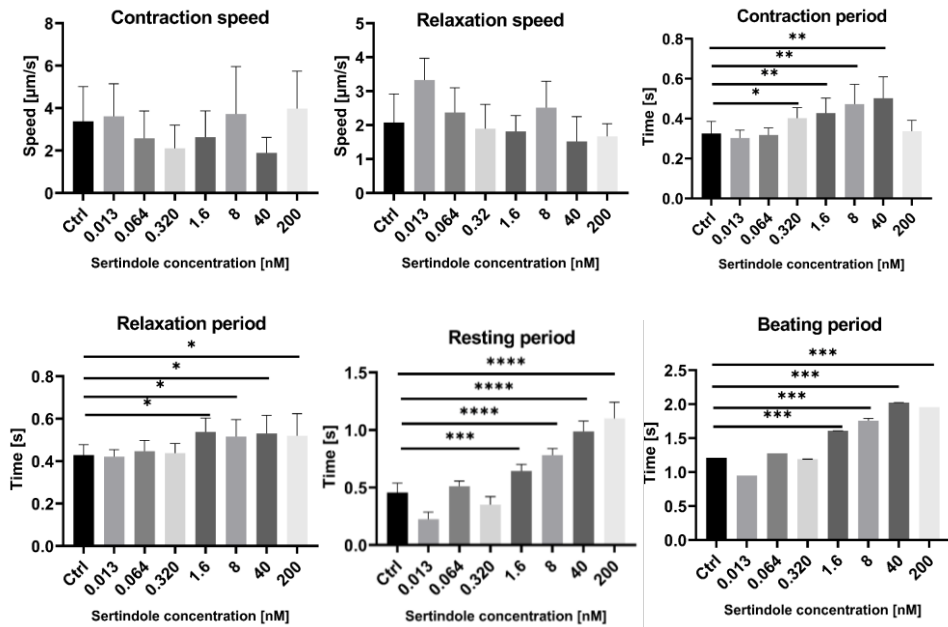


Figure 2.27. Effect of sertindole on critical parameters of the average population of single cells. The graph shows a summary of the changes in the mean and standard deviation. The unpaired t-test was performed to detect



significant differences between average groups.

As one can see from Figure 2.26, 27 the sertindole treatment exhibited significant prolongation of the resting time. As can be seen, Sertindole does not significantly change the contraction period while the relaxation period is significantly prolonged. There is variation in contractile motion speed between individual single cells while a declining trend was observed in averaging the population for relaxation motion speed. The difference level of the other critical parameters is evaluated by an unpaired T-test.

### *Effects of isoprenaline treatment*

isoprenaline, a b-adrenoceptor agonist, increased the beating rate frequency while decreasing the overall duration of each beat.

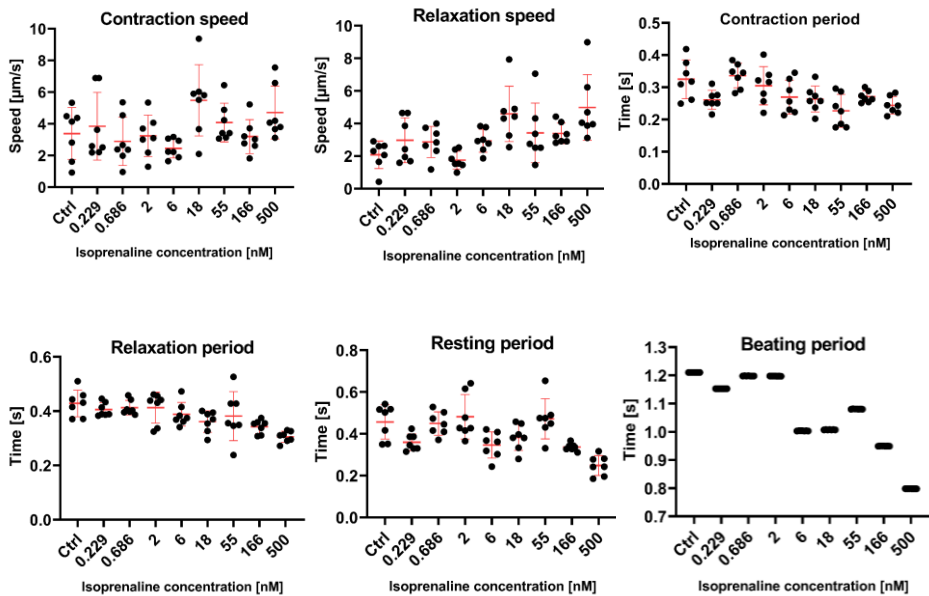


Figure 2.28: Multiple parameter measurements per each extracted cells treated with different concentrations of isoprenaline drug. The effect of the drug by increasing the concentration on each cell behavior is investigated.

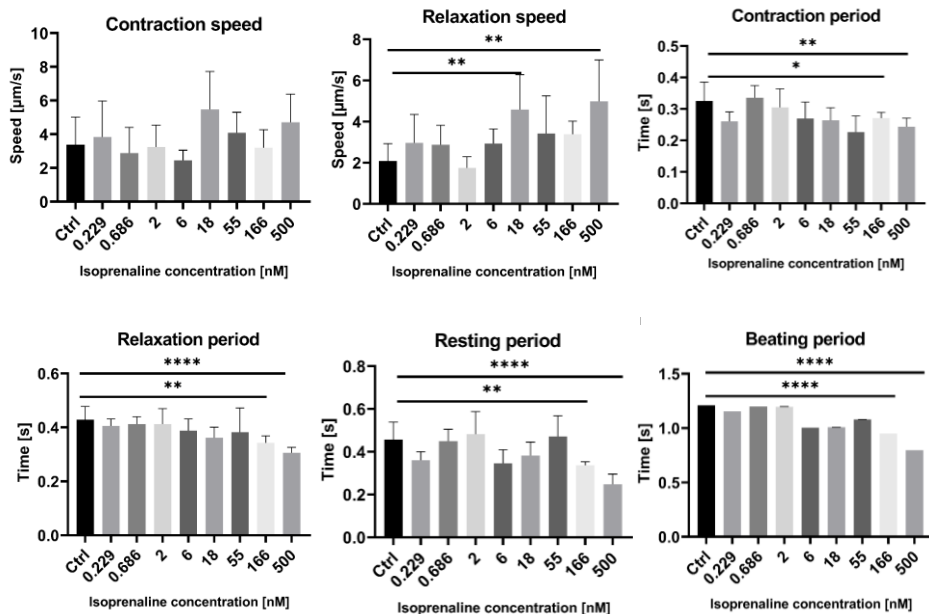


Figure 2.29: Characterization of the Effect of isoprenaline with different concentrations on critical parameters of the average population of single cells. The graph shows the changes in the mean and standard deviation of each quantification parameters calculated from the average of the single cells population. The unpaired T-test was performed.

Figure 2.28,29 shows the contractile motion of individual single cells and average of population in control and drug-treated conditions in presence of different concentrations of isoprenaline and corresponding quantification results. As can be seen from Fig.2.29 contraction-relaxation motion speed is raised compared to the control condition. Accordingly, the contraction-relaxation period, resting period and, beating period are declined due to the increase in beating frequency.

### *Effects of E-4031 treatment:*

We monitored the effects of E-4031 (a class III antiarrhythmic drug). The E-4031 declined

contraction and relaxation motion speed and prolonged the resting period of hiPSC-CMs depending on the concentration level which is in line with our previous study.

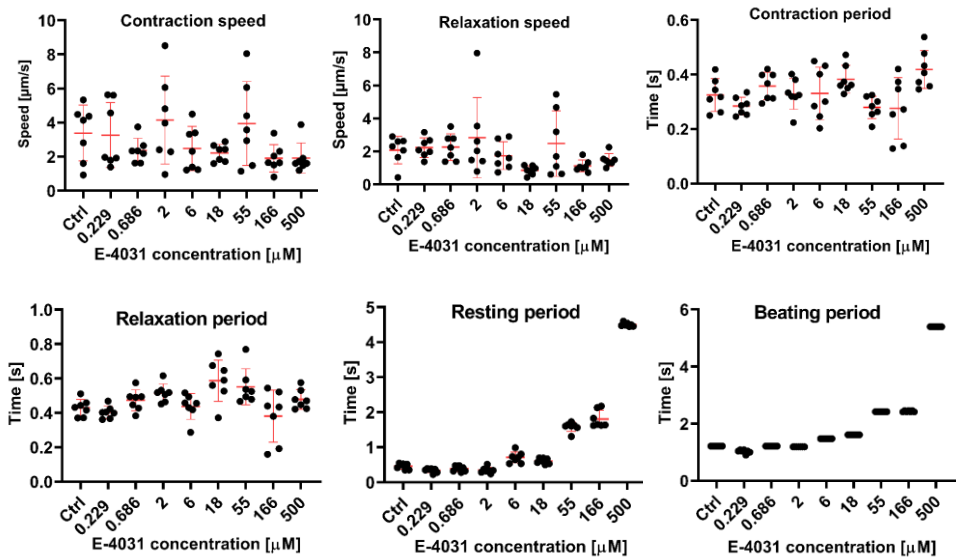


Figure 2.30: Assessment of multiple parameters per each cardiac cells. The effect of the E-4031 different concentrations of the drug on each cardiomyocyte is shown.

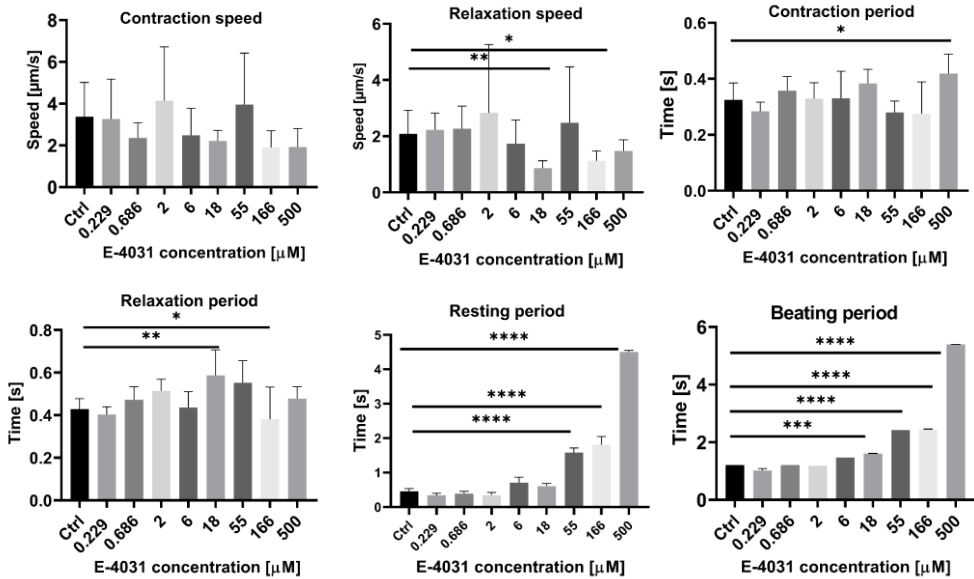


Figure 2.31: Characterization of the effect of E-4031 with different concentrations on critical parameters of the average population of single cells. The graph shows a summary of the changes in mean and standard deviation calculated from the average of the single cells population.

All drugs have one principle common to share the ability of alternation in the resting period and thus in beating frequency as regards their mechanism of action and could often be selected based solely on this criterion. However, the degree of changes in beating frequency varies significantly between different levels of drug concentrations.

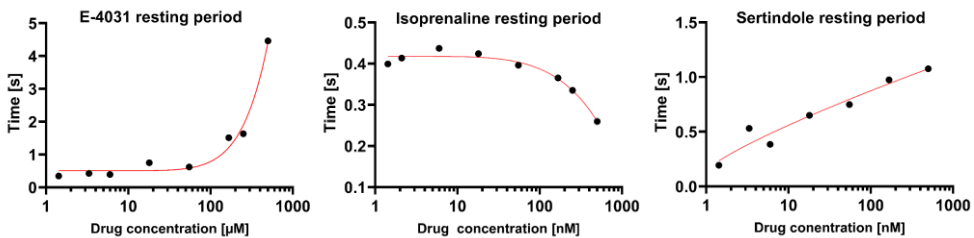


Figure 2.32: The average resting period of single cells population in the presence of different drug concentrations of E-4031, isoprenaline, and sertindole.

Different concentrations of E-4031 the resting duration dramatically changes with the increasing of E-4031 concentration and thus results in the beat duration increase .From Fig. 13 one can see by increasing the concentration of the isoprenaline, the resting period will gradually decrease and thus the beating frequency rises. The underlying mechanism sertindole compound shows the ability to increase in resting period linearly by increasing the concentration.

### ***Discussion***

Various shortcomings are found in the state-of-the-art methods for *in vitro* detection of changes in drug-induced cardiac contractility. However, a single cardiomyocytes contractile motion characterization is challenging. The present study aimed to evaluate the contractile characteristics of single drug-treated cardiomyocytes by measuring changes in beating frequency along with other comparable baseline parameters form the quantitative phase images that allow measuring hiPSC-CMs kinetic responses of drugs at the single-cell level which cant be identified ordinary methods. we present a novel system for contractile motion characterization of single cardiomyocytes by a combination of dense Farneback optical flow method and quantitative phase images (QPI) that can identify drug-induced cardiac effects at the single-cell level. The effects of three drugs (Sertindole, Isoprenaline, and E-4031) in different concentrations are effectively analyzed. Our experimental results of E-4031 and Isoprenalie showed good agreement with a previous study <sup>25</sup>. Isoprenaline exhibited a rise in contraction-relaxation motion speed while sertindole cause only increases in contraction motion speed, in contrast, declined the relaxation motion speed and significantly prolonged relaxation period. E-4031 showed a decrease in both contraction-relaxation motion speed. All drugs cause alternation in the resting period thus changed the beating frequency. All drugs investigated in this study also affected other critical parameters including (contraction-relaxation period, beating period and resting period). The goals of these experiments were to not only monitoring the kinetics of single CMs but also

measure other critical parameters regarding the beating activity profile generated using contractile motion speed measurement. Measured features from the contractile motion profile at the single-cell level are including (Maximum contraction-relaxation motion speed contraction-relaxation period, beating period, and resting period ). We have shown that the current platform can quantitative prediction of the potential cardiotoxicity by single CM kinetics monitoring and can be used to promote the maturation of *in vitro* hiPSC-CMs and reduce animal testing for cardiac safety screening.

### **e. Conclusions**

In this paper, we used the combination of quantitative phase images obtained from DHM and dense Fareneback optical flow methods for motion characterization of single cardiomyocytes in control and drug-treated conditions. The motion waveform generated from the proposed method further provided complementary information about critical parameters regarding CM's beating activity profile. The effects of three drugs (Sertindole, E-4031, and isoprenaline) were analyzed. The system includes two parts: first, we extract multiple single cardiac cells from the whole slide of QPI and calculated the contractile motion speed of beating cells using a dense Farenack optical flow method. Our experimental results of Sertindole treated CMs exhibited raise in contraction motion speed while the decline in relaxation motion speed. Other critical parameters E-4031 treated cardiomyocytes show that the decrease in contraction-relaxation motion speed while the concentration of E-4031 increases the resting duration. We also found out that contraction duration is shorter than the relaxation duration. Isoprenaline shows its effect on the sample by increasing both contraction-relaxation motion speed and results in to decrease in the resting period. our experimental results represent thus a promising label-free approach for drug discovery.

## **D. Integrated platform for simultaneously monitoring human cardiomyocytes contractile motion and kinetics force generation at the single-cell level from holographic imaging informatics**

### **a. Abstract**

We describe a novel platform for in vitro monitoring contractile motion and force generation of the human induced pluripotent stem cell-derived cardiomyocytes(hiPS-CM) at the single-cell level from digital holographic imaging informatics. We extract single CM dry mass using an FCN model. Consequently, the Farneback optical flow method was applied to measure the single CM contraction kinetics, force generation using dry mass redistribution monitoring. We demonstrate the proposed approach allows multiple analyses of single CM contractility from motion waveform including contractile force, speed, acceleration, velocity along with temporal parameters including contraction period, relaxation period, resting period, beating period. The applicability of the CM force measurement method was tested to reveal the pharmacological effects of two cardiovascular drugs, isoprenaline (166nM, 500nM) and E-4031 (166 $\mu$ M, 500 $\mu$ M), on whole slide QPI in comparison to the control condition. Validation of our approach was tested by measuring the contractile force generation of live cardiomyocytes versus fixed cardiomyocytes. The experimental results demonstrate that the cardiomyocytes responded to isoprenaline by increasing the action potential (AP) contractile force with a decrease in the resting period. In the presence of E-4031, the AP contractile force was declined and the resting period was prolonged. Accordingly, our CM force measurement method has the potential application in the study of cardiac disease, drug discovery, and cardiotoxicity screening.

## **b. Motivations and introductions:**

Heart failure contributes to a major cause of mortality around the world. Cardiomyocytes (CMs) muscle cells are the main elements of the human myocardium that produce force to pump the blood to the entire body through spontaneous contraction-relaxation mechanical beating activity [59]. The main functionality of the cardiac muscle cell is the ability to spontaneous contraction-relaxation beating activity by dry mass redistribution leading to generate contractile force. The quantification of the contractile forces generation and the cardiac motion activity at the single-cell level allows interpreting the relationship between mechanical and biochemical signaling pathways [60]. Human-induced pluripotent stem cell-derived cardiomyocytes (hiPSC-CMs) are elastic elements used for in vitro human disease modeling and cardiotoxicity screening [61]. The simultaneously monitoring human cardiomyocytes contractile motion and force generation at the single-cell level can provide valuable information about cell functionality and health [62]. Digital holographic microscopy (DHM) is a promising tool for real-time monitoring cardiomyocytes dry mass redistribution by providing a quantitative phase image (QPI) in a label-free manner [63–66]. By simultaneously monitoring single CM contractile motion and kinetics force generation, one can ensure the muscle cell health and proper behavior [67,68]. To date several different methods previously reported for CM force generation assessment using highly specialized advanced instrumentation including fluorescent microsphere-based traction force microscopy and atomic force microscopy [69–76]. The biosensors are the most widely used tool utilized for simultaneously monitoring cardiac cell mechanical beating activity and contractile force [77, 78]. These need expensive equipment or cardiomyocytes to be cultured into specific materials which render the process challenging and may alter the originality of the samples. Yet there is a lack of a simplified platform for single CM motion monitoring to provide detailed information about contractile motion and force generation at the single-cell level. Optical flow-based



methods are low cost, high throughput, contactless, methods able to real-time motion tracking of the cardiomyocytes without physical contact which preserves samples originality [77-80]. While cardiac cell beating activity, dry mass redistribution occurs which leads to force generation. Single CM dry mass size can be precisely measured from QPI images captures using DHM [81,82]. The cell's dry mass size has a strong correlation with the amount of the force generated by single cardiac cells. Precise measurement of the cells dry mass from QPI is crucially important for subsequent contractile force measurement. A fully convolutional neural network (FCN) method is a promising tool for single CM's contour extraction from QPI images [83–86]. We previously reported an FCN-based method for single CM functional behavior characterization using nucleus extraction from QPI images [87]. This rapid dry mass screening using DHM can be useful for high-throughput, low-cost monitoring for compound toxicity screening. Furthermore, we previously established an optical flow-based method for motion characterization of the single cardiac cells. We successfully demonstrated the applicability of the optical flow-based method for single CM motion characterization of drug-treated cardiomyocytes. The proposed optical flow-based method can yield several temporal and dynamic parameters related to the beating activity of single CMs.

Here we present a novel contactless and low cost in vitro platform allowing us simultaneous monitoring of the cardiac mechanical beating activity and force generation at the single-cell level combined with digital holographic imaging informatics. Our proposed method is a combination of the fully convolutional neural network and optical flow method which can return functional parameters for in vitro single CM motion and force generation analysis simultaneously. In the first step, we extracted seven single cardiac cells from whole slide QPI of multiple cardiomyocytes and removed the unnecessary background to measure the cell dry mass precisely using a fully convolutional neural network. Secondly, we tracked the spatial-temporal coordinates  $x$ ,  $y$  of the cell dry mass while beating activity using the Farneback optical flow method. This allowed us to monitor contractile force along with multiple parameters related to

dynamic beating activity of the cell (contractile force, speed, velocity, acceleration ) in addition to multiple temporal beating activity-related parameters (contraction period, relaxation period, resting period, beating period). The applicability of CM contractile kinetics and force generation of the proposed method was tested to reveal the pharmacological effects of two cardiovascular drugs, isoprenaline (166nM, 500nM) and E-4031 (166  $\mu$ M, 500 $\mu$ M), on whole slide QPI of multiple cardiomyocytes compared to the control condition. The results demonstrate that the cardiomyocytes responded to isoprenaline by increasing the action potential (AP) contractile force with a decrease in the resting period. In the presence of E-4031, the AP contractile force was declined and the resting period was prolonged. Validation of our approach was tested by measuring the contractile force generation of live cardiomyocytes versus fixed cardiomyocytes.

### **c. Materials and methods**

#### **Single cardiomyocytes dry mass extraction using fully convolutional neural network**

Convolutional neural network (CNN) models are based on the sequential application of the convolutional layer, where the output of one convolution layer is the input to the next one. CNN captures features of input data via multiple consecutive convolution kernels followed by max-pooling layers for data dimension reduction. CNN mainly consists of the following elements. 1) A set of learnable filters to extract local features. 2) A nonlinear function as an activation function and 3) a max-pooling layer that aggregates the local feature specification to reduce the data dimensions. However, depending on the different tasks, different network architectures are proposed which might be more efficient than simple CNN-based networks [25, 34]. A fully convolutional neural network (FCN) is a type of CNN in which the fully connected layer is replaced with another convolution layer. We extracted a single CMs region of interest (ROI) from whole slide QPI using our proposed FCN Model in [87] (see Fig. 2.33a). The segmented region mostly includes the nucleus section (see Fig. 2.33b).

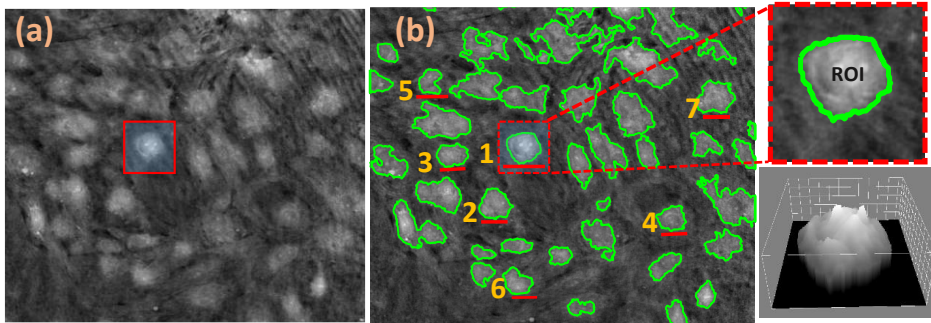


Figure 4.33. Steps of single CM dry mass extraction using a fully convolutional neural network. (a) original QPI of multiple CMs, (b) single CMs captured using the FCN model marked with the green line, inset shows a single CM dry mass denoted with a green line (top), 3D representation of single CM dry mass (bottom).

### *Single CM motion tracking with Farneback optical flow*

The Farneback algorithm is a dense optical flow method that performs motion tracking in multi-resolution levels. The Farneback method uses a polynomial expansion for displacement estimation. In the first step, the algorithm generates a hierarchy of resolution levels from the original image using Gaussian pyramids, where each level has a lower resolution compared to the previous level. The tracking starts from the lowest resolution and continues to the highest resolution. Displacement of two local patches in consecutive image frames is calculated by approximating the neighborhood of each pixel with a quadratic polynomial [53].

The tracking is refined in each resolution level by initializing from the lowest resolution level to the highest resolution. The detected tracking points at each level are the base point for the next level and large displacement can be detected.

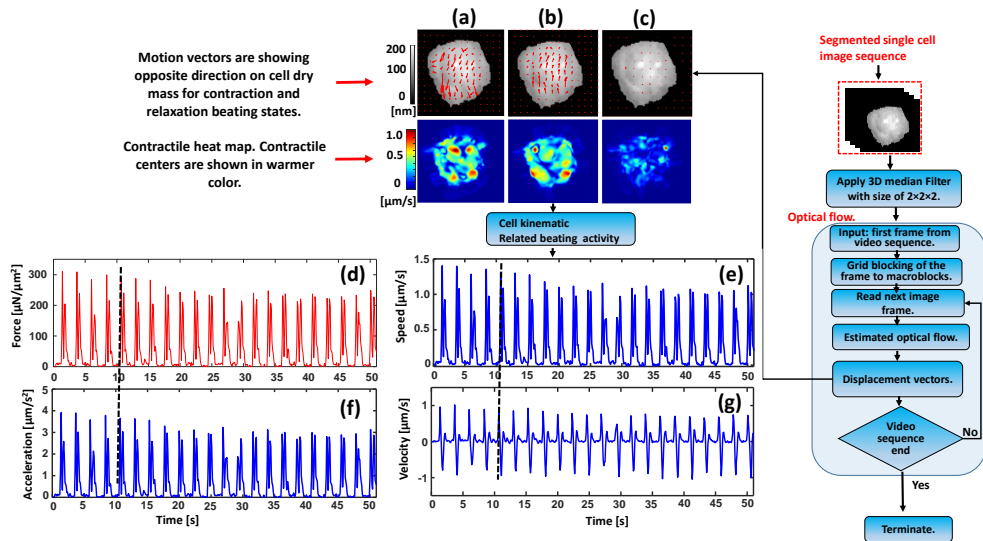


Figure 2.34 The workflow of single CMs kinematic beating activity signal extraction. Single CM dry mass extracted using FCN method with superimposed motion vectors for contraction (a), relaxation (b), resting (c) (top) and their corresponding heat map (bottom), (d) Single CM's contractile force profile, (d) single CM motion speed profile (f), motion acceleration profile, (g) motion velocity profile.

Seven single CMs are extracted using the FCN model from different parts of the cardiomyocytes QPI. The extracted cell area mostly includes the nucleus section which is the center of the motion. While the cardiac cell's beating activity, by repeating the optical flow procedure shown in Fig. 2.34, an array of motion vectors is generated which shows the CM's motion direction and the kinetics waveform is generated. A single cardiac cell with superimposed motion vectors on the image referring to the motion directions for different beating statuses for contraction, relaxation, and resting beating status respectively (Fig. 2.34(a, b, c) top). The corresponding heat map generated from absolute motion for each beating status is shown in (Fig. 2.34(a, b, c) bottom). Heat map represents the specific regions of the cells which is a center of contraction. Consequently, the single CM's contractile force profile, motion speed profile, motion acceleration profile, motion velocity profile ((Fig. 2.34(d, e, f, g) respectively)) was generated. This led us to normalize all force measurements to the cell area to obtain a more accurate representation of cellular contractile performance.

*Single CM dry may measurement*

**Projected cell area:** stands for the cell area size calculated as follow.

$$S = NP^2 \quad (13)$$

Where N stands for the number of pixels inside the cardiac cells and P denotes the pixel size (here is 0.28 $\mu$ m).

**Dry mass (DM)** denotes the mass of the cardiac cell:

$$DM_{pg} = \frac{10\lambda}{2\pi a} \int_s \phi ds = \frac{10\lambda}{2\pi a} \Phi s \quad (14)$$

where  $\lambda$  is the wavelength of the light source (666 nm),  $\Phi$  is the average phase value induced by the the whole cell, a is known as the specific refraction increment (0.002 m<sup>3</sup>/Kg) [24].

### ***Kinematic parameters quantification***

Table 2.6 Description of kinematic parameters measured for each extracted single cardiac cell.

Parameter name	Equation	Description
Displacement	$Displacement_{\mu m} = \sqrt{(dx)^2 + (dy)^2}$ ,	The displacement between two consecutive movie frame
Speed	$Speed_{\mu m/s} = \frac{\sqrt{(dx)^2 + (dy)^2}}{Time}$ ,	The motion speed between two consecutive image frame
Velocity	$Velocity_{\mu m/s} = \frac{dx + dy}{Time}$ ,	The cardiac cell velocity between two consecutive image frames
Acceleration	$Acceleration_{\mu m/s^2} = \frac{Velocity}{Time}$ ,	The acceleration between two consecutive frame
Force	$Force_{\mu N} = Acceleration \times DM$ ,	Single CM kinetics force generation

where  $dx$  and  $dy$  are displacements in  $x$  and  $y$  directions estimated by Farneback optical flow method representing CM motion in the  $x$  and  $y$  direction, and time is considered as the time between two consecutive frames.

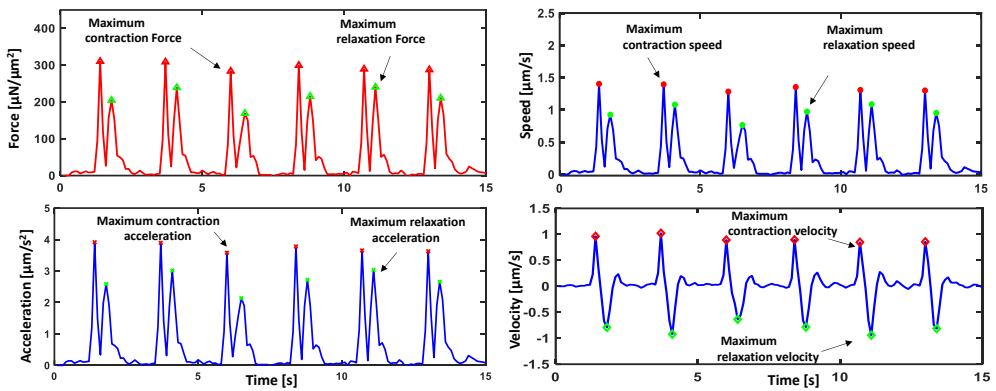


Figure 2.35. Schematic of single cells kinematic signals quantification using contraction-relaxation peak identification method.

The CM beating activity quantification was analyzed using an automated contraction-relaxation peak identification using the Otus thresholding method along with multiple auxiliary points for precise kinetics and temporal parameter quantification method proposed in [87].

*CM Beating activity temporal parameter quantification.*

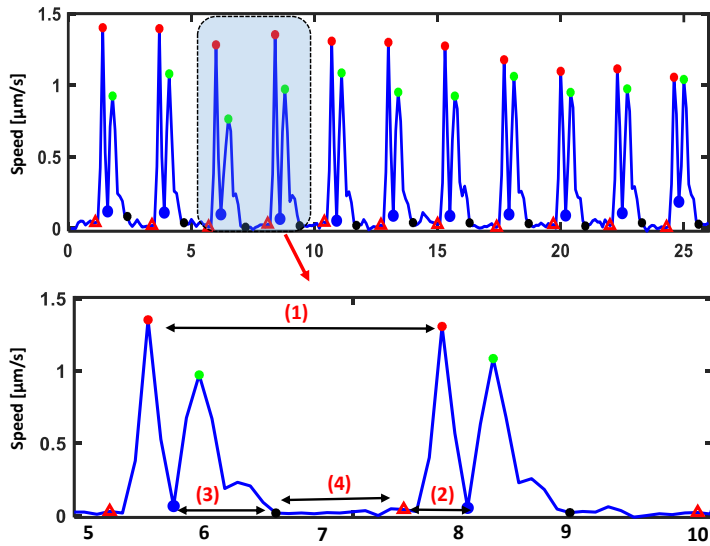


Figure 2.36. Details of beating activity related temporal parameters quantification calculated from motion speed waveform explained in the table 2.7.




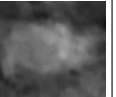
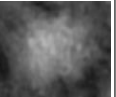
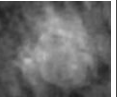
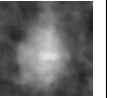
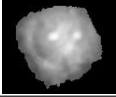
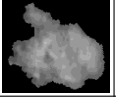
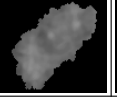
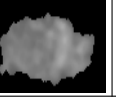
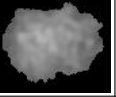
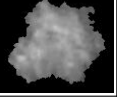
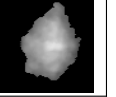
Table 2.7 Description of temporal parameters measured for each extracted single cardiac cell.

Dynamic parameter		Description
Contraction	Beating period [see #1 in Fig. 2.36 inset]	The time between two adjacent contraction peaks
	Contraction period [see #2 in Fig. 2.36 inset]	The average time between the Start-of-Contraction and End-of-Contraction points
Relaxation	Relaxation period [see #3 in Fig. 2.36 inset]	The average time between Start-of-Relaxation to the End-of-Relaxation points
Resting	Resting period [see #4 in Fig. 2.36 inset]	The average time between the End-of-Relaxation to the next Start-of-Contraction points

#### d. Results and discussion

In this study, we aimed to develop a high throughput method for simultaneous monitoring of single human cardiomyocytes contractile motion and kinetics force generation along with temporal beating activity-related parameter assessment. The cardiomyocytes kinetic related parameters which are related to the cardiac cell's ability to produce force is its morphology, including total cell area and dry mass sizes. The relationship between cell mass area and the amount of generated force is important. Using the FCN we have precisely extracted the cell mass area and investigated the correlation between cell size and produced force. Table.3 shows the extracted single cells from whole slide QPI of multiple cardiac cells and cells dry mass extraction using the proposed FCN based network model.

Table 5.8 The single CM quantitative images before and after segmentation for precise cell dry mass extraction using a fully convolutional neural network method.

Cell number	Cell #1	Cell #2	Cell #3	Cell #4	Cell #5	Cell #6	Cell #7
Original QPI of single cardiomyocyte							
Extracted cell dry mass using FCN							

Cell area size depends on the cells' maturation level. The cells' dry mass is precisely extracted using the FCN model.



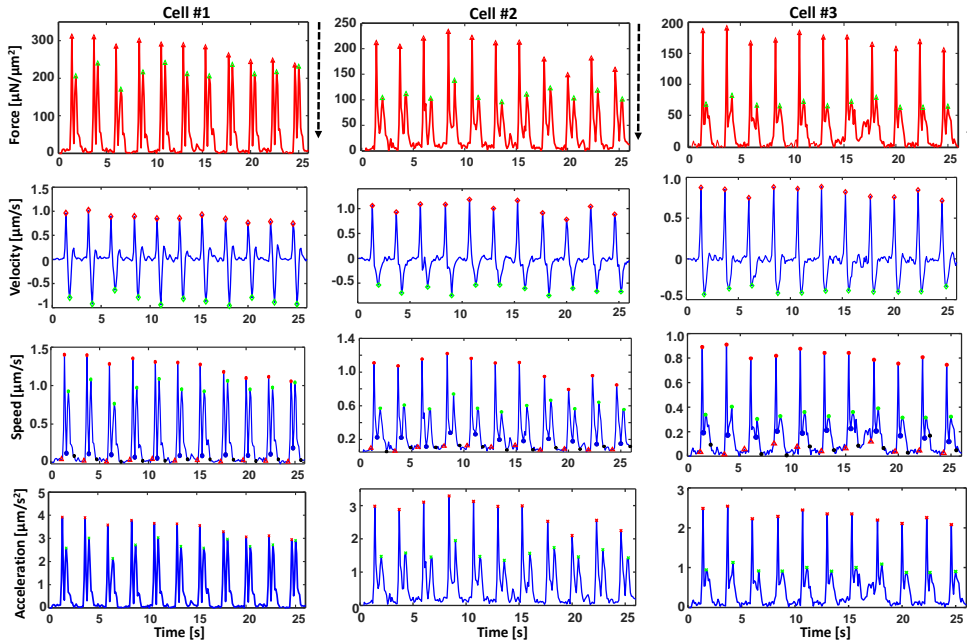


Figure 2.37 Single CMs (#1 to #3) autonomous mechanics beating activity signals.

Figure 2.37 demonstrates the mechanical beating activity signal of single CMs (#1 to #3). Our proposed method can analyze both the direction and magnitude of the vectors which provides more detailed information. The single CM study allowed us to study the properties of temporal and cell-autonomous mechanics which can be used for the health and function of the single CMs. Currently, little is known about single hiPSC-CM kinematics force generation. The maximum peak force of contraction and relaxation action potential were extracted using an automated peak identification technique. Besides, using motion waveform generated from cell kinematics beating activity, we can monitor contraction and relaxation beating activity duration. Single CMs produce different amounts of force. The contractile force generation is in direct relation with the cell's mass size. To normalize the force generated by variation of different cells with different area sizes, the total force was normalized to cell surface area and expressed as ( $\mu\text{N}/\mu\text{m}^2$ ).

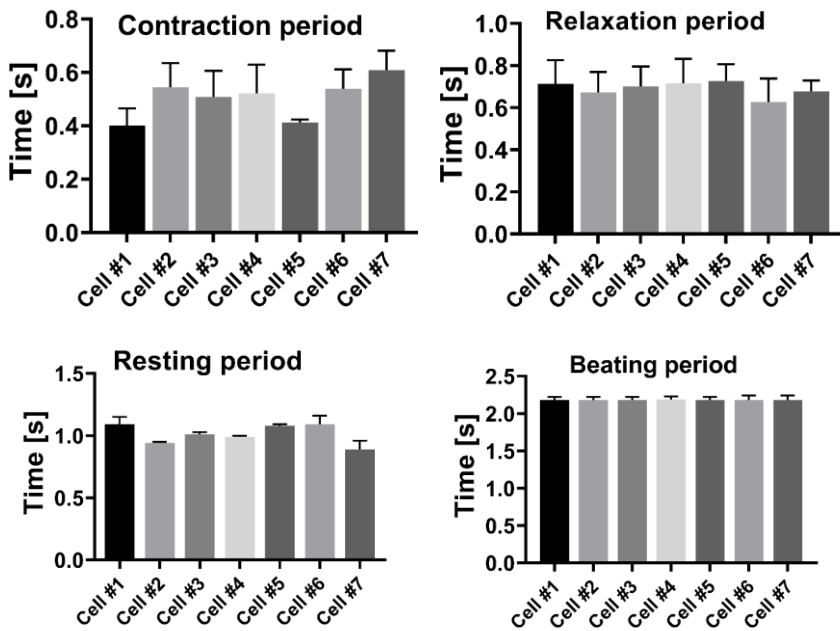


Figure 2.38. Single CM beating activity-related temporal parameter quantification results.

Figure 2.38 demonstrates the temporal beating activity quantification results. As can be seen, there is a small variation in the contraction period between single cells while the relaxation and resting beating activity duration show almost similar results for all extracted single cells. The beating period shows a similar period for all extracted single cells meaning they are beating at regular intervals. This phenomenon demonstrates the synchronization of the single cells in beating activity. We have precisely measured the temporal beating activity using the peak identification method for every single cell and demonstrated the importance of the temporal parameters. Single CMs kinematics analysis is an important functional readout for cardiotoxicity screening applications.

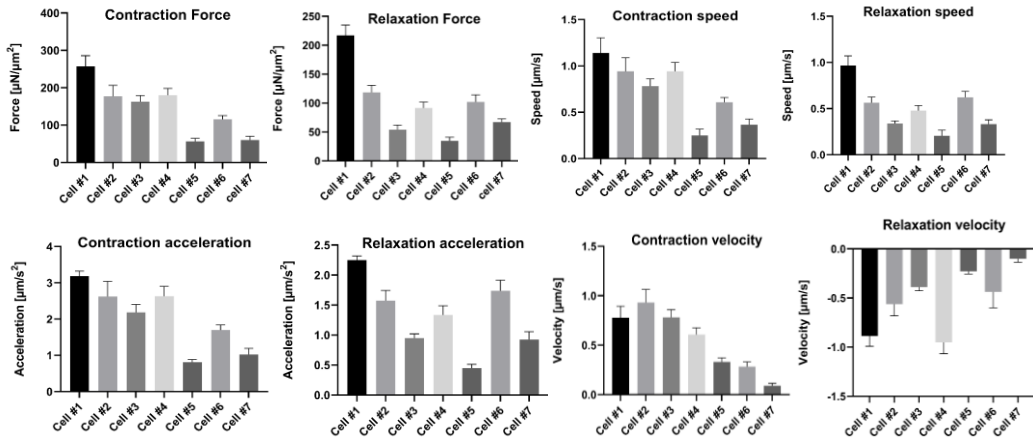


Figure. 2.39. Single CM kinetic beating activity quantification results.

Figure 2.39 demonstrates the maximum contraction force and speed is larger than the maximum relaxation force and speed. Accordingly, the maximum contraction acceleration is larger than the relaxation acceleration.

### *Quantitative Analysis of CM Function in Response to E-4031 and Isoprenaline*

To evaluate the sensitivity of our methodology in detecting the effects of the pharmacological substance on CMs kinetics, force generation, and temporal parameters, we examined the dose-response of two cardiovascular drugs used widely in cardiovascular research (E-4031, isoprenaline).

#### *Quantitative Analysis of CM in Response to E-4031*

E-4031 is a known class III antiarrhythmic drug that blocks the  $\text{K}^+$  channel and subsequently prolongs the AP interval.

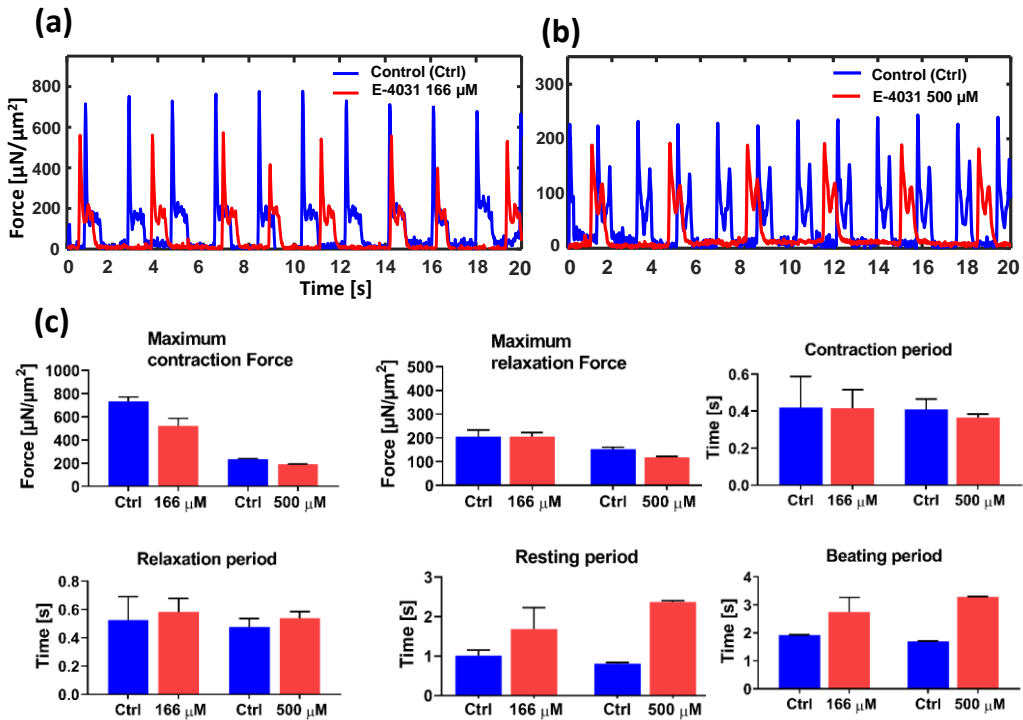


Figure. 2.40. Cardiomyocytes response to 166  $\mu\text{M}$ , 500  $\mu\text{M}$  of E-4031 drug kinetic force generation, and beating activity temporal parameters analysis in control (ctrl) versus drug-treated conditions. (a) whole-slide QPI contractile force profile in control versus drug-treated conditions in response 166  $\mu\text{M}$ , 500  $\mu\text{M}$  of E-4031(a, b), (c) quantification results in comparison of the control conditions (blue bars) versus drug-treated conditions (red bars).

Figure 2.40 (a,b) demonstrates a whole-slide QPI of multiple CMs contractile force profile in control versus drug-treated conditions in response to 166  $\mu\text{M}$ , 500  $\mu\text{M}$  of E-4031. Analysis of E-4031, a  $\text{K}^+$  channel blocker known to prolong the AP interval was expected to reduce the contractile force generation and prolongation of beating activity intervals. The experimental analysis demonstrated the cardiomyocytes responded to the E-4031 drug by decreasing the contractile force generation and prolongation of the beating period. The cardiomyocytes respond to E-4031 drugs were further examined on for temporal beating activity parameters for better comprehend analysis and the ability of the force measurement method to differentiate between different drug concentrations multiple parameters from waveforms has been pursued. The

quantification analysis demonstrated E-4031 prolonged resting period. Besides, the cardiomyocytes demonstrated a slight prolongation of the relaxation period.

*Quantitative Analysis of CM in Response to isoprenaline*

The proposed cardiomyocytes contractile force generation method was further examined on two different concentrations of isoprenaline.

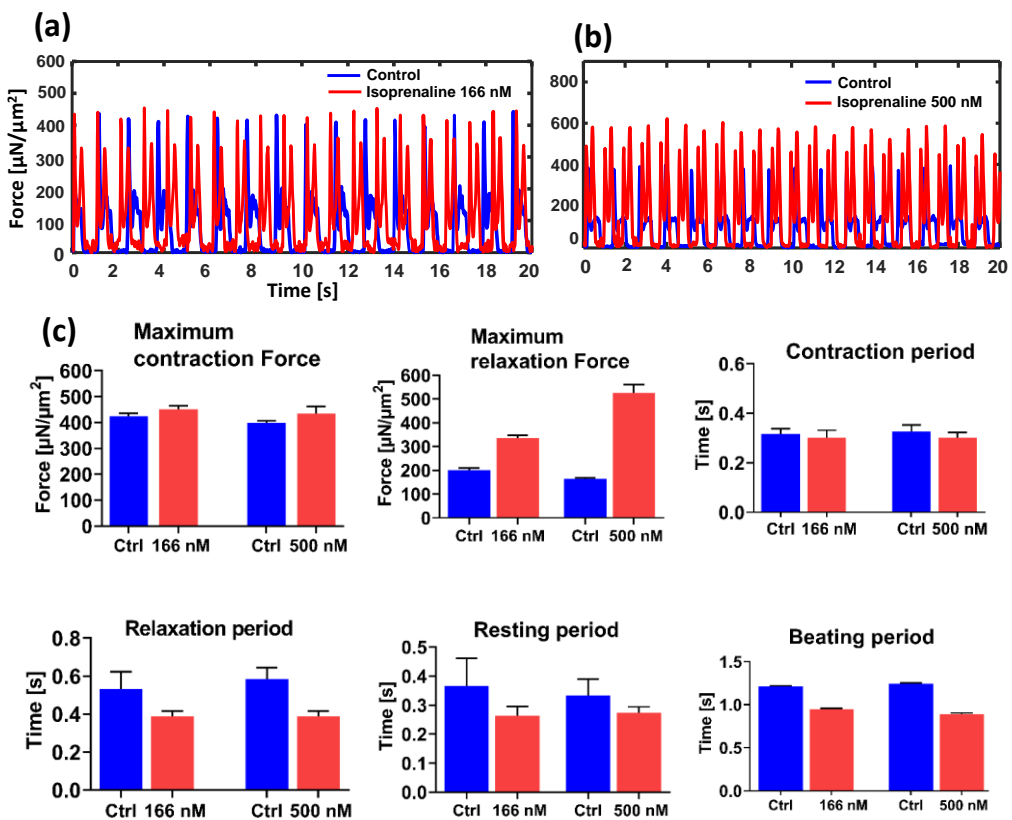


Figure. 2.41. Cardiomyocytes response to 166 nM, 500 nM of isoprenaline drug kinematic force generation and beating activity temporal parameters analysis in control (ctrl) versus drug-treated conditions. Whole-slide QPI contractile Force profile in control versus drug-treated conditions in response to 166 nM (a), 500 nM (b) of isoprenaline, (c) quantification result comparison of the control conditions (blue bars) versus drug-treated

conditions (red bars).

We analyzed the cardiomyocyte's response to 166 nM (Fig. 2.41a), 500 nM (Fig. 2.41b) of isoprenaline drug kinematic force generation and beating activity temporal parameters analysis in control (ctrl) versus drug-treated conditions (Fig. 2.41c). Isoprenaline demonstrated an increase in CM contractility. The cardiomyocytes responded to isoprenaline drug by increasing the contractile force generation. For a better understanding of the isoprenaline drug effect on temporal beating activity properties, we analyzed multiple temporal parameters related to the beating activity. The experimental result demonstrated the cardiomyocytes responded to isoprenaline drug by a reduction in beating activity intervals along with a decrease in resting period thus raised the beating frequency. Besides, the relaxation period demonstrated a reduction.

#### ***Verification of the proposed method***

Afterward, We validated this quantitative analysis of beating frequency (BPM) correlation with contractile force generation using Pearson's correlation coefficients. We found Pearson's correlation coefficients of above 0.91 for isoprenaline treated cardiomyocytes (see Fig.2.42a). Pearson's correlation analysis for E-4031 demonstrated a moderate coefficient (0.32) between contractile force generation and beating frequency (see Fig.2.42 b).

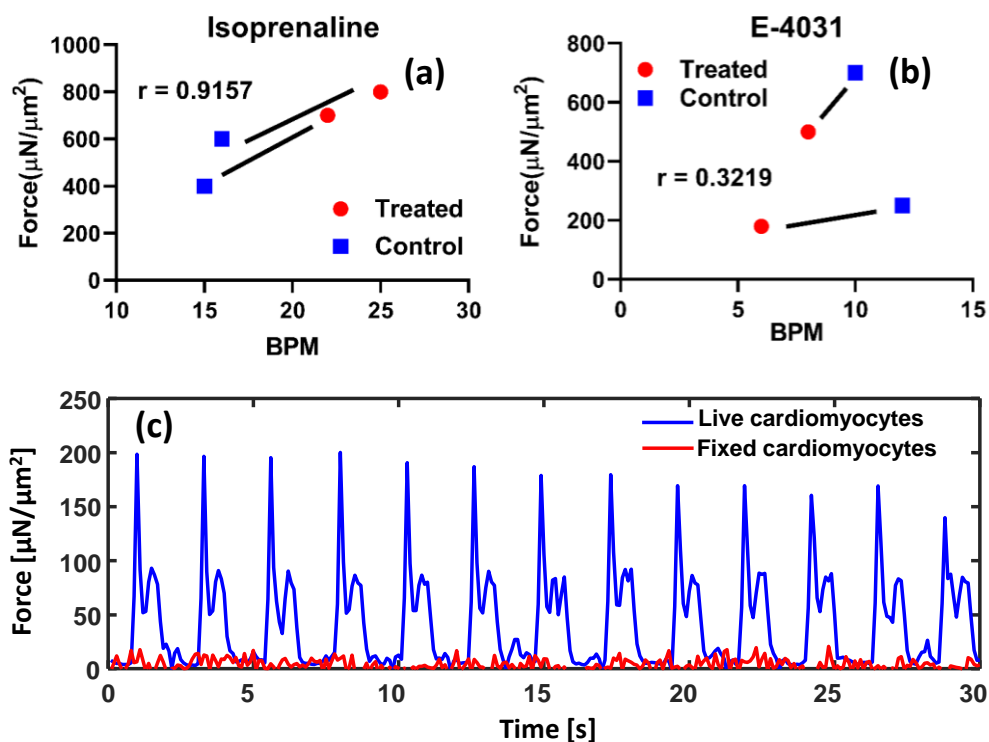


Figure. 2.42. Pearson's correlation analysis (Pearson's  $r$ ) between beating frequency and contractile force generation. (a) Isoprenaline, (b) E-4031, (c) Contractile force measurement of fixed cardiomyocytes versus live cardiomyocytes.

The method was verified by measuring the contractile force generation of fixed cardiomyocytes versus live cardiomyocytes (Fig. 2.42b). The amplitude of the contractile force of fixed cells fluctuates around zero. The amplitude is much smaller than both contraction-relaxation peaks and similar to the amplitude of the resting state.

The advent of human-induced pluripotent stem cell-derived cardiomyocytes has opened new prospects for cardiotoxicity screening and disease modeling. The major obstruction in lengthy and costly drug discovery processes is the lack of high throughput, a user-independent method for identifying understanding cardiotoxicity potential of pharmacological substance on single cardiomyocytes. Single CM contractile kinetics, and force generation characteristics is a

challenging task. The traction force microscopy (TFM) approaches is the most widely used method for the measurement of the contractile force of CMs require the use of fluorescent microspheres. This study describes an advanced label-free method for single CM kinetics of force generation analysis using a combination of a fully convolutional neural network and dense Farneback optical flow method form holographic images. In the first step, the single CM's dry mass was precisely extracted using the FCN model. We then applied Dense Farneback optical flow to monitor CM's dry mass redistribution form video microscopy and measured several kinetic related parameters per every single CM. We demonstrate our approach allows the assessment of contractile kinetics and force generation in a fully automated user-independent manner. We quantified the following parameters from a single CM. (1) Contractile force. (2) motion speed, (3) motion velocity, (4) motion acceleration. Furthermore, several temporal beating activity-related parameters (contraction period, relaxation period, resting period, and beating period) were measured from a single CM motion waveform. An automated peak identification algorithm marked the contraction and maximum relaxation peaks for all contraction kinetics and marked them for visual quality control. The proposed computational algorithm for peak identification method allows robust measurements of contraction kinetics. Therefore, the proposed automated system is well suited for monitoring the effects of the pharmacological substance on CM kinetics. The proposed method was validated by contractile force measurement of live cardiomyocytes versus fixed cardiomyocytes. The applicability of the proposed method was tested to reveal the pharmacological effects of two drugs commonly used in cardiovascular research, isoprenaline (166nM, 500nM) and E-4031 (166 $\mu$ M, 500 $\mu$ M), on whole slide QPI of multiple cardiomyocytes in comparison to the control condition. The results demonstrate that the cardiomyocytes responded to isoprenaline by increasing the AP contractile force with a decrease in the resting period. The cardiomyocytes responded to E-4031, with the AP contractile force decline and the resting period was prolonged.



### e. Conclusion

In this article, we proposed an integrated platform for simultaneously monitoring human cardiomyocytes contractile kinetics, force generation at the single-cell level using a combination of FCN and optical flow from holographic imaging informatics. Several single CM were manually extracted from the QPI video sequence of multiple cardiomyocytes and dry mass was extracted using the FCN method. Subsequently, kinetics related parameters including force, speed, velocity, acceleration were calculated using dense Farneback optical flow method. To quantify single CM kinetics force generation and temporal related parameters, a computational algorithm was proposed for amplitude peak identification and contraction-relaxation beating activity was marked for visual quality control. Average values for kinetics parameters were calculated and represented as bar graphs with SD. The applicability of force measurement of the proposed method was tested to reveal the pharmacological effects of two cardiovascular drugs, isoprenaline (166nM, 500 nM) and E-4031 (166  $\mu$ M ,500 $\mu$ M), on whole slide QPI of multiple cardiomyocytes were quantified and compared to the control condition. The results demonstrate that the cardiomyocytes responded to isoprenaline by increasing the action potential (AP) contractile force with a decrease in the resting period. In the presence of E-4031, the AP contractile force was declined and the resting period was prolonged.

### 3 Conclusion and Future Research Opportunities

This dissertation aimed to show the application of the holographic imaging method for cardiac cell analysis. Cardiac cells derived from stem cells are transparent or semi-transparent micro object which is used for human disease modeling and cardiotoxicity screening application. Despite that many researchers reported different ways of cardiac cell analysis, yet little is known about the single cardiac cell. In this desertion, we demonstrated four different research conducted to show the different analyses of the cardiac cells at the single-cell level. In our new experiment, we would like to see the difference in the kinematic parameter in time dependant cardiac cells at the drug-treated cardiac cells. In a new experiment, we would like to propose a method for the automatic classification of single drug-treated cardiac cells. In the presence of the different drugs, The beating activity profile of different cardiac cells will change the shape. Also, different temporal parameters will dramatically change. This parameter can be used for the automatic classification of drug-treated cardiomyocytes at the single-cell level. The studying of drug-treated single cells contractile force generation changes during time is another study of our interest. The beating profile of cardiac cells dramatically changes the shape and temporal parameters in the presence of different drugs. We would like to investigate the feasibility of the single cardiomyocytes classification based on the beating activity profile.

## 4 References

- [1] C. Wheeler-Jones, "Cell signaling in the cardiovascular system: An overview," *Heart* 91(10), 1366-1374 (2005).
- [2] N. Shaked, L. Satterwhite, N. Bursac, and A. Wax, "Whole-cell-analysis of live cardiomyocytes using wide-field interferometric phase microscopy," *Biomed. Opt. Express* 1(2), 706-719 (2010).
- [3] A. Totaro, F. Urciuolo, G. Imparato, and P. A. Netti, "Engineered cardiac micromodules for the in vitro fabrication of 3D endogenous macro-tissues," *Biofabrication* 8(2), (2016).
- [4] D. Ossola, M. Amarouch, P. Behr, J. Vörös, H. Abriel, and T. Zambelli, "Force-controlled patch clamp of beating cardiac cells," *Nano Lett.* 15(3), 1743-1750 (2015).
- [5] A. Brüggemann, C. Haarmann, M. Rapedius, T. Goetze, I. Rinke, M. George, and N. Fertig, "Characterization of iPS Derived Cardiomyocytes in Voltage Clamp and Current Clamp by Automated Patch Clamp," *Biophys. J.* 112(3), 236a (2017).
- [6] N. Huebsch, P. Loskill, M. Mandegar, N. Marks, A. Sheehan, Z. Ma, A. Mathur, T. Nguyen, J. Yoo, L. Judge, C. Spencer, A. Chukka, C. Russell, P. So, B. Conklin, and K. Healy, "Automated video-based analysis of contractility and calcium flux in human-induced pluripotent stem cell-derived cardiomyocytes cultured over different spatial scales," *Tissue Eng. Part C Methods* 21(5), 467-479 (2015).
- [7] E. Grespan, S. Martewicz, E. Serena, V. Houerou, J. Rühle, and N. Elvassore, "Analysis of calcium transients and uniaxial contraction force in single human embryonic stem cell-derived cardiomyocytes on microstructured elastic substrate with spatially controlled surface chemistries," *Langmuir* 32(46), 12190-12201 (2016).

- [8] A. Ahola, A. L. Kiviahho, K. Larsson, M. Honkanen, K. Aalto-Setälä, and J. Hyttinen, "Video image-based analysis of single human induced pluripotent stem cell derived cardiomyocyte beating dynamics using digital image correlation," *Biomed. Eng.* 13(1), 1-18 (2014).
- [9] C. Bazan, D. Barba, P. Blomgren, and P. Paolini, "Image processing techniques for assessing contractility in isolated neonatal cardiac myocytes," *J. Biomed. Imaging* 16 (2011).
- [10] I. Nitsan, S. Drori, Y. Lewis, S. Cohen, and S. Tzlil, "Mechanical communication in cardiac cell synchronized beating," *Nat. Phys.* 12(5), 472-477 (2016).
- [11] Y. Abassi, B. Xi, N. Li, W. Ouyang, A. Seiler, M. Watzele, R. Kettenhofen, H. Bohlen, A. Ehlich, E. Kolossov, X. Wang, and X. Xu, "Dynamic monitoring of beating periodicity of stem cell-derived cardiomyocytes as a predictive tool for preclinical safety assessment," *Br. J. Pharmacol.* 165(5), 1424-1441 (2012).
- [12] K. Jaferzadeh, S. Hwang, I. Moon, and B. Javidi, "No-search focus prediction at the single cell level in digital holographic imaging with deep convolutional neural network," *Biomed. Opt. Express* 10, 4276-4289 (2019).
- [13] Y. Wu, A. Ray, Q. Wei, A. Feizi, X. Tong, E. Chen, Y. Luo, and A. Ozcan, "Deep Learning Enables High-Throughput Analysis of Particle-Aggregation-Based Biosensors Imaged Using Holography," *ACS Photonics* 6(2), 294-301 (2019).
- [14] D. Fortun, P. Bouthemy, C. Kervrann, "Optical Flow Modeling and Computation: A Survey," *Computer Vision and Image Understanding* 134, 1-21 (2015).
- [15] A. Plyer, G. Le Besnerais, F. Champagnat, "Massively Parallel Lucas Kanade Optical Flow for Real-Time Video Processing Applications," *Journal of Real-Time Image Processing* 11(4), 713-730 (2016).
- [16] Matsa, E., Burridge, P. W. & Wu, J. C. Human stem cells for modeling heart disease and for drug discovery. *Science Translational Medicine* 6, 1–8 (2014).

- [17] Rappaz, B. et al. Automated multi-parameter measurement of cardiomyocytes dynamics with digital holographic microscopy. *Optics Express* 23, 13333 (2015).
- [18] Shaked, N. T., Satterwhite, L. L., Bursac, N. & Wax, A. Whole-cell-analysis of live cardiomyocytes using wide-field interferometric phase microscopy. *Biomedical Optics Express* 1, 706 (2010).
- [19] Carl, D. microscope for high-resolution living-cell analysis. (2004).
- [20] Boss, D. et al. Measurement of absolute cell volume, osmotic membrane water permeability, and refractive index of transmembrane water and solute flux by digital holographic microscopy. *Journal of Biomedical Optics* 18, 036007 (2013).
- [21] Merola, F. et al. Digital holography as a method for 3D imaging and estimating the biovolume of motile cells. *Lab on a Chip* 13, 4512–4516 (2013).
- [22] Moon, I., Daneshpanah, M., Javidi, B. & Stern, A. Automated three-dimensional identification and tracking of micro/nanobiological organisms by computational holographic microscopy. *Proceedings of the IEEE* 97, 990–1010 (2009).
- [23] Kühn, J. et al. Label-free cytotoxicity screening assay by digital holographic microscopy. *Assay and Drug Development Technologies* 11, 101–107 (2013).
- [24] Rappaz, B. et al. Noninvasive characterization of the fission yeast cell cycle by monitoring dry mass with digital holographic microscopy. *Journal of Biomedical Optics* 14, 034049 (2009).
- [25] Moon, I., Jaferzadeh, K., Ahmadzadeh, E. & Javidi, B. Automated quantitative analysis of multiple cardiomyocytes at the single-cell level with three-dimensional holographic imaging informatics. *Journal of Biophotonics* 1–12 (2018). doi:10.1002/jbio.201800116
- [26] Annabi, N. et al. Highly elastic micropatterned hydrogel for engineering functional cardiac tissue. *Advanced Functional Materials* 23, 4950–4959 (2013).
- [27] Chandrashekhara, R., Rao, A., Sanchez-Ortiz, G. I., Mohiaddin, R. H. & Rueckert, D. Construction of a statistical model for cardiac motion analysis using nonrigid image registration.

- Lecture Notes in Computer Science (including subseries Lecture Notes in Artificial Intelligence and Lecture Notes in Bioinformatics) 2732, 599–610 (2003).
- [28] Hoang, P. et al. quantitatively characterizing drug-induced arrhythmic contractile motions of human stem cell-derived cardiomyocytes. *Biotechnology and Bioengineering* 115, 1958–1970 (2018).
- [29] Maddah, M. et al. A non-invasive platform for functional characterization of stem-cell-derived cardiomyocytes with applications in cardiotoxicity testing. *Stem Cell Reports* 4, 621–631 (2015).
- [30] Czirik, A. et al. Optical-flow based non-invasive analysis of cardiomyocyte contractility. *Scientific Reports* 7, 1–11 (2017).
- [31] He, J. Q., Ma, Y., Lee, Y., Thomson, J. A. & Kamp, T. J. Human embryonic stem cells develop into multiple types of cardiac myocytes: Action potential characterization. *Circulation Research* 93, 32–39 (2003).
- [32] Cuhe, E., Marquet, P. & Depeursinge, C. Simultaneous amplitude-contrast and quantitative phase-contrast microscopy by numerical reconstruction of Fresnel off-axis holograms. *Applied Optics* 38, 6994 (1999).
- [33] Marquet, P. et al. Digital holographic microscopy: a noninvasive contrast imaging technique allowing quantitative visualization of living cells with subwavelength axial accuracy. *Optics Letters* 30, 468 (2005).
- [34] Schnars, U. & Juptner, W. *Digital recording and numerical. Institute of Physics Publishing* 13, 17 (2002).
- [35] G. Litjens, T. Kooi, B. Bejnordi, A. Setio, F. Ciompi, M. Ghafoorian, J. Laak, B. Ginneken, and C. Sánchez, “A survey on deep learning in medical image analysis,” *Med. Image Anal.* 42, 60–88 (2017).

- [36] A. Garcia, S. Escolano, S. Oprea, V. Martinez, P. Gonzalez, and J. Rodriguez, "A survey on deep learning techniques for image and video semantic segmentation," *Appl. Soft Comput. J.* 70, 41-65 (2018).
- [37] Shen, Dinggang, Guorong Wu, and Heung-Il Suk. "Deep learning in medical image analysis." *Annual review of biomedical engineering* pp.221-24819 (2017).
- [38] G. Huang, Z. Liu, L. Maaten, and K. Weinberger, "Densely connected convolutional networks," *IEEE Conf. Comput. Vis. Pattern Recognition, CVPR 2017*, 2261-2269 (2017).
- [39] Dolz, Jose, et al. "HyperDense-Net: a hyper-densely connected CNN for multi-modal image segmentation." *IEEE transactions on medical imaging*; pp.1116-11263; 8.5; (2018)
- [40] M. Khened, V. Kollerathu, and G. Krishnamurthi, "Fully convolutional multi-scale residual DenseNets for cardiac segmentation and automated cardiac diagnosis using ensemble of classifiers," *Med. Image Anal.* 51, 21-45 (2019).
- [41] S. Jastrzębski, D. Arpit, N. Ballas, V. Verma, T. Che, and Y. Bengio, "Residual Connections Encourage Iterative Inference," *ICLR 2018*, 1-14 (2018).
- [42] Jaferzadeh, K. et al. "Marker-Free Automatic Quantification of Drug-Treated Cardiomyocytes with Digital Holographic Imaging". *ACS Photonics* 7, 105–113 (2020).
- [43] N. Huebsch, P. Loskill, MA. Mandegar, NC. Marks, AS. Sheehan, Z. Ma ,A. Mathur, TN. Nguyen, JC. Yoo, LM. Judge and CI. Spencer , "Automated video-based analysis of contractility and calcium flux in human-induced pluripotent stem cell-derived cardiomyocytes cultured over different spatial scales," *Tissue Engineering Part C: Methods.* 21(5), 467-79 (2015).
- [44] Weiger, Michael C., et al. "Real-time motion analysis reveals cell directionality as an indicator of breast cancer progression." *PLoS One* 8.3 (2013).
- [45] Hoang, Plansky, et al. "Quantitatively characterizing drug-induced arrhythmic contractile motions of human stem cell-derived cardiomyocytes." *Biotechnology and bioengineering* 115.8: 1958-1970. (2018).

- [46] Maddah, Mahnaz, et al. "A non-invasive platform for functional characterization of stem-cell-derived cardiomyocytes with applications in cardiotoxicity testing." *Stem cell reports* 4.4: 621-631. (2015).
- [47] Czirok, Andras, et al. "Optical-flow based non-invasive analysis of cardiomyocyte contractility." *Scientific reports* 7.1: 1-11. (2017).
- [48] Hayakawa, Tomohiro, et al. "Noninvasive evaluation of contractile behavior of cardiomyocyte monolayers based on motion vector analysis." *Tissue Engineering Part C: Methods* 18.1: 21-32. (2012).
- [49] Ahola, A.; Pradhapan, P.; Laurila, E.; Aalto-Setälä, K.; Hyttinen, J. Motion Analysis Method for Determining Cardiomyocyte Beating Properties Based on Digital Image Correlation and Templates. *Computing in Cardiology*, 41 (January), 1137–1140. (2014).
- [50] Ting S, Liew SJ, Japson F, Shang F, Chong WK, Reuveny S, Tham JY, Li X, Oh S. Time-resolved video analysis and management system for monitoring cardiomyocyte differentiation processes and toxicology assays. *Biotechnology journal*. May;9(5):675-83. (2014).
- [51] Wang H, Kläser A, Schmid C, Liu CL. Dense trajectories and motion boundary descriptors for action recognition. *International journal of computer vision*. May 1;103(1):60-79.( 2013)
- [52] Kaltsa V, Briassouli A, Kompatsiaris I, Srinivasan MG. Timely, robust crowd event characterization. In 2012 19th IEEE International Conference on Image Processing Sep (pp. 2697-2700). IEEE.( 2012).
- [53] Farneback, G. Two-Frame Motion Estimation Based on. *Lecture Notes in Computer Science* 2749, 363–370 (2003).
- [54] Arzeno, N. M., Deng, Z. De & Poon, C. S. Analysis of first-derivative based QRS detection algorithms. *IEEE Transactions on Biomedical Engineering* 55, 478–484 (2008).



- [55] Ruha, A., Sallinen, S. & Nissilä, S. A real-time microprocessor QRS detector system with a 1-ms timing accuracy for the measurement of ambulatory HRV. *IEEE Transactions on Biomedical Engineering* 44, 159–167 (1997).
- [56] Christov, I. I. Real time electrocardiogram QRS detection using a combined adaptive threshold. *Biomedical Engineering Online* 3, 1–9 (2004).
- [57] Luo, C., Wang, K. & Zhang, H. Modelling the effects of quinidine, disopyramide, and E-4031 on short QT syndrome variant 3 in the human ventricles. *Physiological Measurement* 38, 1859–1873 (2017).
- [58] Roy, S. J. & Mainzen Prince, P. S. Protective effects of sinapic acid on cardiac hypertrophy, dyslipidaemia and altered electrocardiogram in isoproterenol-induced myocardial infarcted rats. *European Journal of Pharmacology* 699, 213–218 (2013).
- [59] Y.A. Abassi, B. Xi, W. Zhang, P. Ye, S.L. Kirstein, M.R. Gaylord, S.C. Feinstein, X. Wang, X. Xu, Kinetic Cell-Based Morphological Screening: Prediction of Mechanism of Compound Action and Off-Target Effects, *Chem. Biol.* 16 (2009) 712–723. <https://doi.org/10.1016/j.chembiol.2009.05.011>.
- [60] J.M. Pioner, A.W. Racca, J.M. Klaiman, K.C. Yang, X. Guan, L. Pabon, V. Muskheli, R. Zaunbrecher, J. Macadangang, M.Y. Jeong, D.L. Mack, M.K. Childers, D.H. Kim, C. Tesi, C. Poggesi, C.E. Murry, M. Regnier, Isolation and mechanical measurements of myofibrils from human induced pluripotent stem cell-derived cardiomyocytes, *Stem Cell Reports*. 6 (2016) 885–896. <https://doi.org/10.1016/j.stemcr.2016.04.006>.
- [61] I. Moon, K. Jaferzadeh, E. Ahmadzadeh, B. Javidi, Automated quantitative analysis of multiple cardiomyocytes at the single-cell level with three-dimensional holographic imaging informatics, *J. Biophotonics*. (2018) 1–12. <https://doi.org/10.1002/jbio.201800116>.
- [62] I. Mannhardt, K. Breckwoldt, D. Letuffe-Brenière, S. Schaaf, H. Schulz, C. Neuber, A. Benzin, T. Werner, A. Eder, T. Schulze, B. Klampe, T. Christ, M.N. Hirt, N. Huebner, A. Moretti, T.

- Eschenhagen, A. Hansen, Human Engineered Heart Tissue: Analysis of Contractile Force, *Stem Cell Reports*. 7 (2016) 29–42. <https://doi.org/10.1016/j.stemcr.2016.04.011>.
- [63] N.T. Shaked, L.L. Satterwhite, N. Bursac, A. Wax, Whole-cell-analysis of live cardiomyocytes using wide-field interferometric phase microscopy, *Biomed. Opt. Express*. 1 (2010) 706. <https://doi.org/10.1364/BOE.1.000706>.
- [64] B. Kemper, G. von Bally, Digital holographic microscopy for live cell applications and technical inspection, *Appl. Opt.* 47 (2008) A52. <https://doi.org/10.1364/AO.47.000A52>.
- [65] E. Cuche, P. Marquet, C. Depeursinge, Simultaneous amplitude-contrast and quantitative phase-contrast microscopy by numerical reconstruction of Fresnel off-axis holograms, *Appl. Opt.* 38 (1999) 6994. <https://doi.org/10.1364/AO.38.006994>.
- [66] B. Rappaz, I. Moon, F. Yi, B. Javidi, P. Marquet, G. Turcatti, Automated multi-parameter measurement of cardiomyocytes dynamics with digital holographic microscopy, *Opt. Express*. 23 (2015) 13333. <https://doi.org/10.1364/OE.23.013333>.
- [67] T. Hayakawa, T. Kunihiro, T. Ando, S. Kobayashi, E. Matsui, H. Yada, Y. Kanda, J. Kurokawa, T. Furukawa, Image-based evaluation of contraction-relaxation kinetics of human-induced pluripotent stem cell-derived cardiomyocytes: Correlation and complementarity with extracellular electrophysiology, *J. Mol. Cell. Cardiol.* 77 (2014) 178–191. <https://doi.org/10.1016/j.yjmcc.2014.09.010>.
- [68] N. Huebsch, P. Loskill, M.A. Mandegar, N.C. Marks, A.S. Sheehan, Z. Ma, A. Mathur, T.N. Nguyen, J.C. Yoo, L.M. Judge, C.I. Spencer, A.C. Chukka, C.R. Russell, P.L. So, B.R. Conklin, K.E. Healy, Automated video-based analysis of contractility and calcium flux in human-induced pluripotent stem cell-derived cardiomyocytes cultured over different spatial scales, *Tissue Eng. - Part C Methods*. 21 (2015) 467–479.

- [69] U. Saleem, I. Mannhardt, I. Braren, C. Denning, T. Eschenhagen, A. Hansen, Force and Calcium Transients Analysis in Human Engineered Heart Tissues Reveals Positive Force-Frequency Relation at Physiological Frequency, *Stem Cell Reports*. 14 (2020) 312–324.
- [70] Z. Liu, J.L. Tan, D.M. Cohen, M.T. Yang, N.J. Sniadecki, S.A. Ruiz, C.M. Nelson, C.S. Chen, Mechanical tugging force regulates the size of cell-cell junctions, *Proc. Natl. Acad. Sci. U. S. A.* 107 (2010) 9944–9949.
- [71] J.L. Ruan, N.L. Tulloch, M. V. Razumova, M. Saiget, V. Muskheli, L. Pabon, H. Reinecke, M. Regnier, C.E. Murry, Mechanical Stress Conditioning and Electrical Stimulation Promote Contractility and Force Maturation of Induced Pluripotent Stem Cell-Derived Human Cardiac Tissue, *Circulation*. 134(2016)1557–1567.
- [72] S. Yin, X. Zhang, C. Zhan, J. Wu, J. Xu, J. Cheung, Measuring single cardiac myocyte contractile force via moving a magnetic bead, *Biophys. J.* 88 (2005) 1489–1495.
- [73] D. Sasaki, K. Matsuura, H. Seta, Y. Haraguchi, T. Okano, T. Shimizu, Contractile force measurement of human induced pluripotent stem cell-derived cardiac cell sheet-tissue, *PLoS One*. 13 (2018) 1–21. <https://doi.org/10.1371/journal.pone.0198026>.
- [74] F. Pillekamp, M. Reppel, O. Rubenchyk, K. Pfannkuche, M. Matzkies, W. Bloch, N. Sreeram, K. Brockmeier, J. Hescheler, Force Measurements of Human Embryonic Stem Cell-Derived Cardiomyocytes in an In Vitro Transplantation Model, *Stem Cells*. 25 (2007) 174–180.
- [75] R.E. Taylor, K. Kim, N. Sun, S.J. Park, J.Y. Sim, G. Fajardo, D. Bernstein, J.C. Wu, B.L. Pruitt, Sacrificial layer technique for axial force post assay of immature cardiomyocytes, *Biomed. Microdevices*. 15 (2013) 171–181.
- [76] K.S. Bielawski, A. Leonard, S. Bhandari, C.E. Murry, N.J. Sniadecki, Real-Time Force and Frequency Analysis of Engineered Human Heart Tissue Derived from Induced Pluripotent Stem Cells Using Magnetic Sensing, *Tissue Eng. - Part C Methods*. 22 (2016) 932–940.

- [77] D. Krinke, H.G. Jahnke, O. Pänke, A.A. Robitzki, A microelectrode-based sensor for label-free in vitro detection of ischemic effects on cardiomyocytes, *Biosens. Bioelectron.* 24 (2009) 2798–2803.
- [78] G. Caluori, J. Pribyl, M. Pesl, S. Jelinkova, V. Rotrekl, P. Skladal, R. Raiteri, Non-invasive electromechanical cell-based biosensors for improved investigation of 3D cardiac models, *Biosens. Bioelectron.* 124–125 (2019) 129–135.
- [79] A. Czirok, D.G. Isai, E. Kosa, S. Rajasingh, W. Kinsey, Z. Neufeld, J. Rajasingh, Optical-flow based non-invasive analysis of cardiomyocyte contractility, *Sci. Rep.* 7 (2017) 1–11.
- [80] D. Fortun, P. Bouthemey, C. Kervrann, Optical flow modeling and computation: A survey, *Comput. Vis. Image Underst.* 134 (2015) 1–21.
- [81] B. Javidi, I. Moon, S. Yeom, E. Carapezza, Three-dimensional imaging and recognition of microorganism using single-exposure on-line (SEOL) digital holography, *Opt. Express.* 13 (2005) 4492.
- [82] B. Rappaz, E. Cano, T. Colomb, J. Kühn, C. Depeursinge, V. Simanis, P.J. Magistretti, P. Marquet, Noninvasive characterization of the fission yeast cell cycle by monitoring dry mass with digital holographic microscopy, *J. Biomed. Opt.* 14 (2009) 034049.
- [83] L. Chen, P. Bentley, K. Mori, K. Misawa, M. Fujiwara, D. Rueckert, DRINet for Medical Image Segmentation, *IEEE Trans. Med. Imaging.* 37 (2018) 2453–2462.
- [84] L.C. Chen, G. Papandreou, I. Kokkinos, K. Murphy, A.L. Yuille, DeepLab: Semantic Image Segmentation with Deep Convolutional Nets, Atrous Convolution, and Fully Connected CRFs, *IEEE Trans. Pattern Anal. Mach. Intell.* 40 (2018) 834–848.
- [85] Y. Wu, A. Ray, Q. Wei, A. Feizi, X. Tong, E. Chen, Y. Luo, A. Ozcan, Deep Learning Enables High-Throughput Analysis of Particle-Aggregation-Based Biosensors Imaged Using Holography, *ACS Photonics.* 6 (2019) 294–301.

- [86] A. Garcia-Garcia, S. Orts-Escolano, S. Oprea, V. Villena-Martinez, P. Martinez-Gonzalez, J. Garcia-Rodriguez, A survey on deep learning techniques for image and video semantic segmentation, *Appl. Soft Comput. J.* 70 (2018) 41–65.
- [87] E. Ahmadzadeh, K. Jaferzadeh, Shin Seokjoo, I. Moon, Automated single cardiomyocyte characterization by nucleus extraction from dynamic holographic images using a fully convolutional neural network, 11 (2020) 1501–1516.
- [88] V. Galvão, J.G.V. Miranda, R. Ribeiro-dos-Santos, Development of a two-dimensional agent-based model for chronic chagasic cardiomyopathy after stem cell transplantation, *Bioinformatics.* 24 (2008) 2051–2056.
- [89] M.P. D. Ghiglia, *Two-dimensional Phase Unwrapping: Theory, Algorithms, And Software*, 2017.